Unveiling Galactic Substructure with Astrometry and Gravitational Lensing

Siddharth Mishra-Sharma

Based on work to appear with Ken Van Tilburg and Neal Weiner

NYU | Center for Cosmology and Particle Physics

Phenomenology Symposium, May 7 2019

Pittsburgh, PA

Pinning down dark matter microphysics…

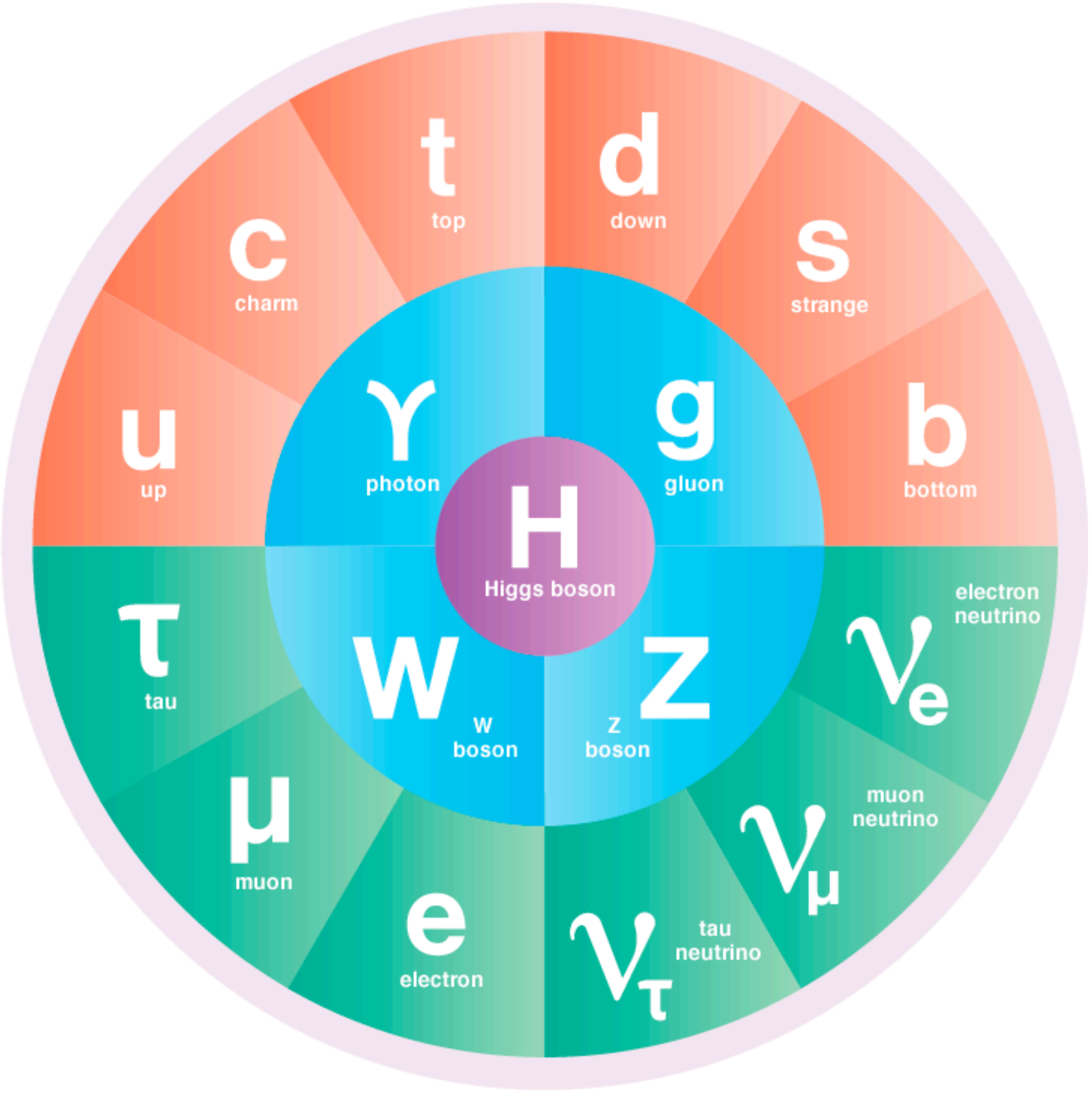

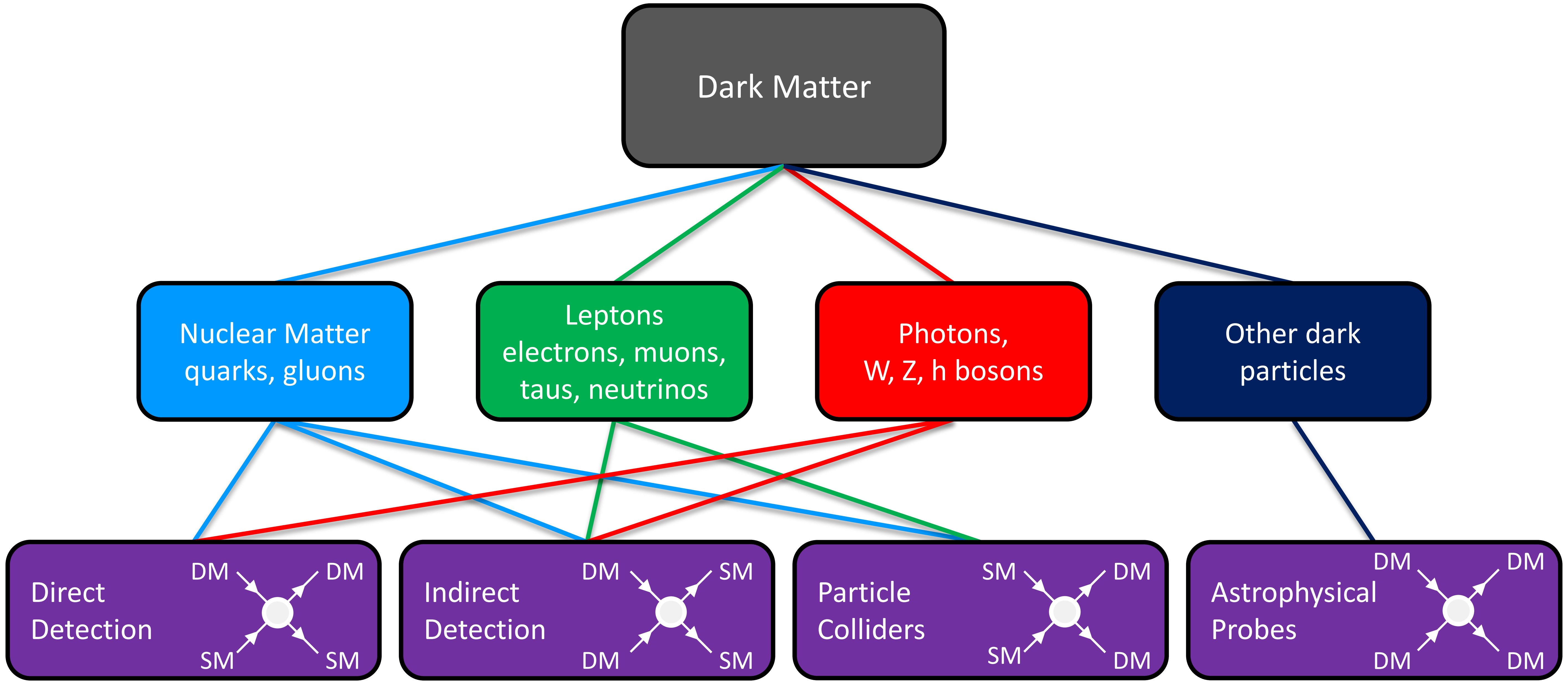

Snowmass CF4 report (Bauer et al, 2015)

...through macroscopic effects

Underlying particle physics can be manifest by understanding macroscopic distribution of dark matter on small scales

Model	Probe	Parameter	Value
Warm Dark Matter	Halo Mass	Particle Mass	$m \sim 18\,\mathrm{keV}$
Self-Interacting Dark Matter	Halo Profile	Cross Section	$\sigma_{\mathrm{SIDM}}/m_\chi \sim 0.1$–$10\,\mathrm{cm}^2/\,\mathrm{g}$
Baryon-Scattering Dark Matter	Halo Mass	Cross Section	$\sigma \sim 10^{-30}\,\mathrm{cm}^2$
Axion-Like Particles	Energy Loss	Coupling Strength	$g_{\phi e} \sim 10^{-13}$
Fuzzy Dark Matter	Halo Mass	Particle Mass	$m \sim 10^{-20}\,\mathrm{eV}$
Primordial Black Holes	Compact Objects	Object Mass	$M > 10^{-4} M_\odot$
Weakly Interacting Massive Particles	Indirect Detection	Cross Section	$\langle\sigma v\rangle \sim 10^{-27}\,\mathrm{cm}^3/\,\mathrm{s}$
Light Relics	Large-Scale Structure	Relativistic Species	$N_{\mathrm{eff}} \sim 0.1$

LSST Dark Matter White Paper (Drlica-Wagner et al, 2019)

Microphysics from **Macrophysics**

(Self-interactions, scalar field DM...)

(Subhalo mass function, subhalo profiles...)

Probe properties of low-mass, non-luminous subhalos through their gravitational effects

Gravitational lensing

Intervening mass causes a shift in the *apparent position* of luminous sources

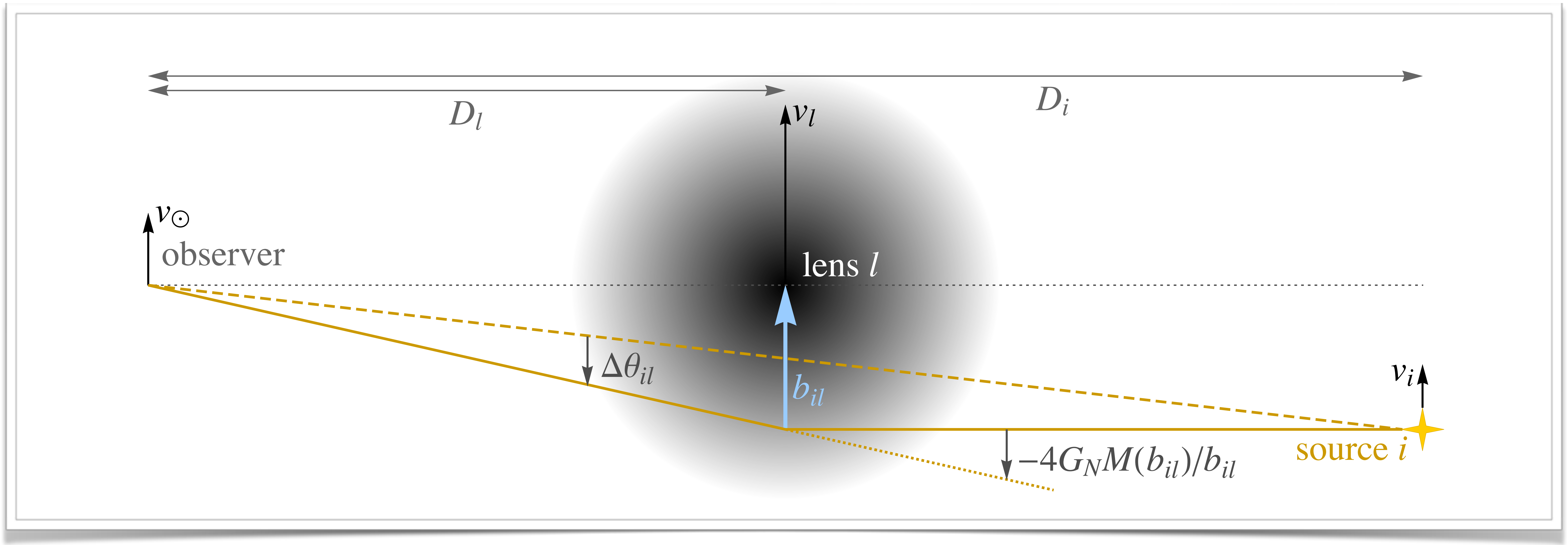

Van Tilburg et al, 2018

Magnitude of the shift for Galactic subhalo lenses

$$\Delta\boldsymbol{\theta}_{il} = -\left(1 - \frac{D_l}{D_i}\right)\frac{4G_N M(b_{il})}{b_{il}}\hat{\mathbf{b}}_{il} \approx 400\ \mu\text{as}\left(\frac{M(b_{il})}{10^6\ M_\odot}\right)\left(\frac{10^2\ \text{pc}}{b_{il}}\right)$$

$1\ \mu\text{as} \approx 5\times10^{-12}$ rad

$M(b)$: projected enclosed mass

Problem: true position of background sources unknown

Shifts in position smaller than typical angular density variations of sources

Potential solution: go into the time-domain

Moving lenses induce motions in background sources

$$\mathbf{v}_{il} \equiv \dot{\mathbf{b}}_{il} = \mathbf{v}_l - \left(1 - \frac{D_l}{D_i}\right)\mathbf{v}_\odot - \frac{D_l}{D_i}\mathbf{v}_i$$

$$\boldsymbol{\mu}(\mathbf{b}) = 4G\left\{\frac{M(b)}{b^2}\left[2\hat{\mathbf{b}}(\hat{\mathbf{b}}\cdot\mathbf{v}_l) - \mathbf{v}_l\right] - \frac{M'(b)}{b}\hat{\mathbf{b}}(\hat{\mathbf{b}}\cdot\mathbf{v}_l)\right\}$$

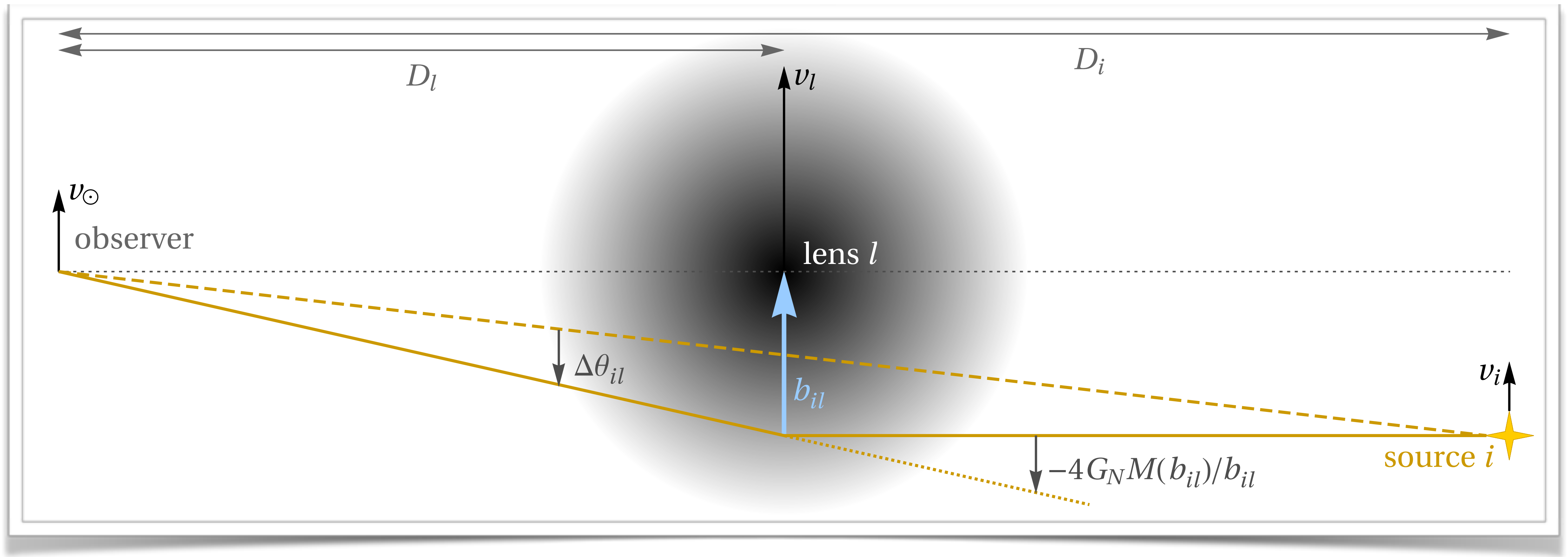

Moving lenses induce motions in background sources

$$\mathbf{v}_{il} \equiv \dot{\mathbf{b}}_{il} = \mathbf{v}_l - \left(1 - \frac{D_l}{D_i}\right)\mathbf{v}_\odot - \frac{D_l}{D_i}\mathbf{v}_i$$

$$\boldsymbol{\mu}(\mathbf{b}) = 4G\left\{\frac{M(b)}{b^2}\left[2\hat{\mathbf{b}}(\hat{\mathbf{b}}\cdot\mathbf{v}_l) - \mathbf{v}_l\right] - \frac{M'(b)}{b}\hat{\mathbf{b}}(\hat{\mathbf{b}}\cdot\mathbf{v}_l)\right\}$$

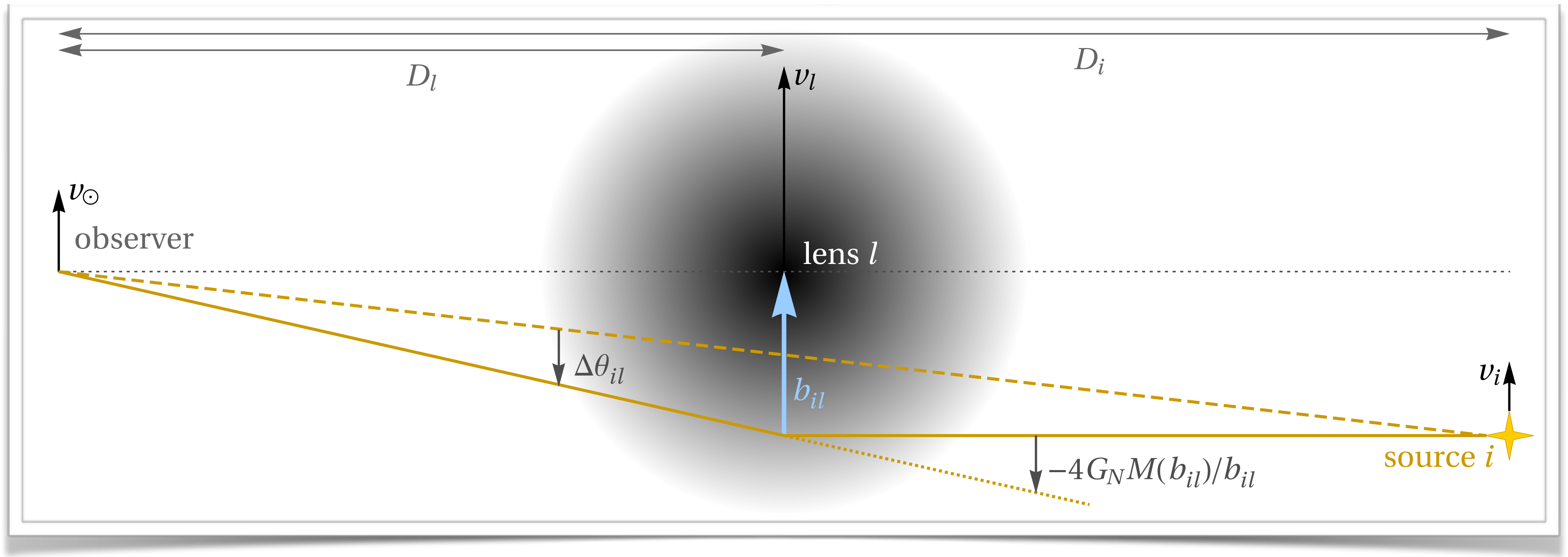

Typical size of time-domain effects for Galactic lenses

Angular velocity shift: $\Delta\dot{\theta}_{il} \sim \frac{4G_N M(b_{il}) v_{il}}{b_{il}^2} \sim 10^{-3}\ \mu\mathrm{as\ y}^{-1}\left(\frac{M(b_{il})}{10^6\ M_\odot}\right)\left(\frac{10^2\ \mathrm{pc}}{b_{il}}\right)^2$

Angular acceleration shift: $\Delta\ddot{\theta}_{il} \sim \frac{4G_N M(b_{il}) v_{il}^2}{b_{il}^3} \sim 4\times10^{-3}\ \mu\mathrm{as\ y}^{-2}\left(\frac{M(b_{il})}{M_\odot}\right)\left(\frac{10^{-2}\ \mathrm{pc}}{b_{il}}\right)^3$

Smaller than current or anticipated astrometric precision

Extended lenses

Problem: extended lenses strongly suppress lensing effects

$$\Delta\dot{\theta}_{il} \sim \frac{4G_N M(b_{il}) v_{il}}{b_{il}^2} \sim 10^{-3}\ \mu\text{as y}^{-1} \left(\frac{M(b_{il})}{10^6\ M_\odot}\right)\left(\frac{10^2\ \text{pc}}{b_{il}}\right)^2$$

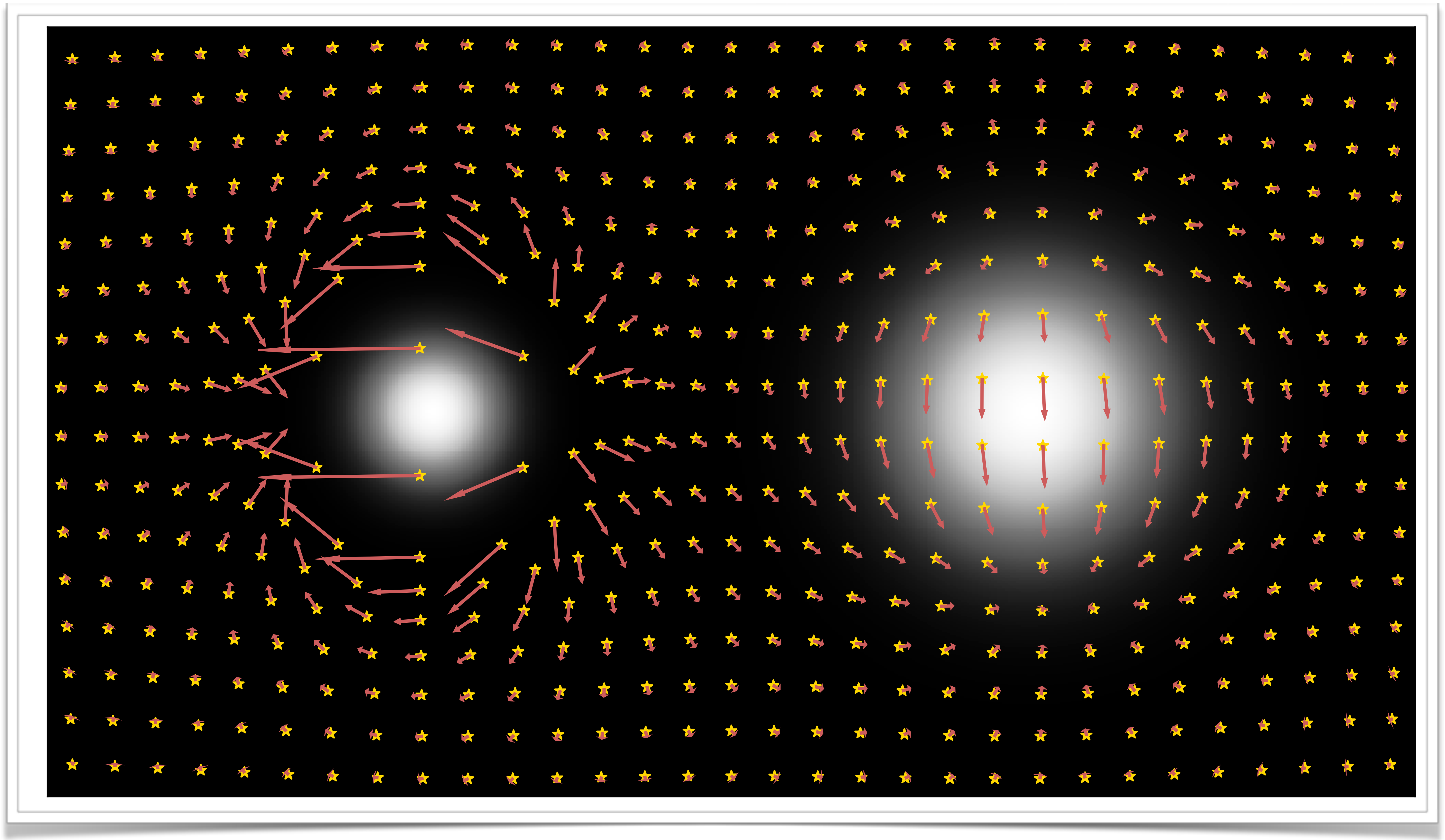

Potential solution: study correlated motions

Global, correlated lens-induced motions

Alternatively, can look for global patterns in induced motion of sources due to a population of lenses

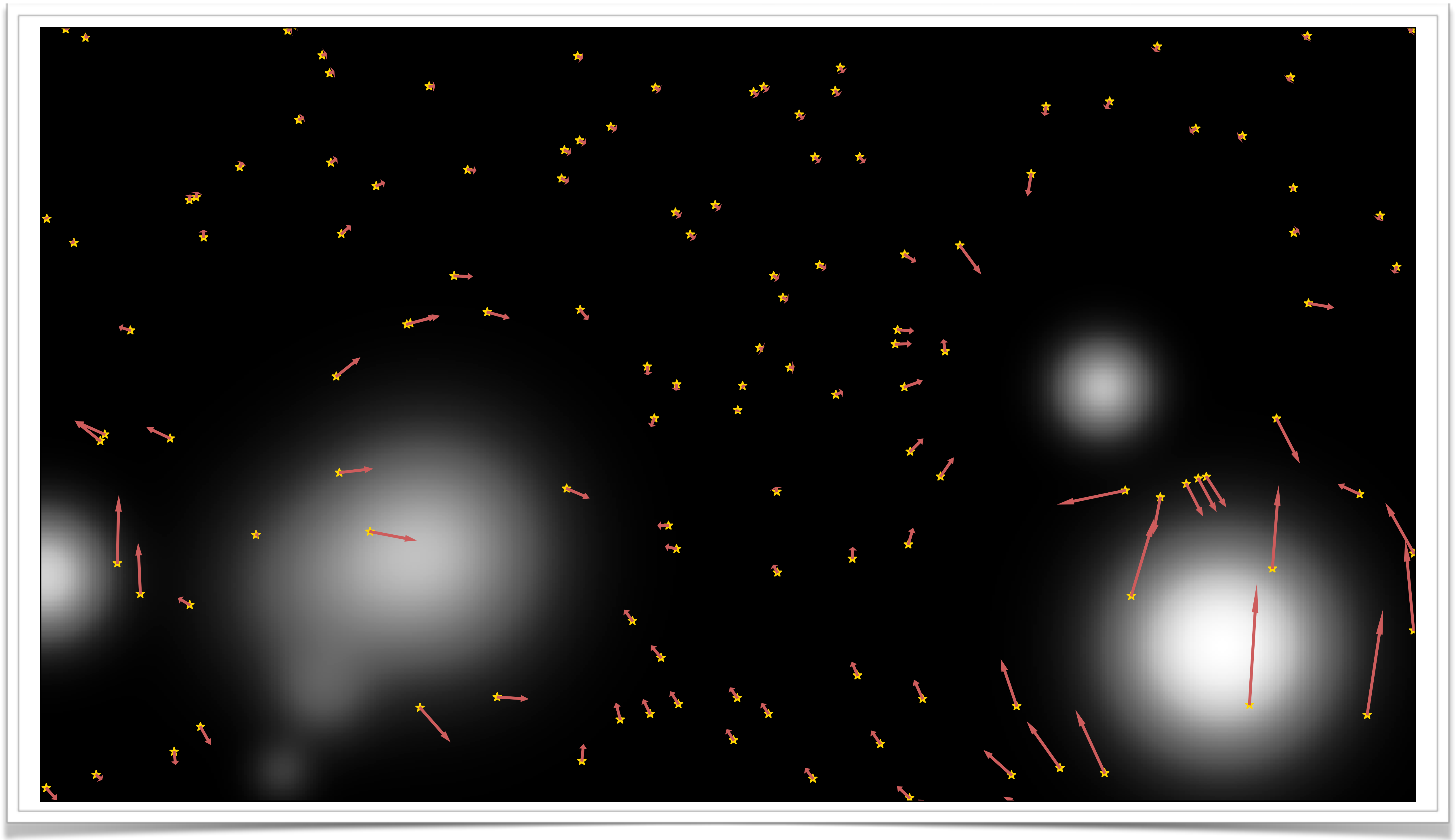

Global, correlated lens-induced motions

Alternatively, can look for global patterns in induced motion of sources due to a population of lenses

$\vec{\mu} = \{$

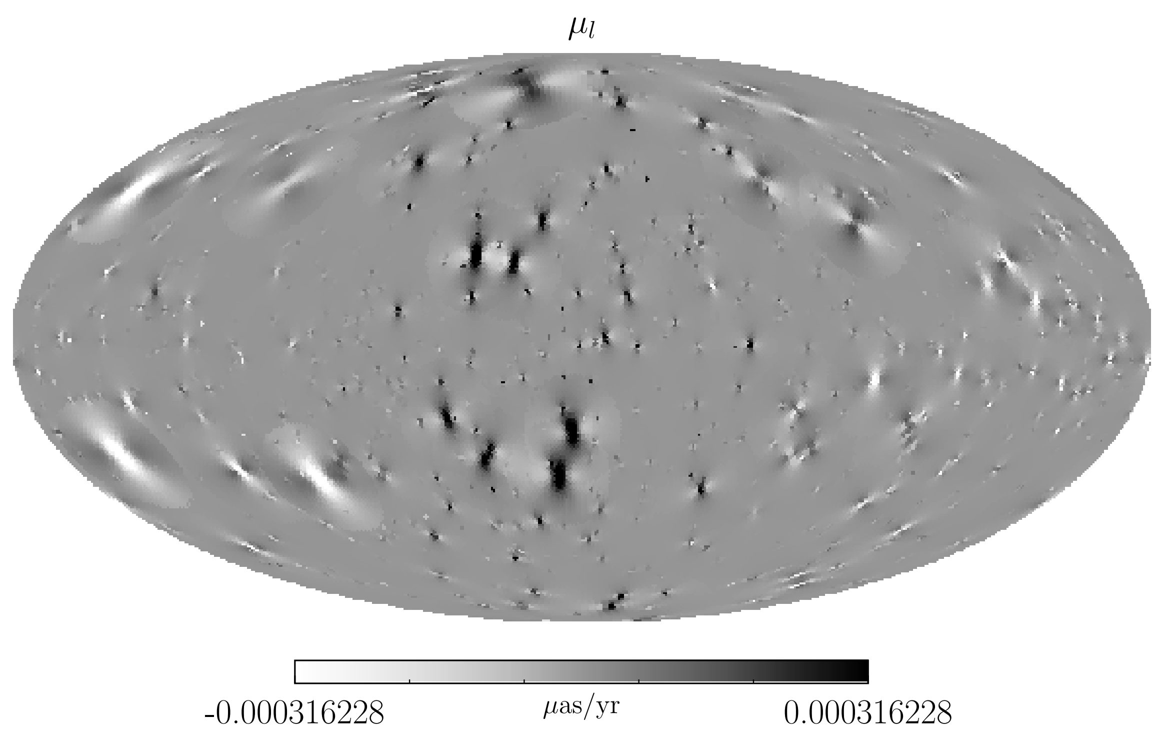

,

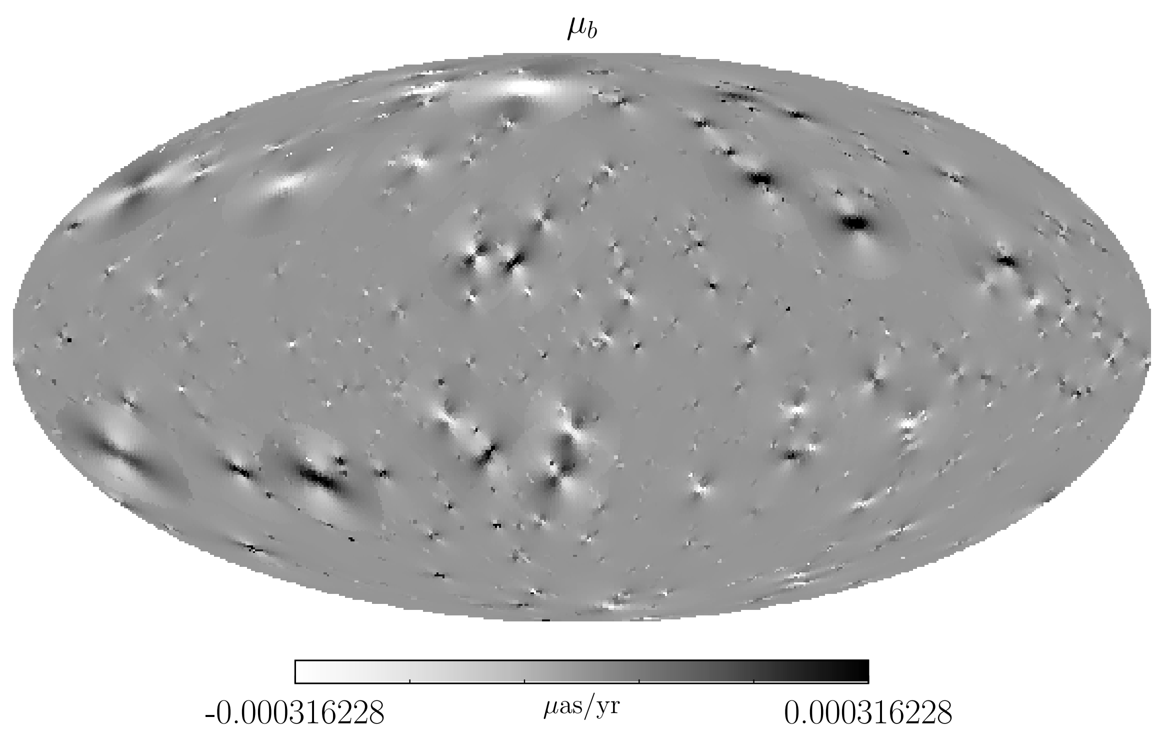

$\}$

One tool to do this: *angular correlation functions*

Large-scale structure power spectra

Data

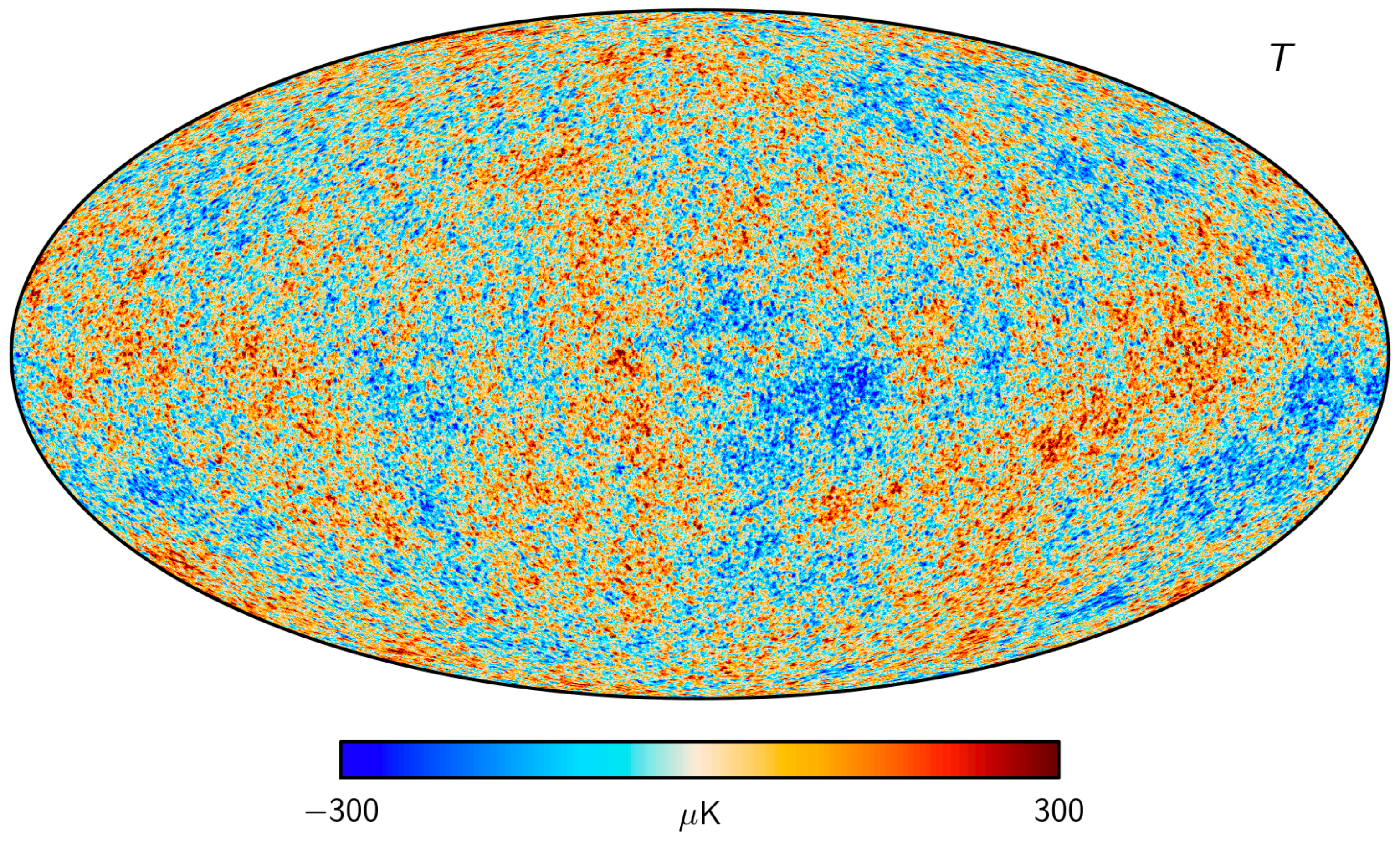

Power spectrum decomposition

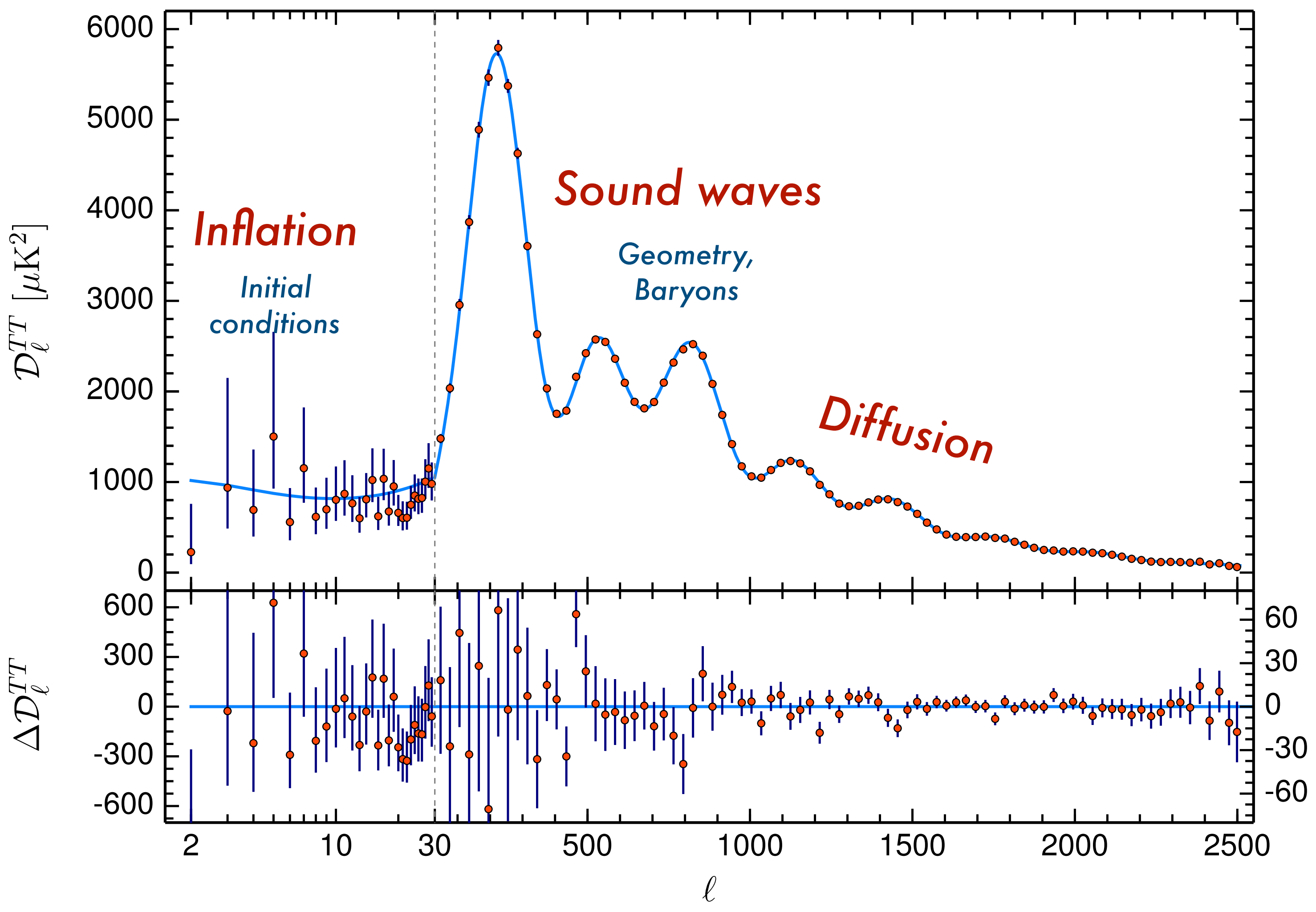

Parameter inference

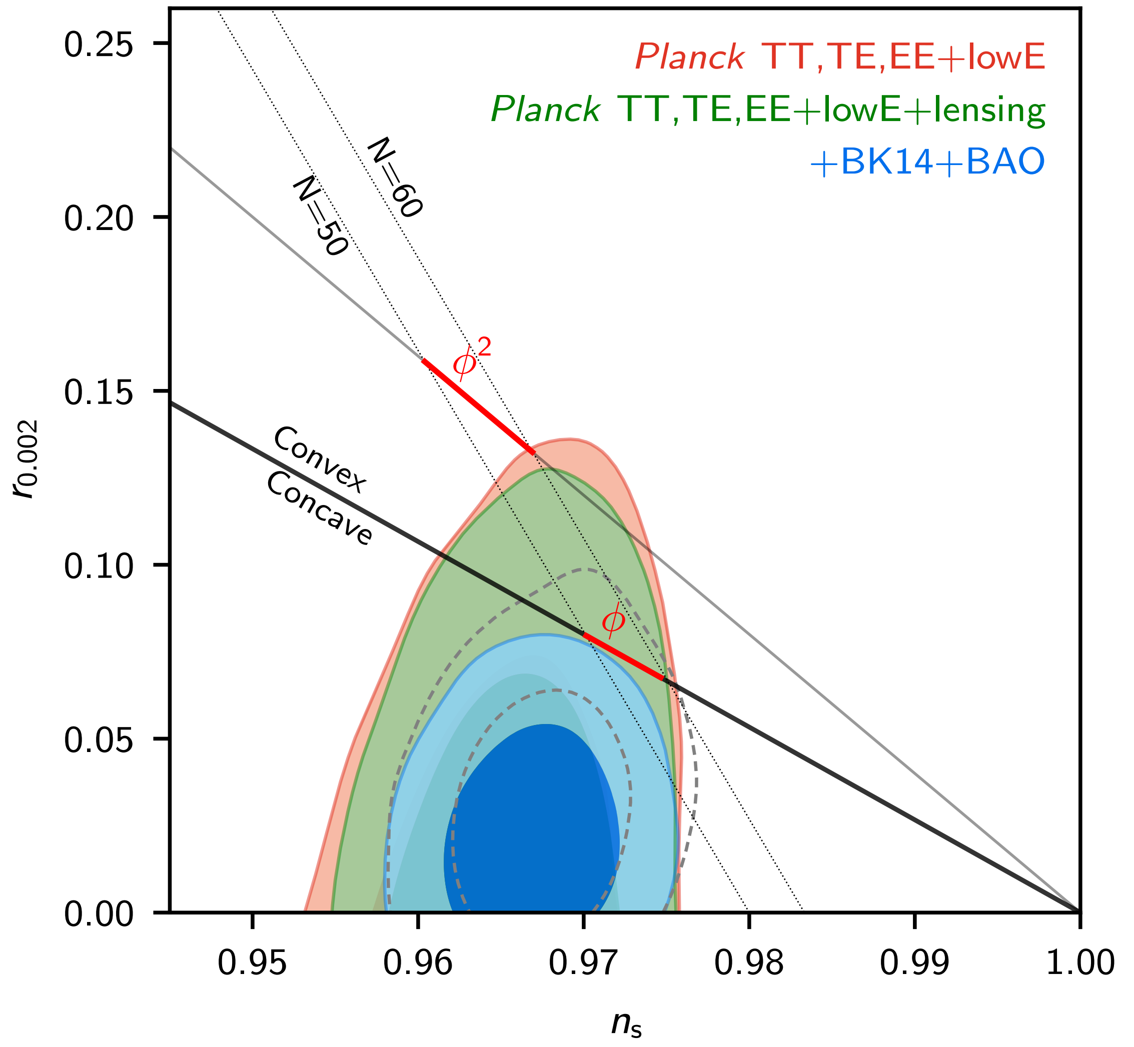

Large-scale structure power spectra

Data

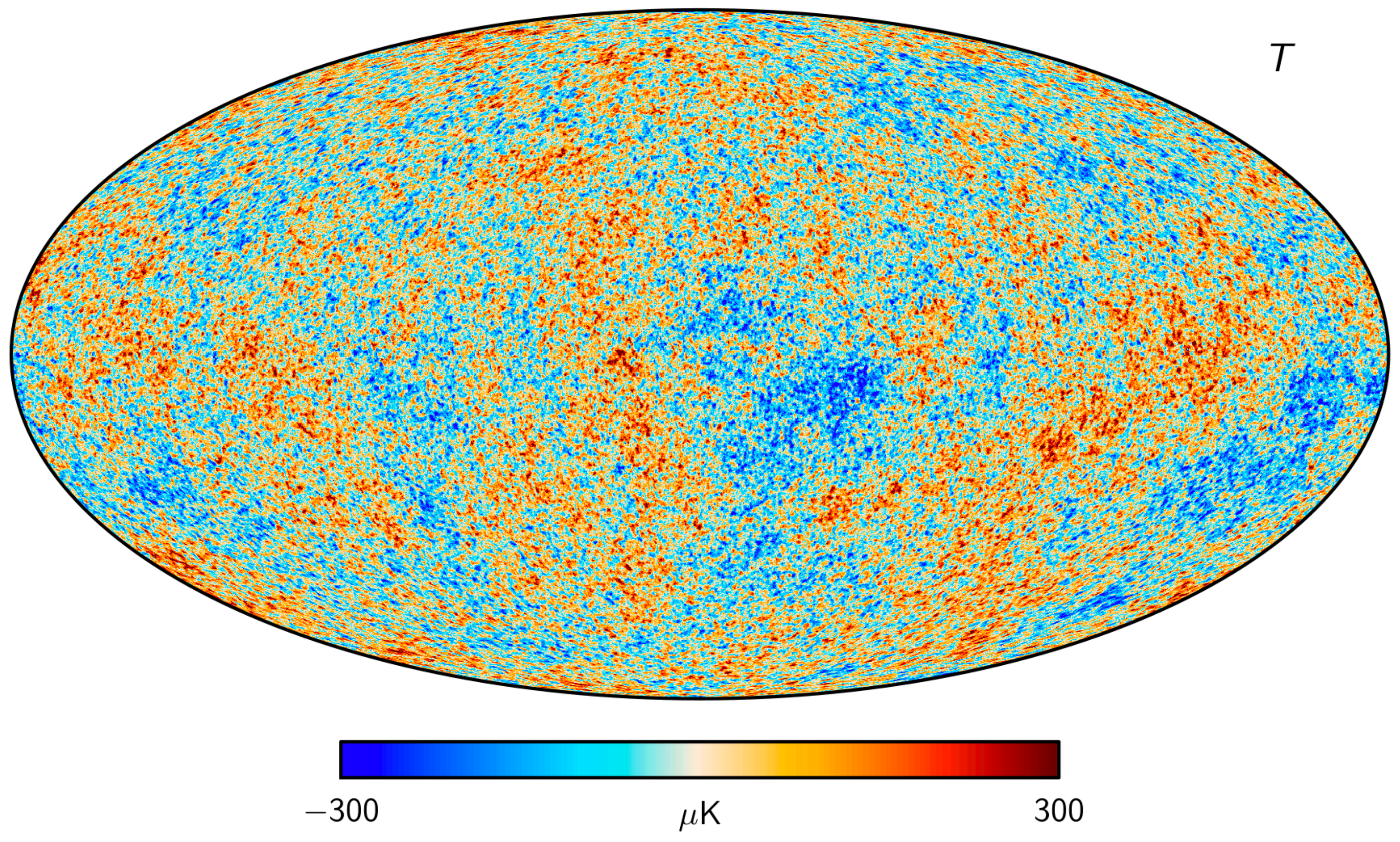

Power spectrum decomposition

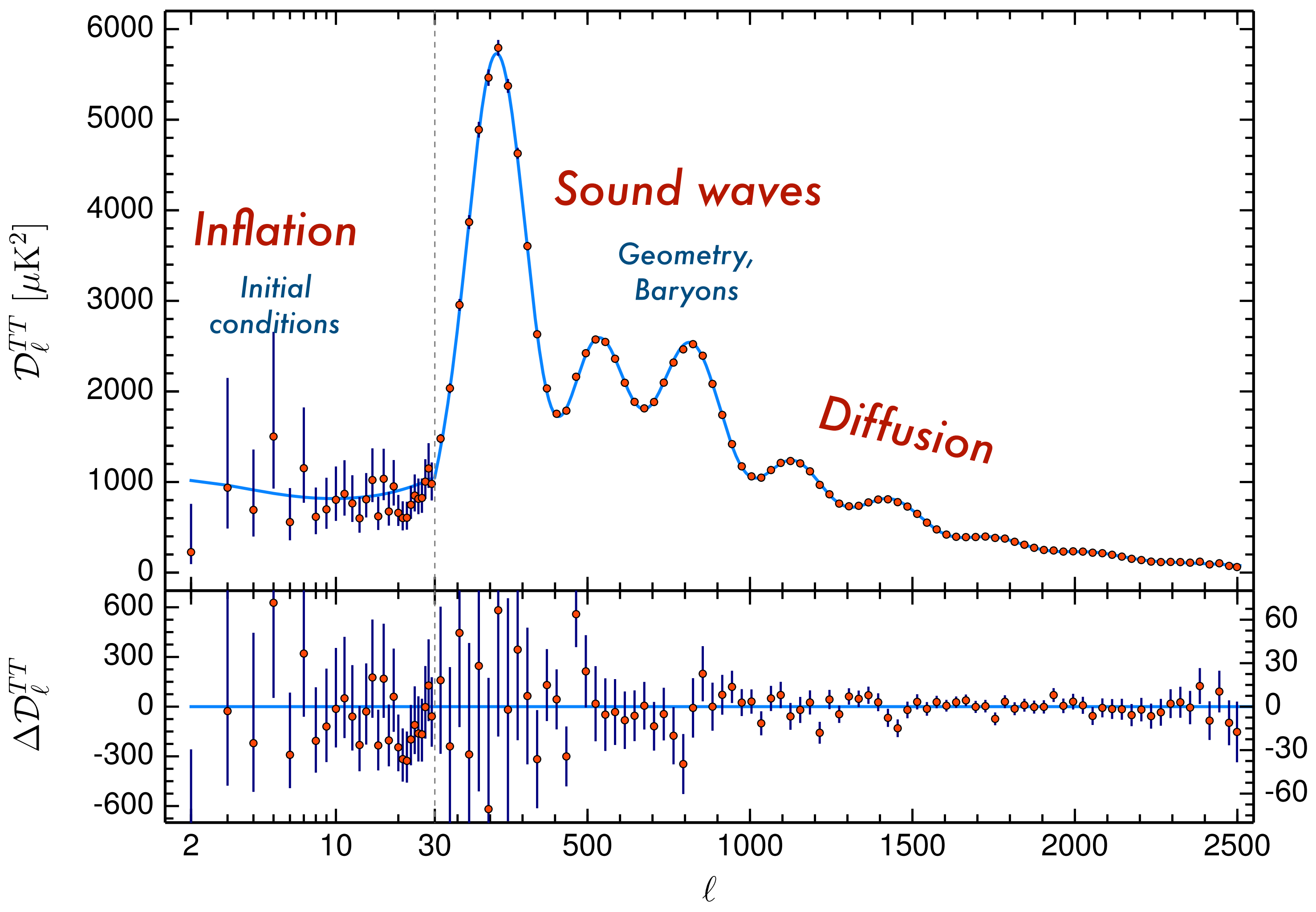

Parameter inference

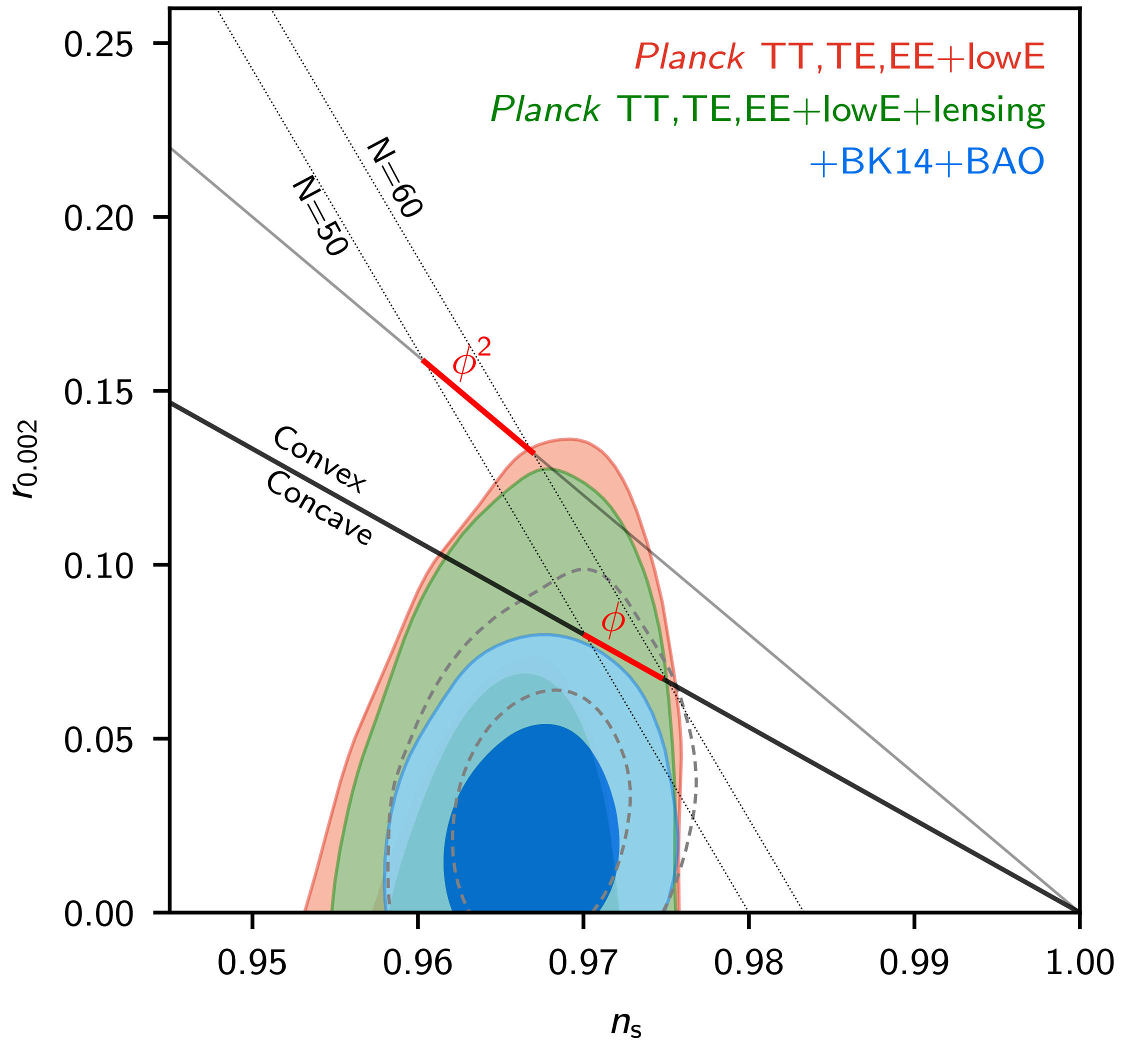

Can map of induced velocities/accelerations due to Galactic dark matter subhalos be analyzed the same way?

{ 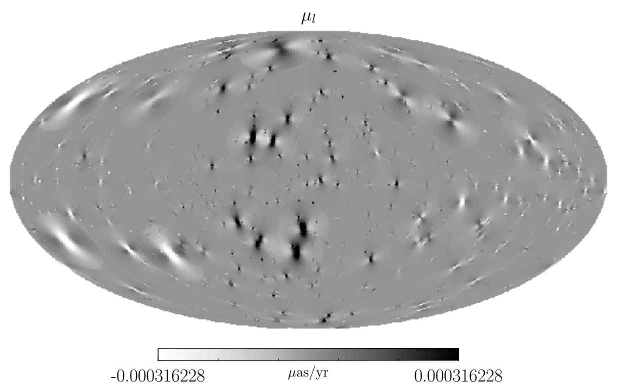 , 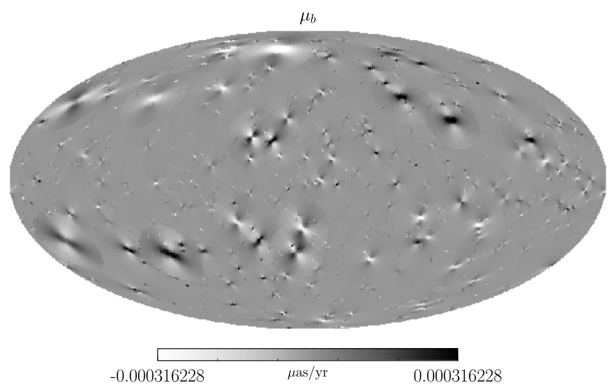 }

Angular Power Spectra 201: vector fields

Any vector field $\vec{\mu}(\hat{n})$ on a sphere can be expressed as a linear superposition of vector spherical harmonics $\vec{\Psi}_{\ell m}(\hat{n})$ and $\vec{\Phi}_{\ell m}(\hat{n})$

$$\vec{\mu}(\hat{n}) = \sum_{\ell m} \underbrace{\mu^{(1)}_{\ell m} \vec{\Psi}_{\ell m}(\hat{n})}_{(\nabla \times) = 0} + \underbrace{\mu^{(2)}_{\ell m} \vec{\Phi}_{\ell m}(\hat{n})}_{(\nabla \cdot) = 0}$$

$$\vec{\Psi}_{\ell m} = \nabla Y_{\ell m}$$
$$\vec{\Phi}_{\ell m} = \hat{n} \times \nabla Y_{\ell m}$$

Physically, corresponds to decomposing vector field in a curl-free and divergence-free part (*Helmholtz-Hodge decomposition*)

Application to lens-induced motions

The lensing deflection is "sourced" from the *gradient* of the gravitational potential

$$\overrightarrow{\Delta\theta} = \frac{2}{D_l}\vec{\nabla}_\theta \int \mathrm{d}z \Psi_G(\vec{r})$$

Induced deflection/velocity/acceleration fields have vanishing curl

$\nabla \times \{$ 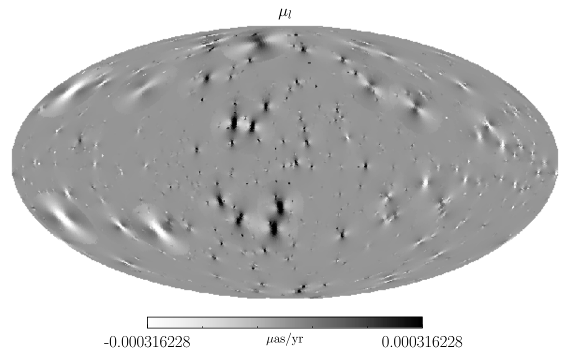 , 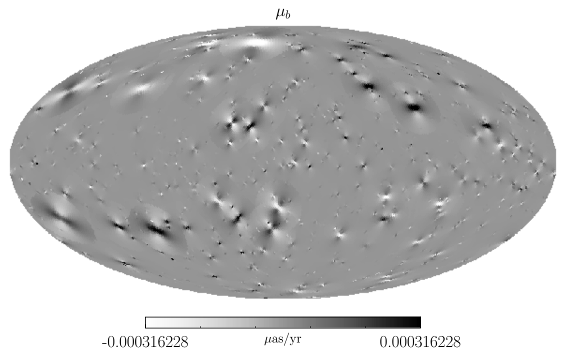 $\} \equiv 0$

Curl-free

$$C_\ell^{\mu(1)} \equiv \frac{1}{2\ell+1}\sum_{m=-\ell}^{\ell}\left|\mu_{\ell m}^{(1)}\right|^2 \simeq \sum_l \left(\frac{4G_N v}{D_l^2}\right)^2 \frac{\pi}{2}\ell(\ell+1)\left[\int_0^\infty \mathrm{d}\beta M\left(\beta D_l\right) J_1(\ell\beta)\right]^2$$

Divergence-free

$$C_\ell^{\mu(2)} \equiv \frac{1}{2\ell+1}\sum_{m=-\ell}^{\ell}\left|\mu_{\ell m}^{(2)}\right|^2 = 0$$

All vector lensing observables have only curl-free modes in harmonic decomposition

Cold dark matter

ΛCDM predicts a *broad, scale invariant* spectrum of subhalos distributed in the Milky Way

Credit: T. Brown and J.Tumlinson

Cold dark matter

ΛCDM predicts a *broad, scale invariant* spectrum of subhalos distributed in the Milky Way

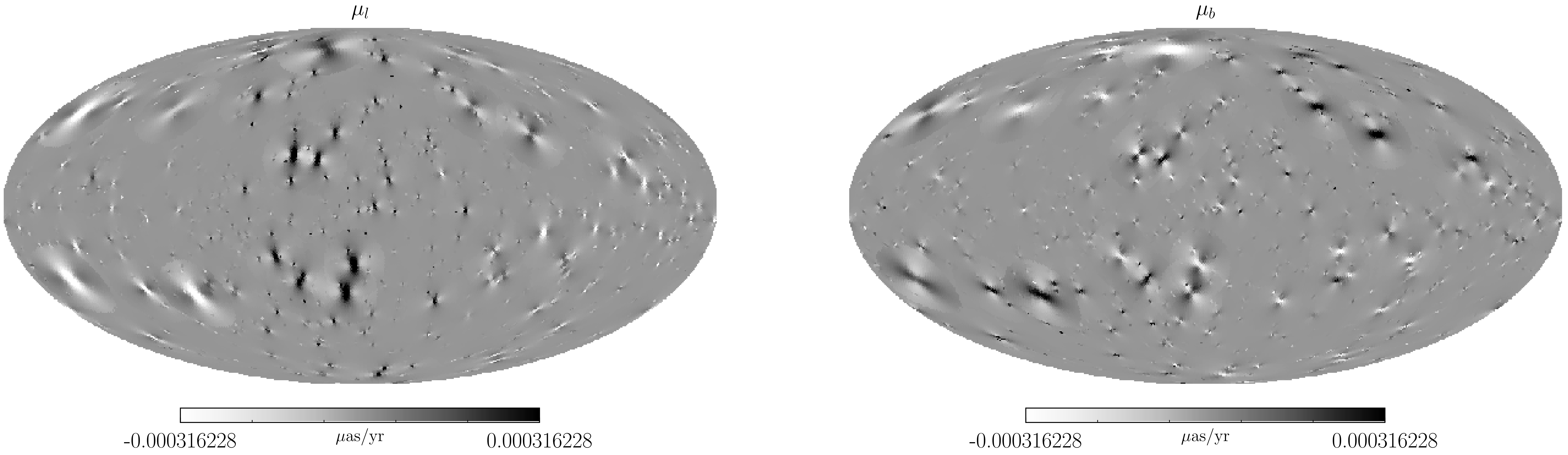

Cold dark matter: total signal and noise

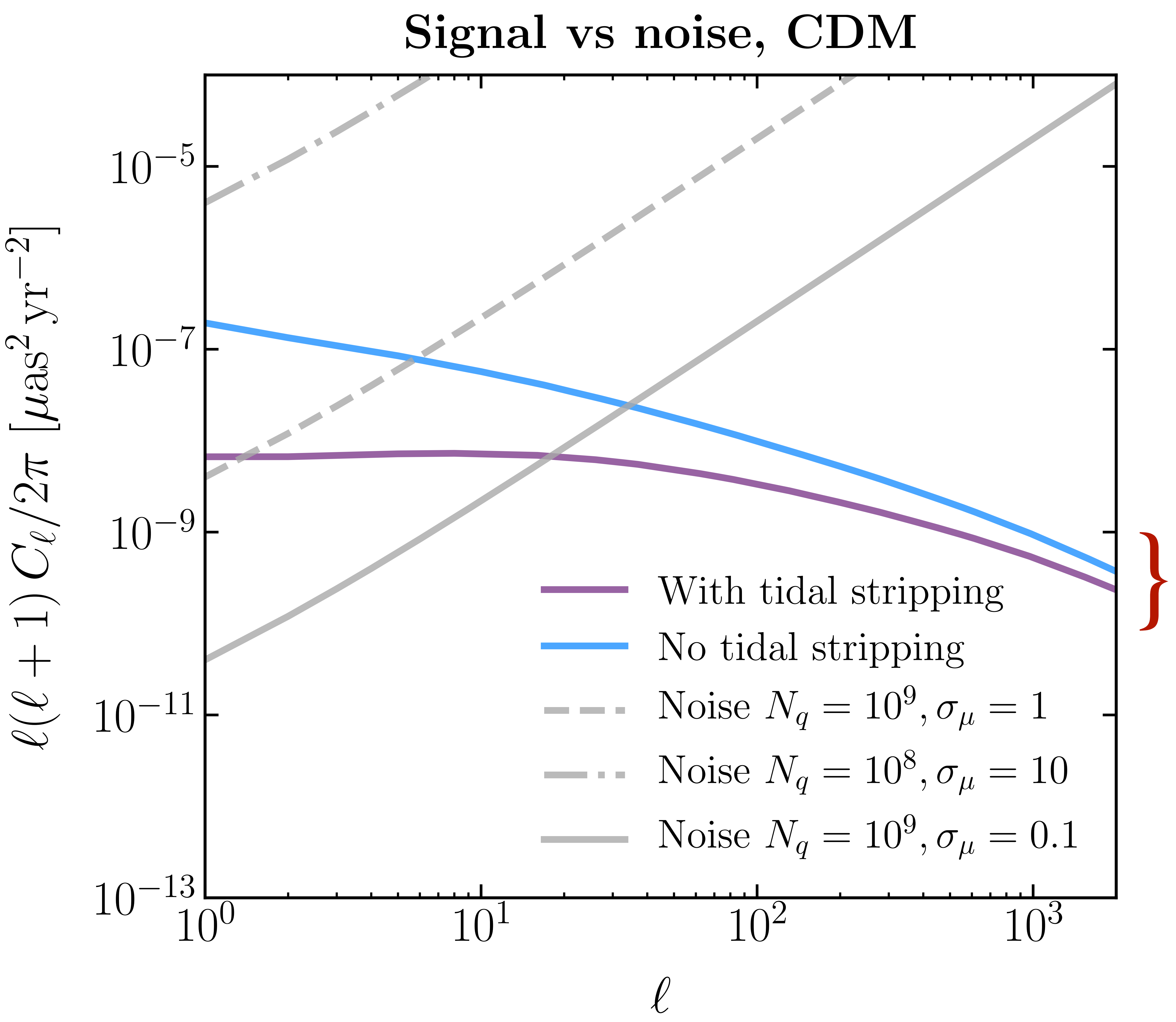

Account for tidal stripping by depleting massive subhalos closer to Galactic center

Brackets uncertainty on CDM halo properties

Tidal disruption may be numerical?

van den Bosch et al, "Disruption of Dark Matter Substructure: Fact or Fiction?", MNRAS [1711.05276]

Cold dark matter: discovery potential

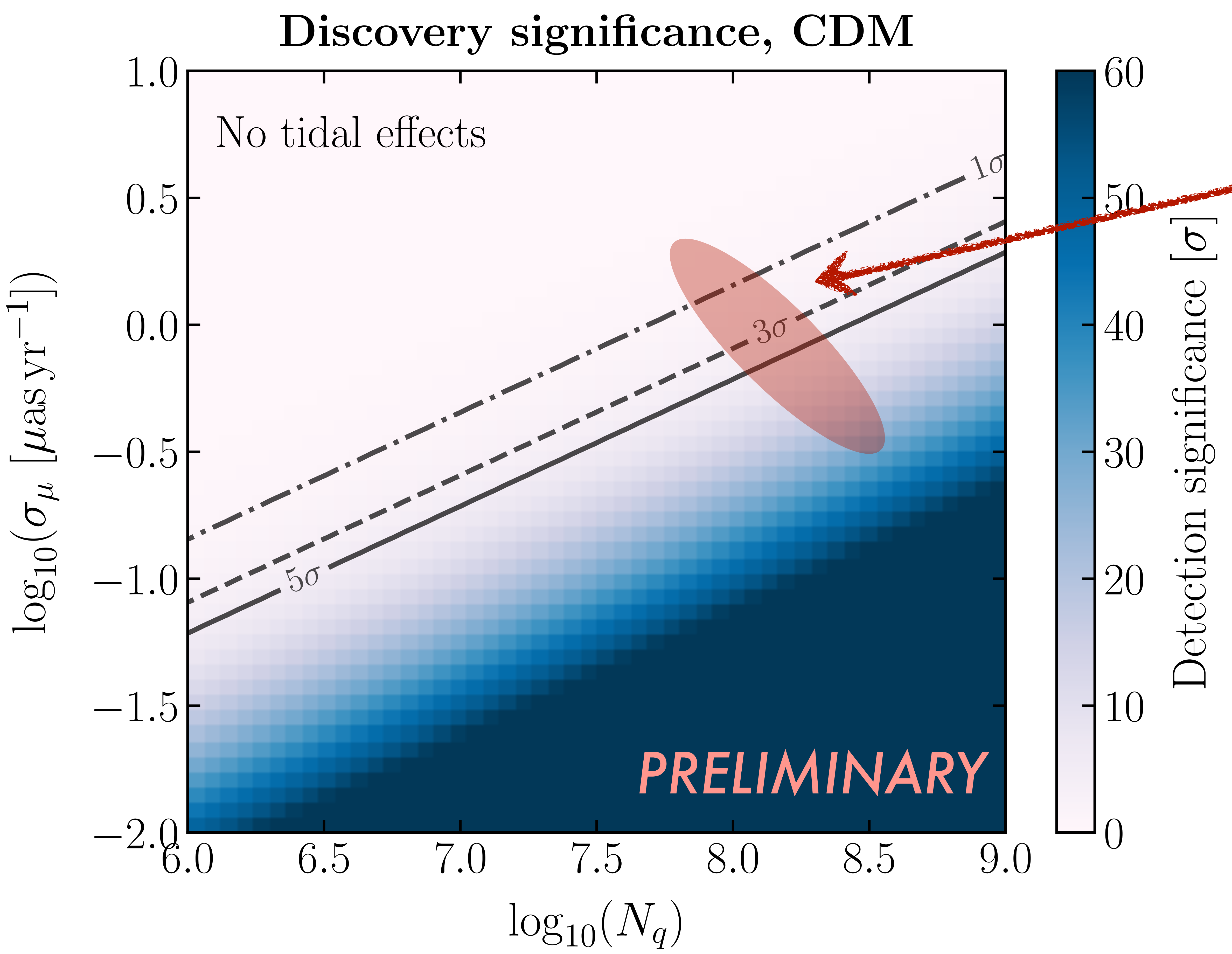

Anticipated noise levels with future surveys

Square Kilometer Array

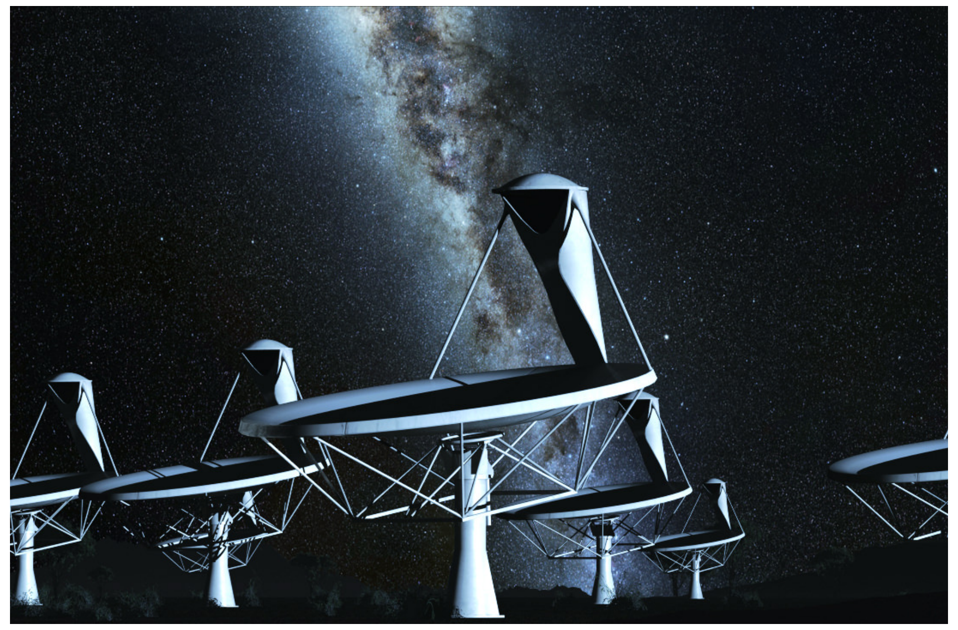

A CDM subhalo population can be detected!

Cold dark matter: discovery potential

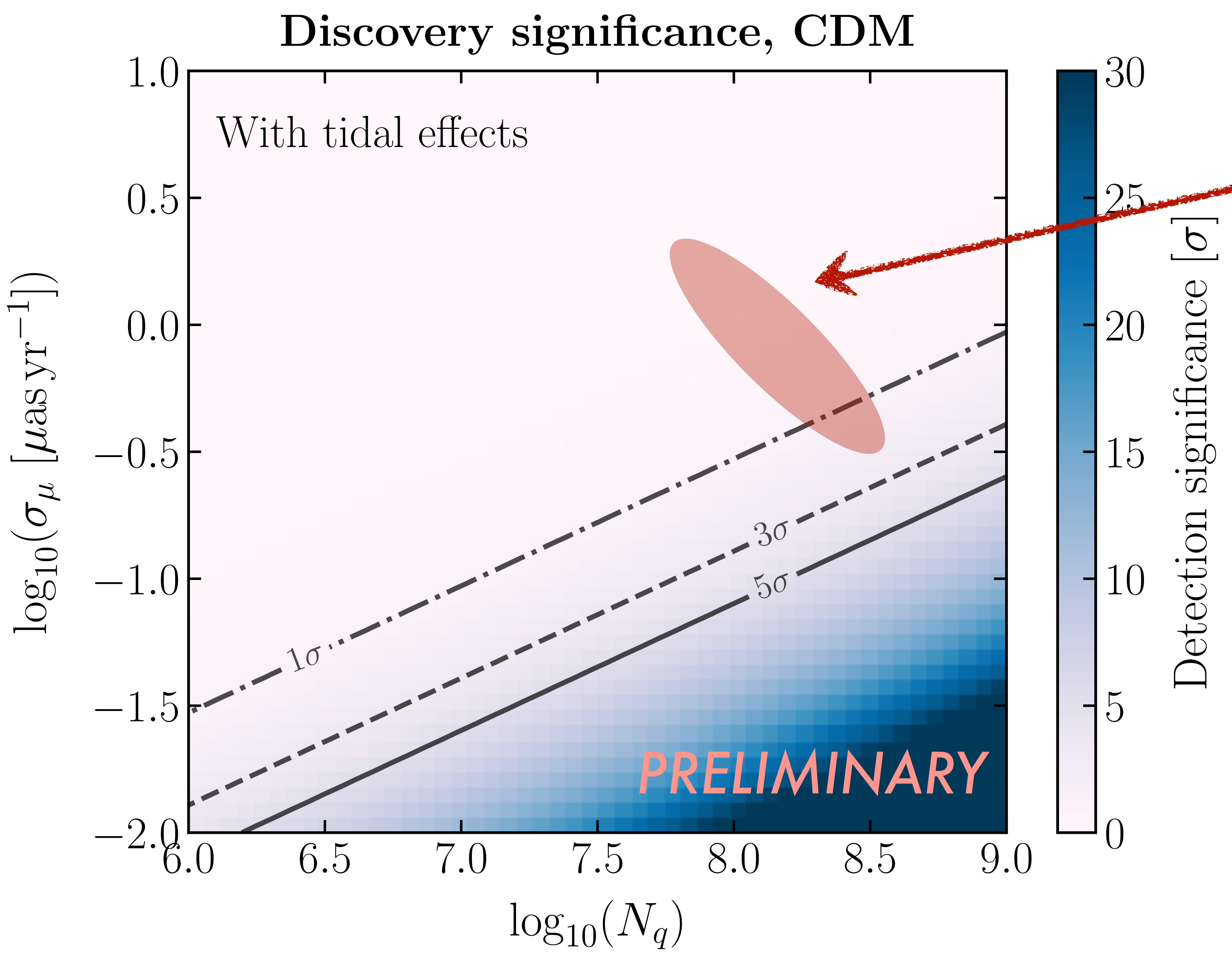

Anticipated noise levels with future surveys

Square Kilometer Array

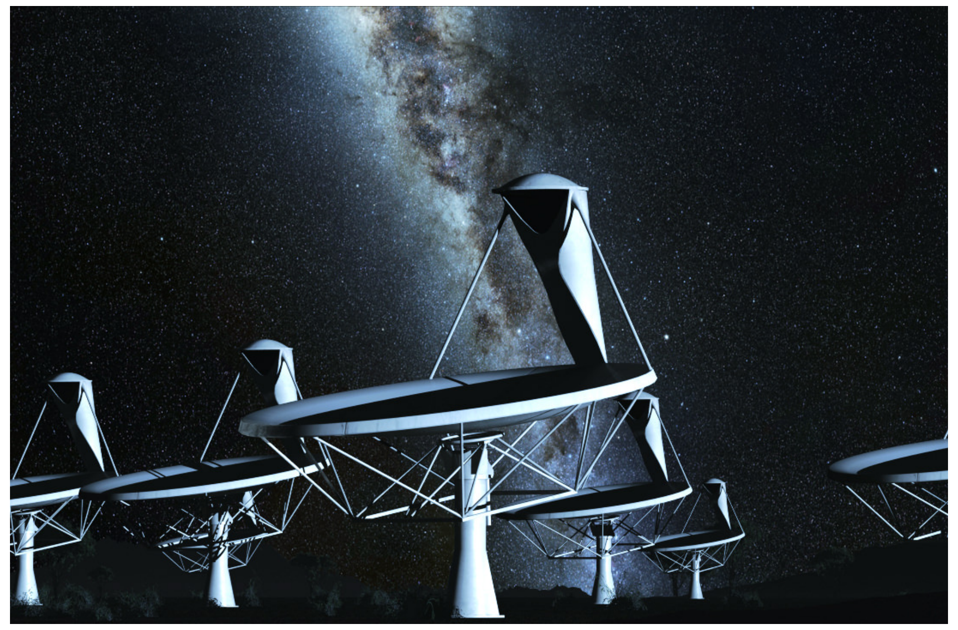

A CDM subhalo population can be detected!

But more difficult for a highly depleted population...

Summary

Astrometry + Gravitational Lensing

Apparent motions induced through gravitational lensing
offer a unique way to probe dark Galactic subhalo populations

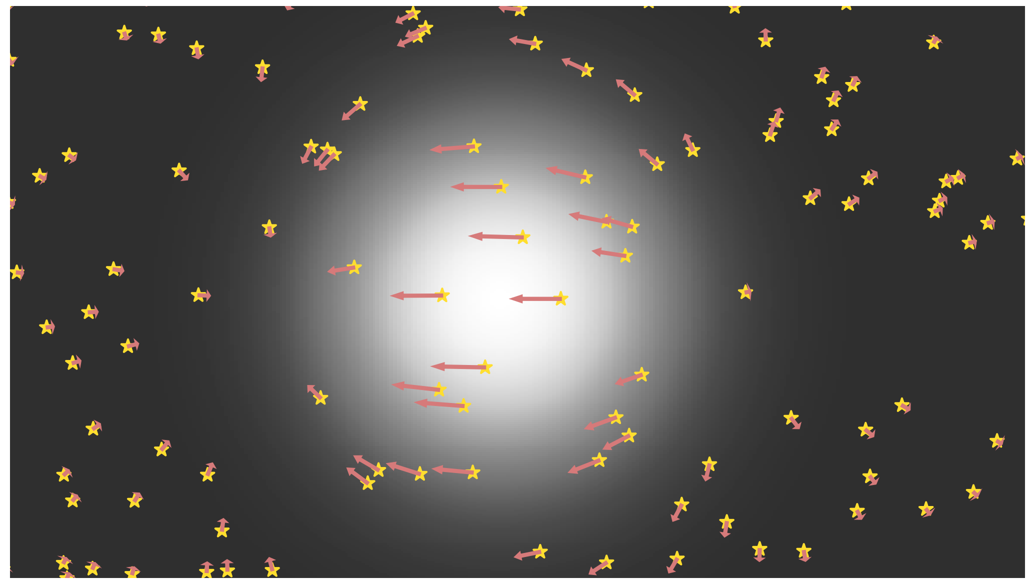

Angular Correlation Functions

Can be used as a tool to look for signatures
of substructure in astrometric data

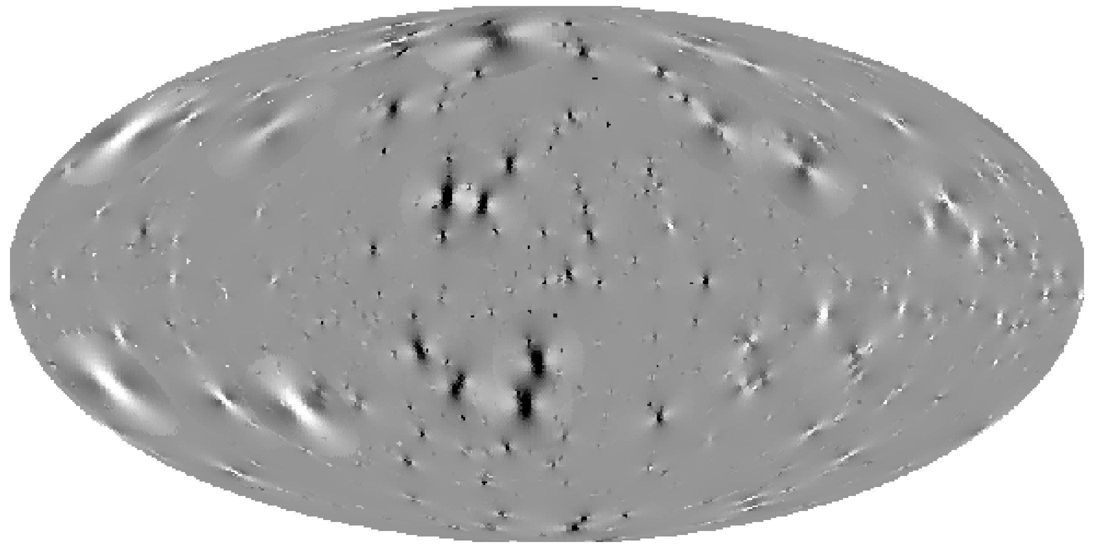

Discovering Substructure Populations

Methods potentially sensitive to cold dark matter,
(not so) compact objects, scalar field dark matter...

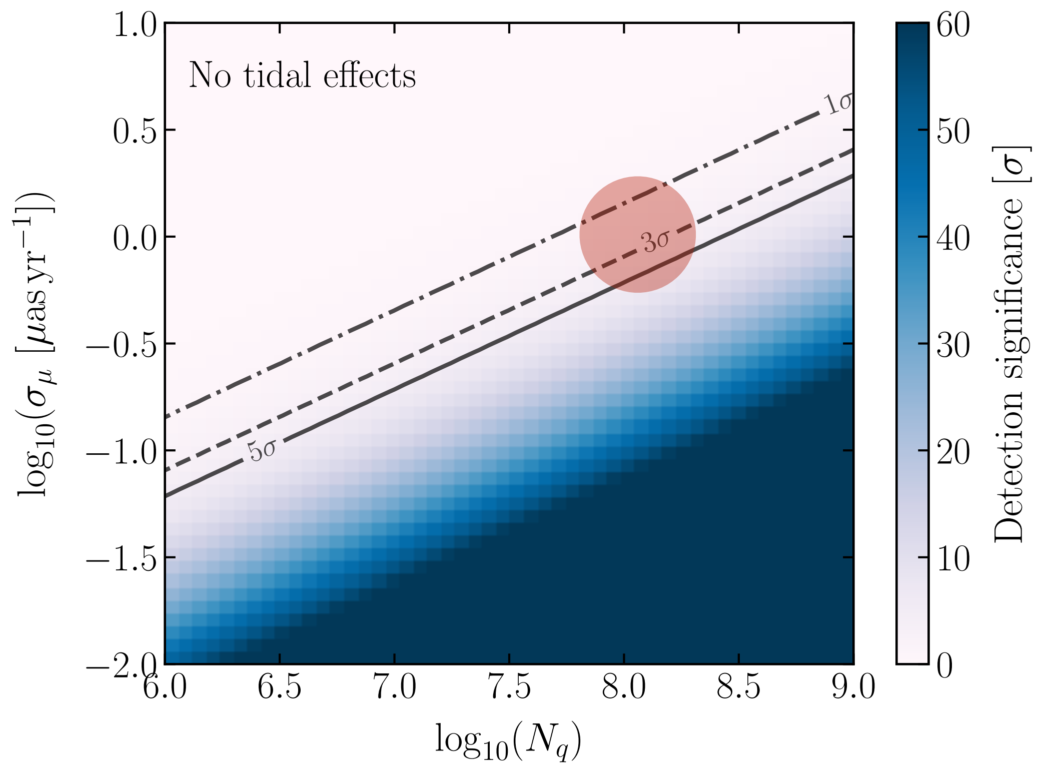

Backup Slides

Compact objects from primordial fluctuations

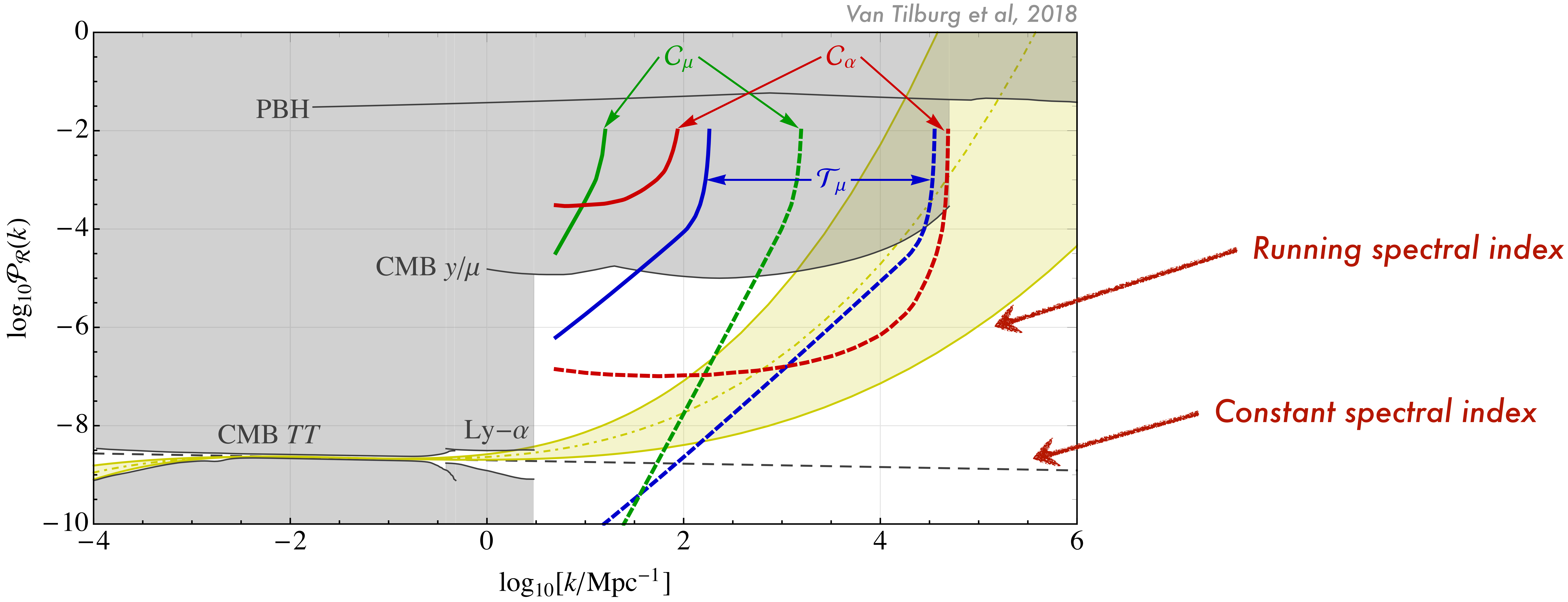

Enhancement in small-scale power is unconstrained and motivated —can have abundance of small clumps

Compact objects in the Milky Way: sensitivity projections

Sensitivity decreases approximately linearly with subhalo size

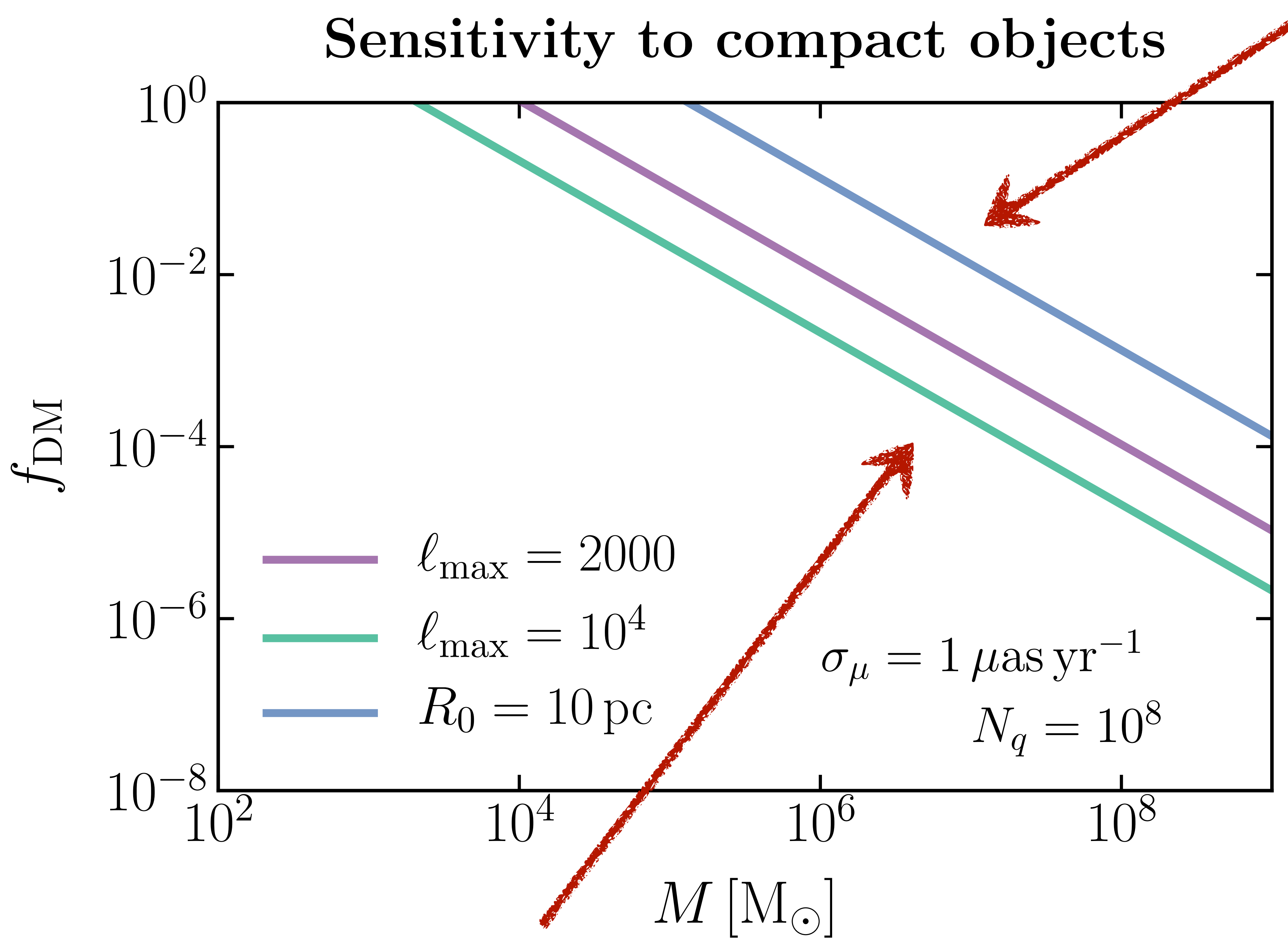

Sensitivity increases linearly with probing smaller scales

Compact objects in the Milky Way: sensitivity projections

Sensitivity decreases approximately linearly with subhalo size

10^{-22} *eV fuzzy dark matter*

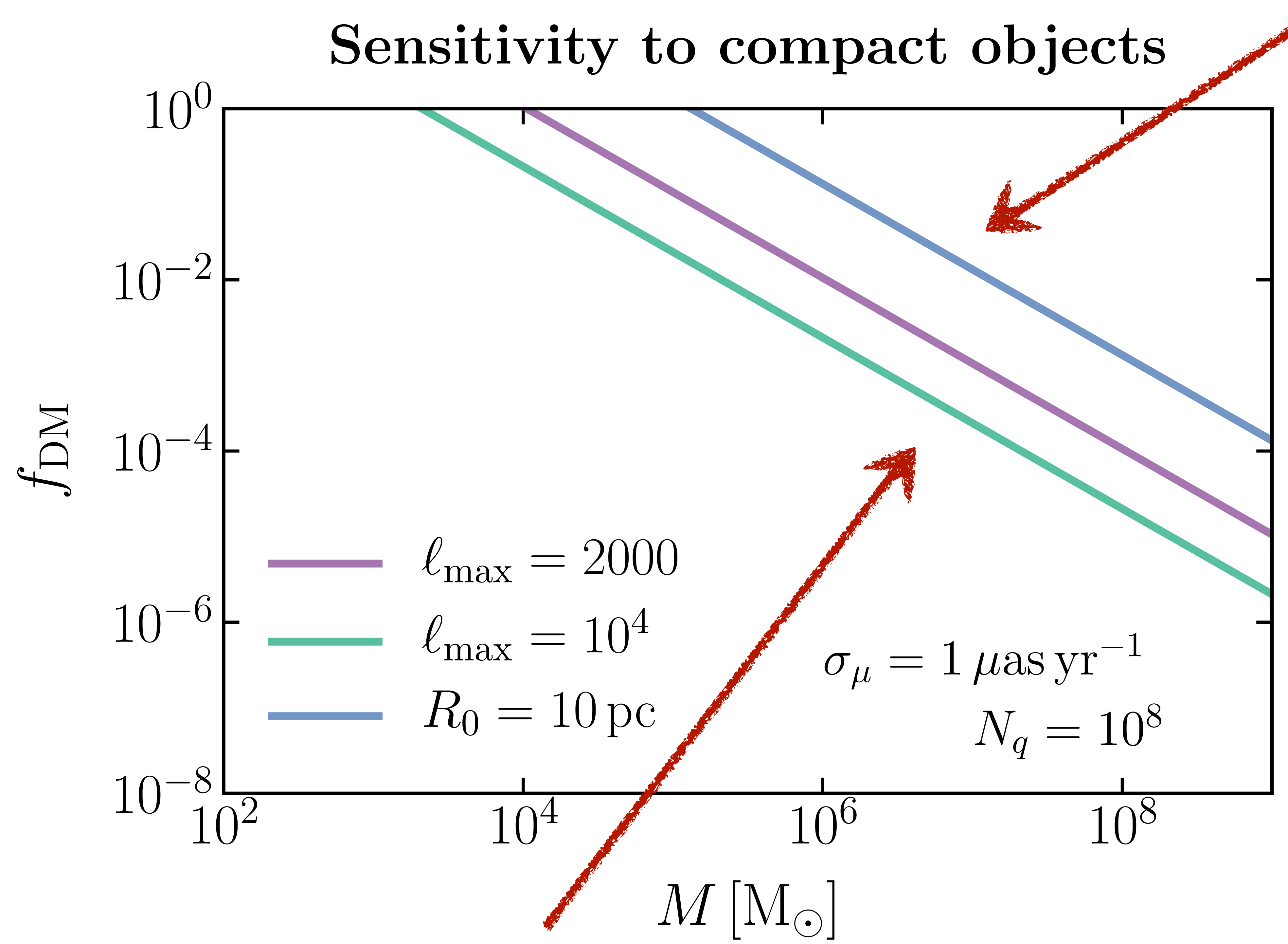

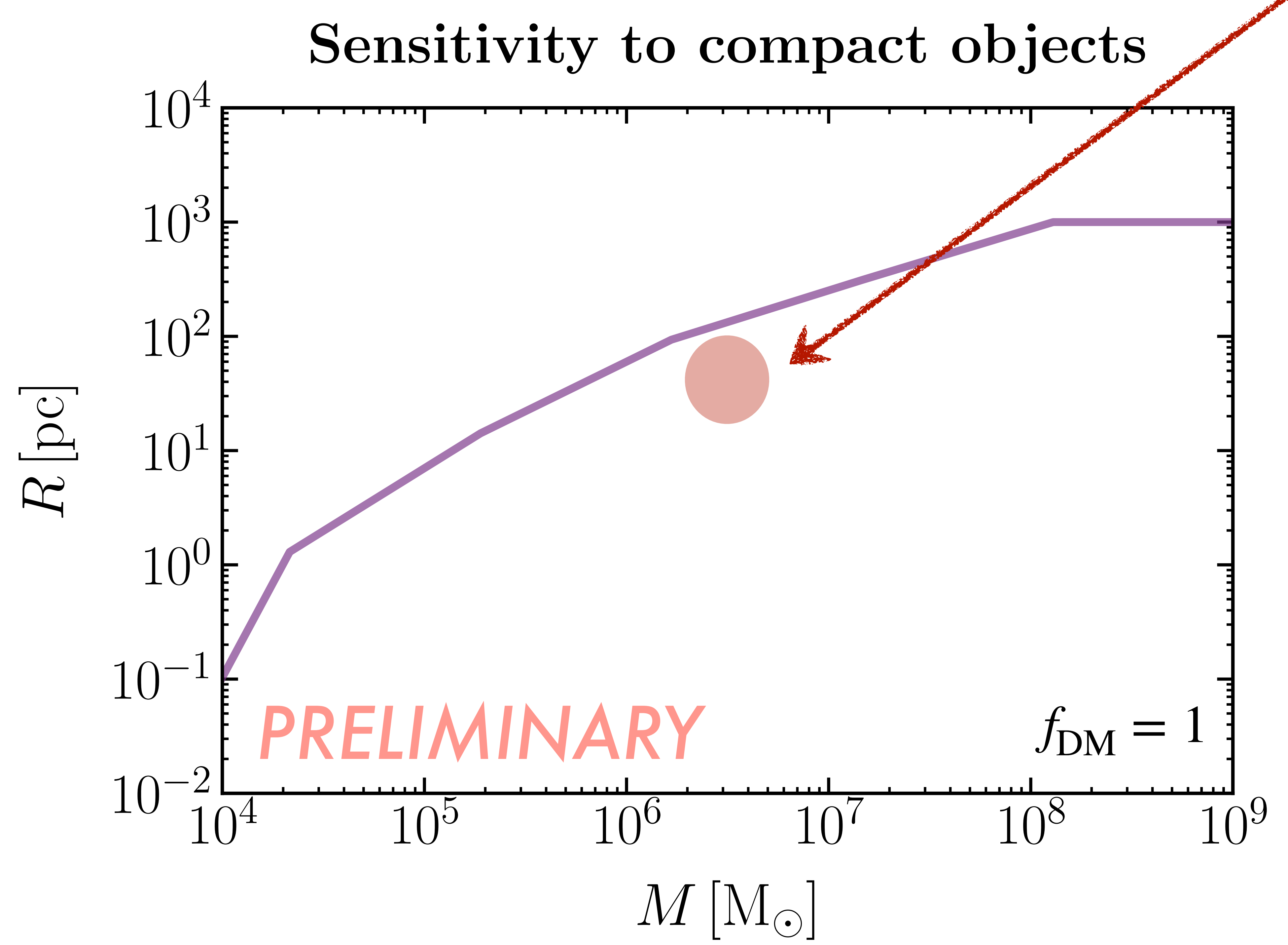

Sensitivity increases linearly with probing smaller scales

Relatively extended subhalos can be detected, unlike conventional searches

Complementary methods

[Bonaca, Hogg, Price-Whelan, Conroy]

(1) Gravitational perturbations (gaps and spurs) in cold stellar streams

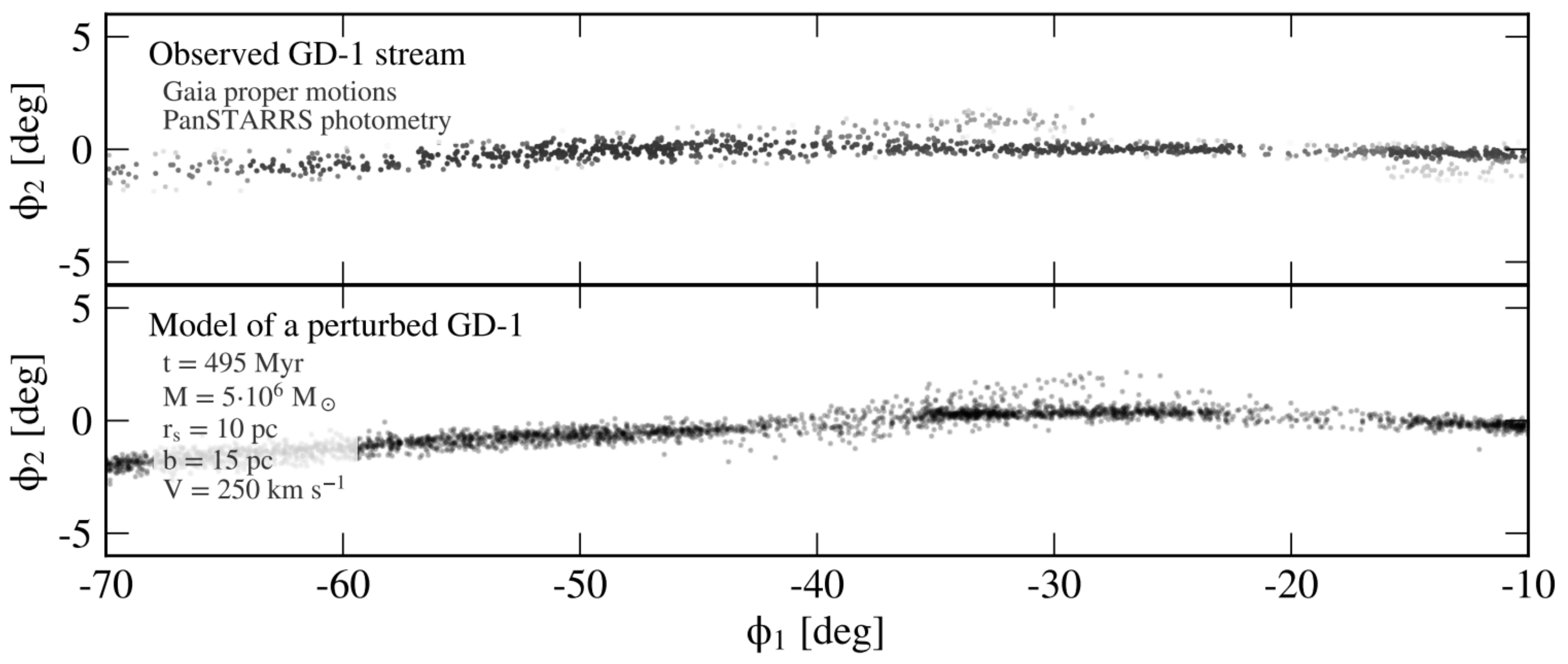

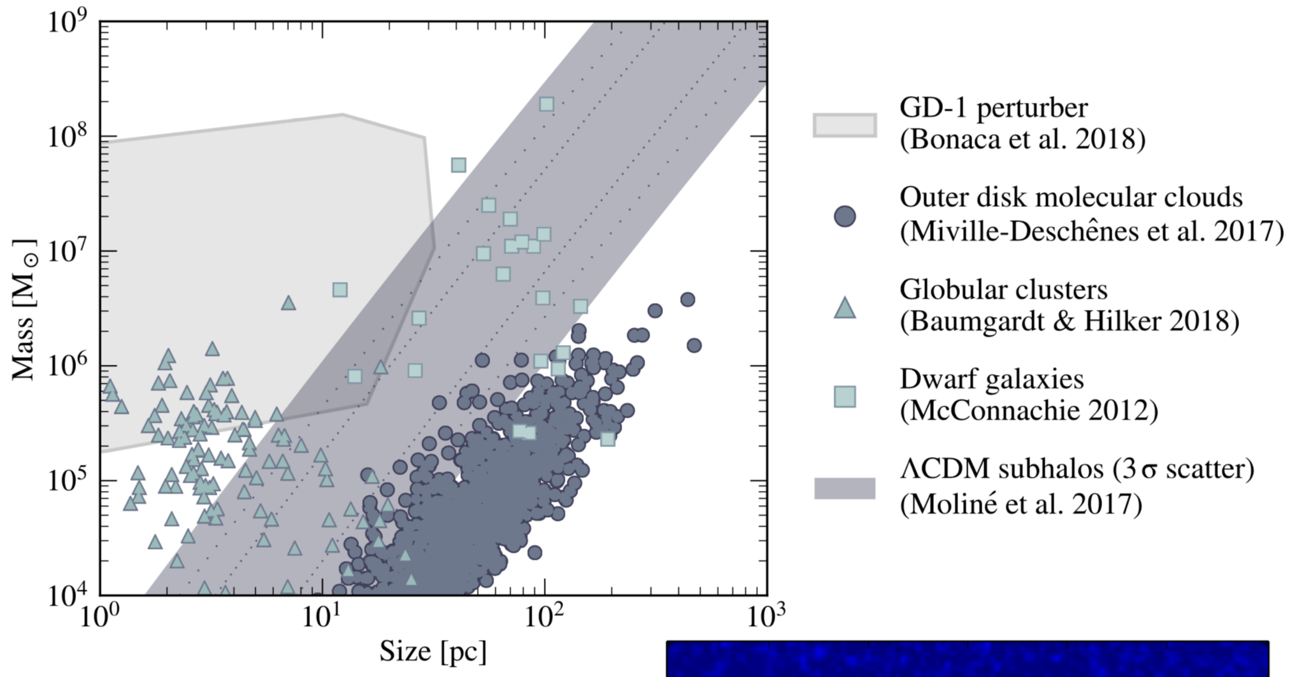

(2) Extragalactic strong gravitational lens systems on galactic scales:

[Mao, Schneider]

Flux-ratio anomalies in multiply-imaged quasars →

[Bayer +]

Surface-brightness perturbations in extended lensed emissions →

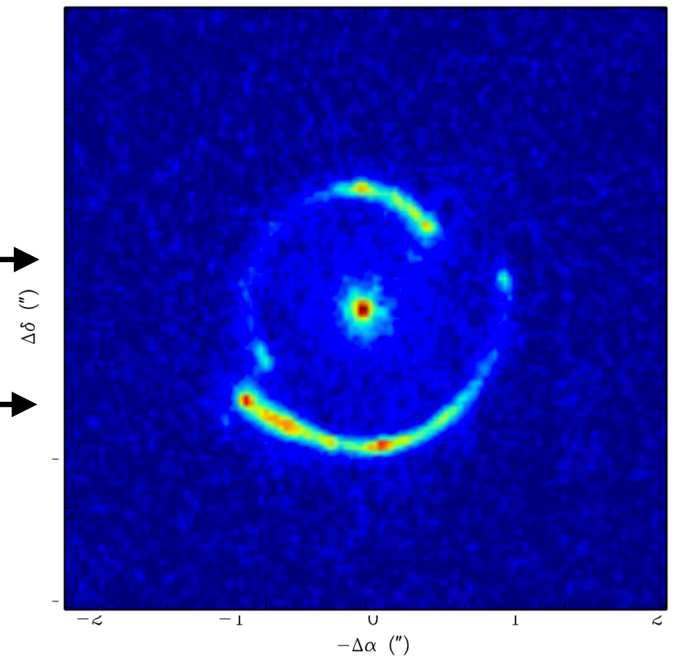

(3) Galactic macro- and micro-evolution constraints

Dynamical friction   Disruption of weakly bound stellar clusters

(4) Photometric microlensing

[Siegel, Hertzberg, Fry], [Baghram, Ashfordi, Zurek]

(5) Doppler and Shapiro effects in pulsar timing arrays

(4,5) (5) (4,5) (1,2,3)

direct, statistics-limited, low mass, low density

Astrometry

Repeatedly measure positions of celestial objects (stars, galaxies…) to get distances (through *parallax*) as well as time-domain information (velocities, accelerations)

$\boldsymbol{\theta}_i(t_n) \longrightarrow$

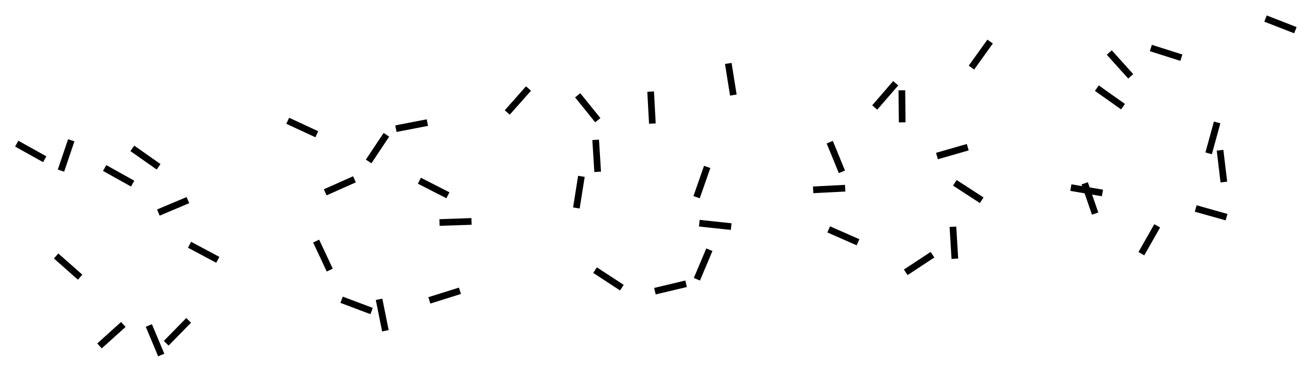

Gaia Satellite

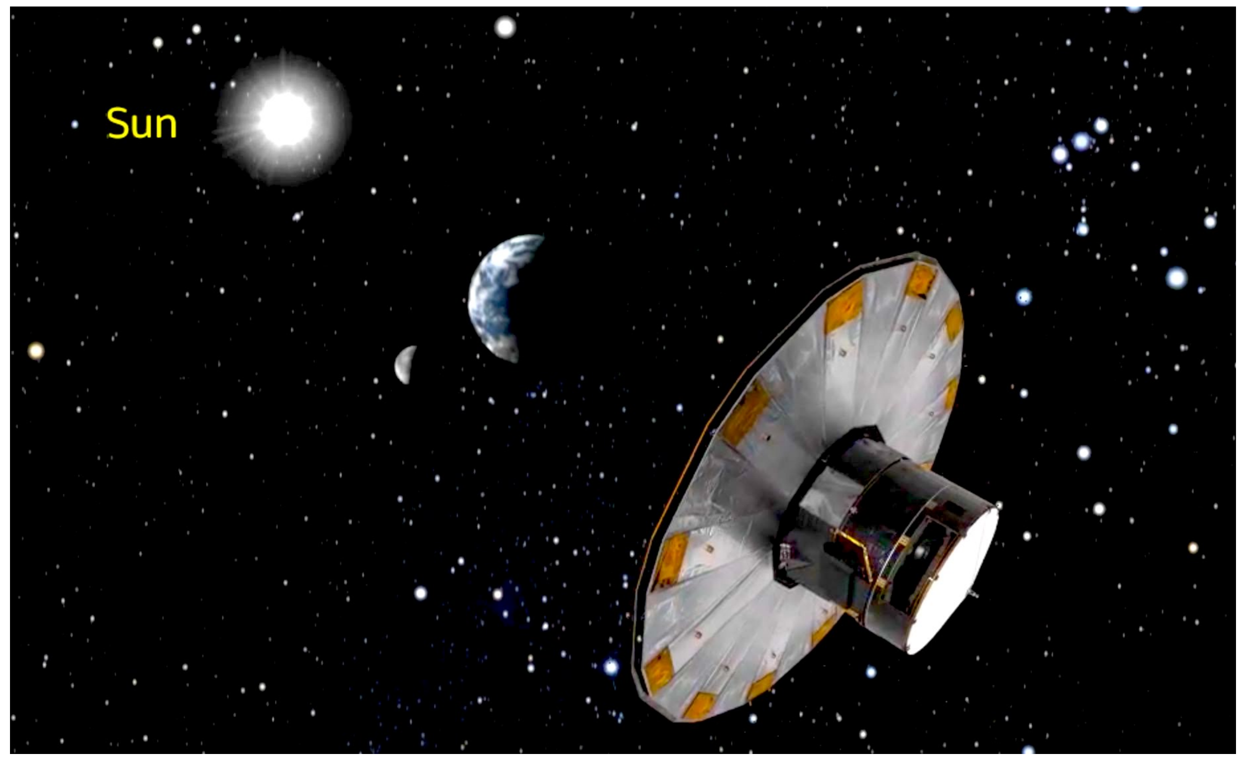

Credits: ESA

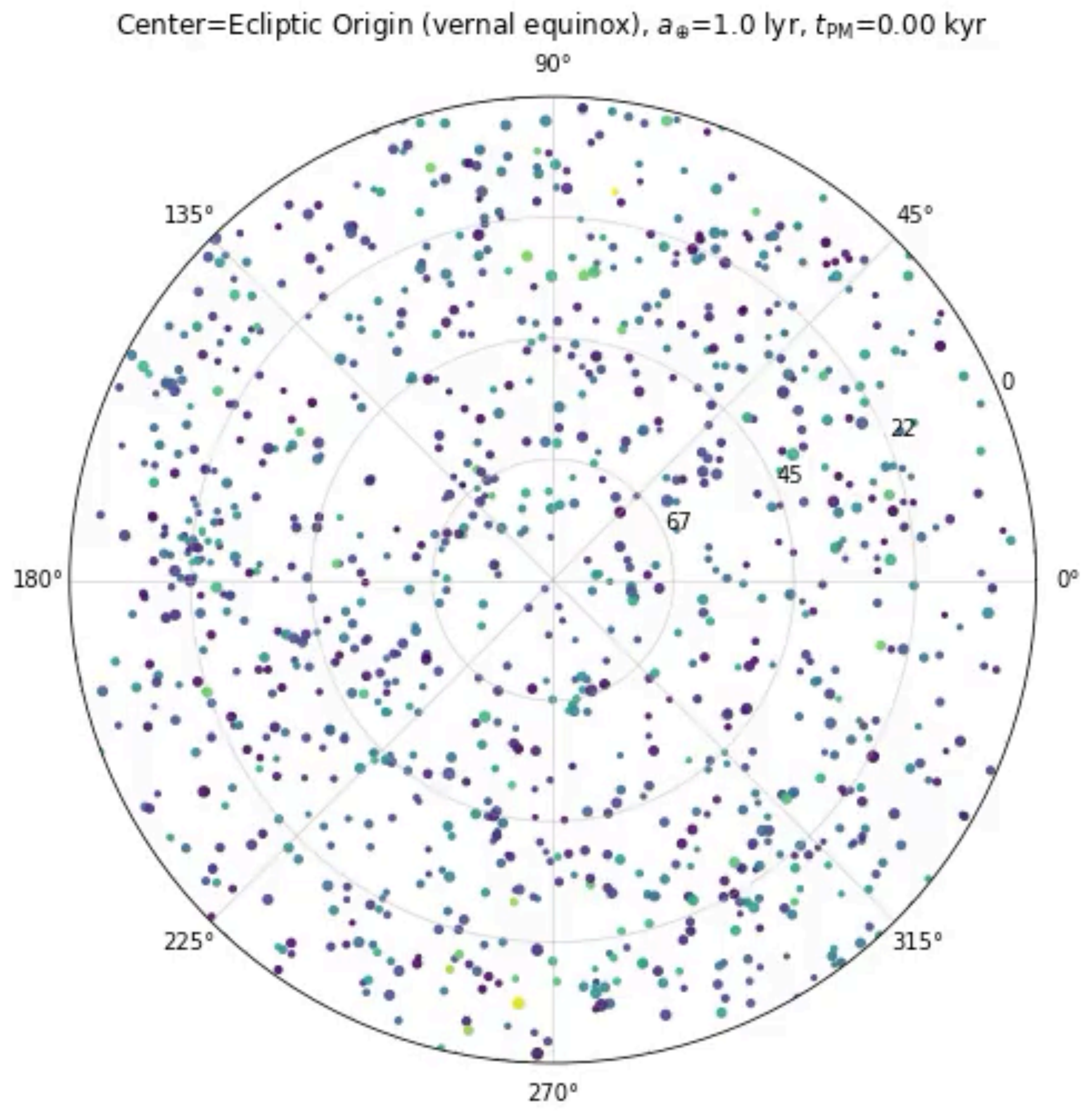

Credits: Erik Tollerud

https://gist.github.com/eteq/02a0065f15da3b3d8c2a9dea146a2a14

Astrometry

Repeatedly measure positions of celestial objects (stars, galaxies…) to get distances (through *parallax*) as well as time-domain information (velocities, accelerations)

$$\boldsymbol{\theta}_i(t_n) \longrightarrow$$

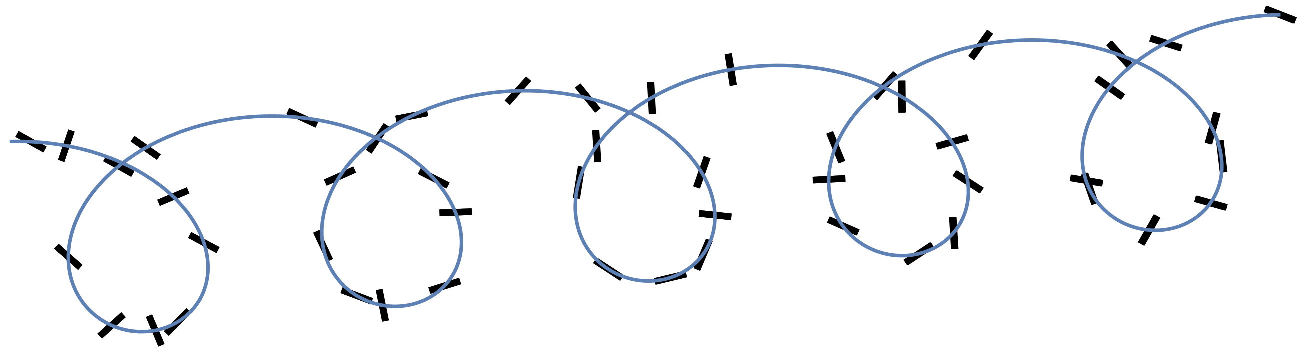

$$\longrightarrow \bar{\boldsymbol{\theta}}_i, \bar{\boldsymbol{\mu}}_i, \frac{\varpi_i}{\mathrm{mas}} = \frac{\mathrm{kpc}}{D_i}$$

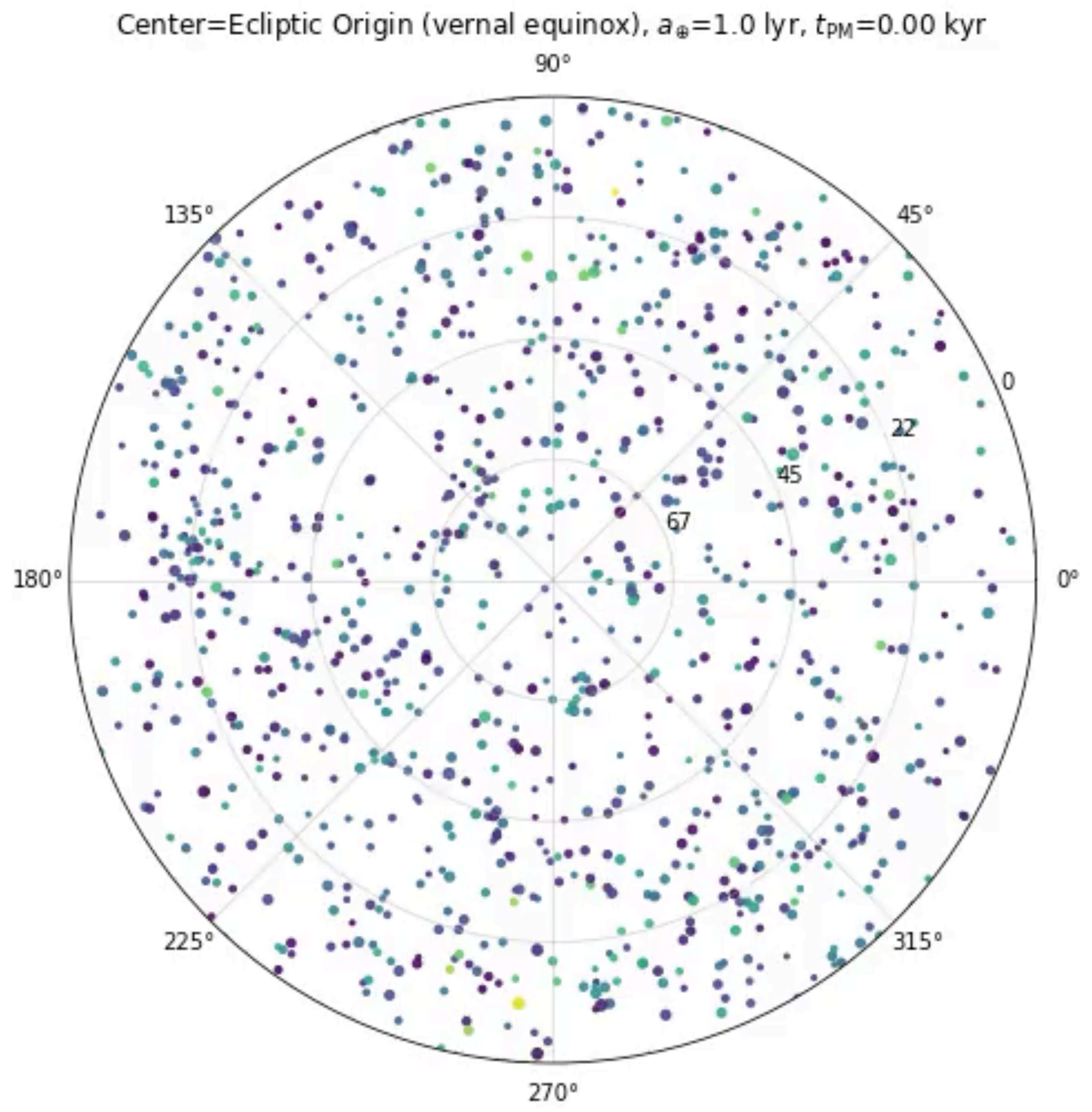

Credits: Erik Tollerud

https://gist.github.com/eteq/02a0065f15da3b3d8c2a9dea146a2a14

Gaia Satellite

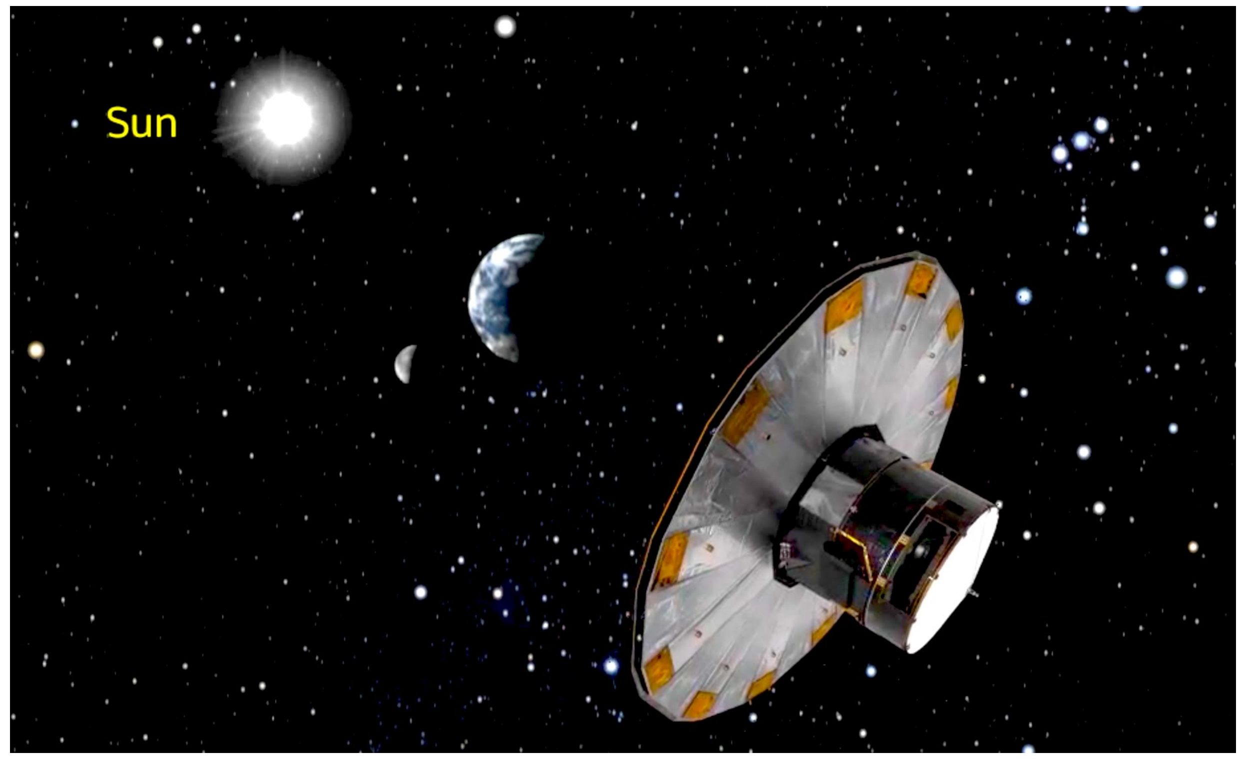

Credits: ESA

Astrometry

Repeatedly measure positions of celestial objects (stars, galaxies...) to get distances (through *parallax*) as well as time-domain information (velocities, accelerations)

$\boldsymbol{\theta}_i(t_n) \longrightarrow$

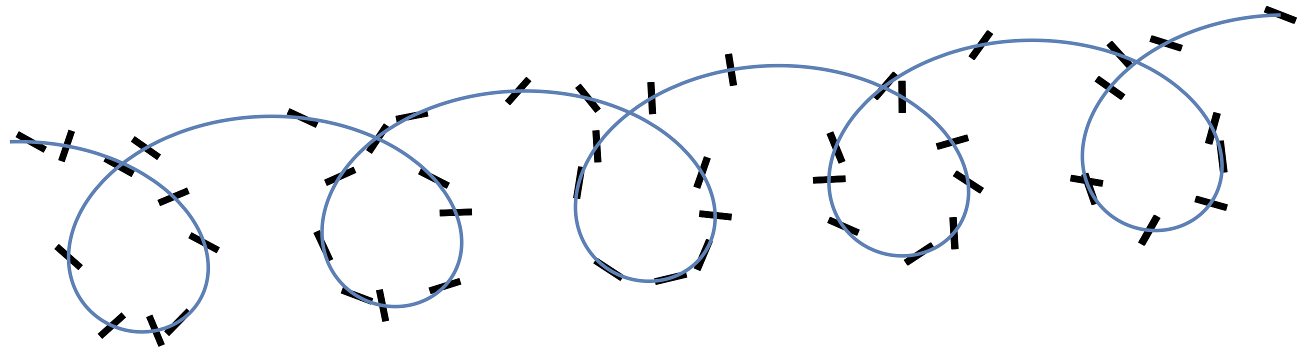

$\longrightarrow \bar{\boldsymbol{\theta}}_i, \bar{\boldsymbol{\mu}}_i, \frac{\varpi_i}{\mathrm{mas}} = \frac{\mathrm{kpc}}{D_i}$

Gaia Satellite

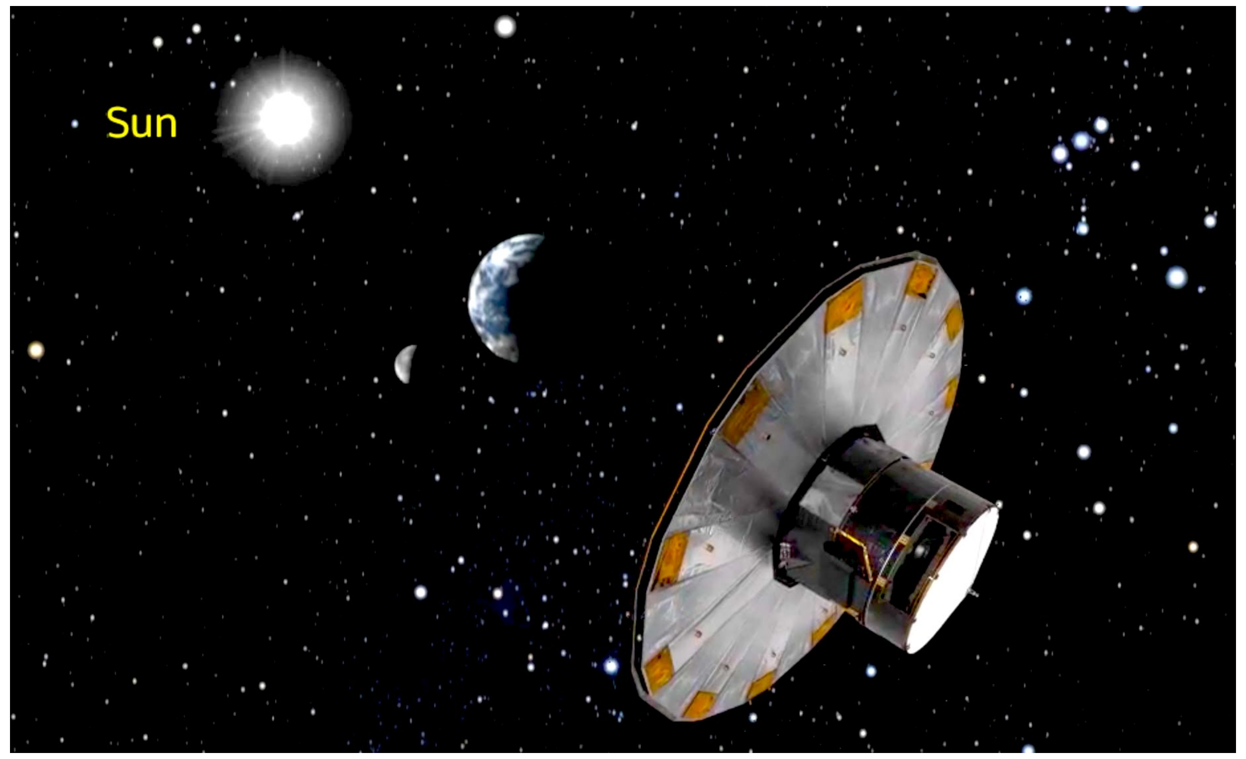

Credits: ESA

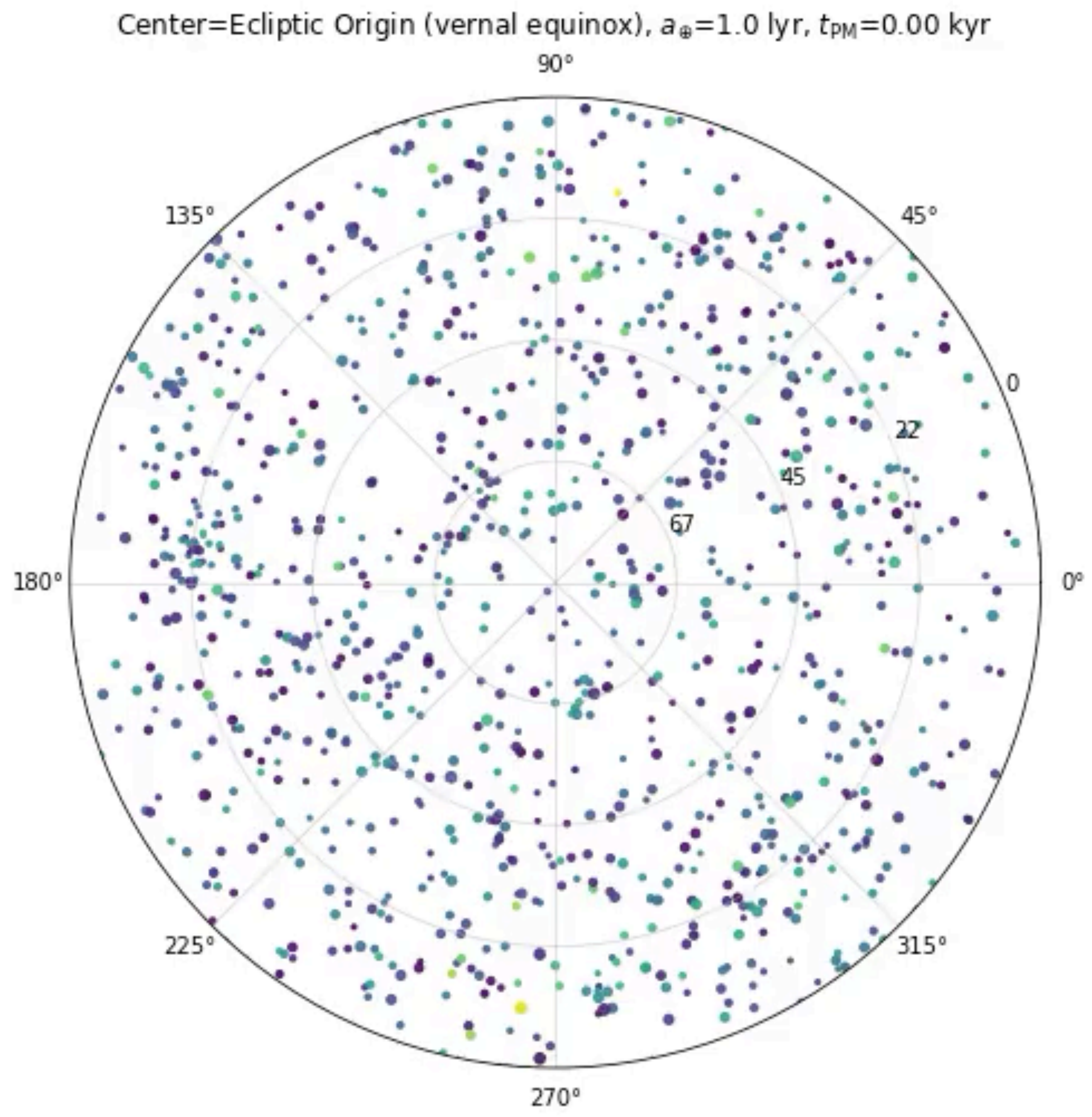

Credits: Erik Tollerud
https://gist.github.com/eteq/02a0065f15da3b3d8c2a9dea146a2a14

Gaia scanning law

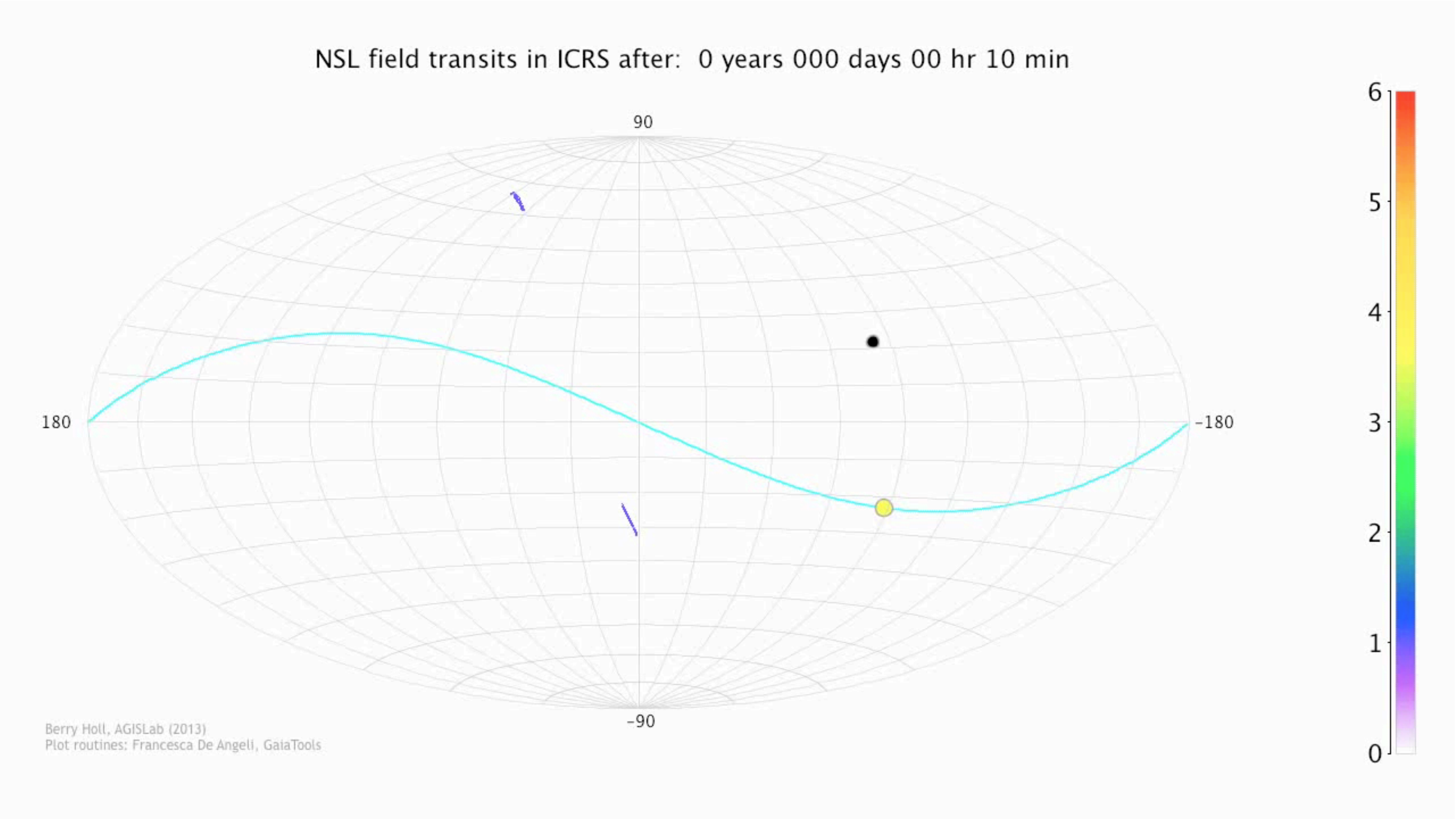

Gaia scanning law

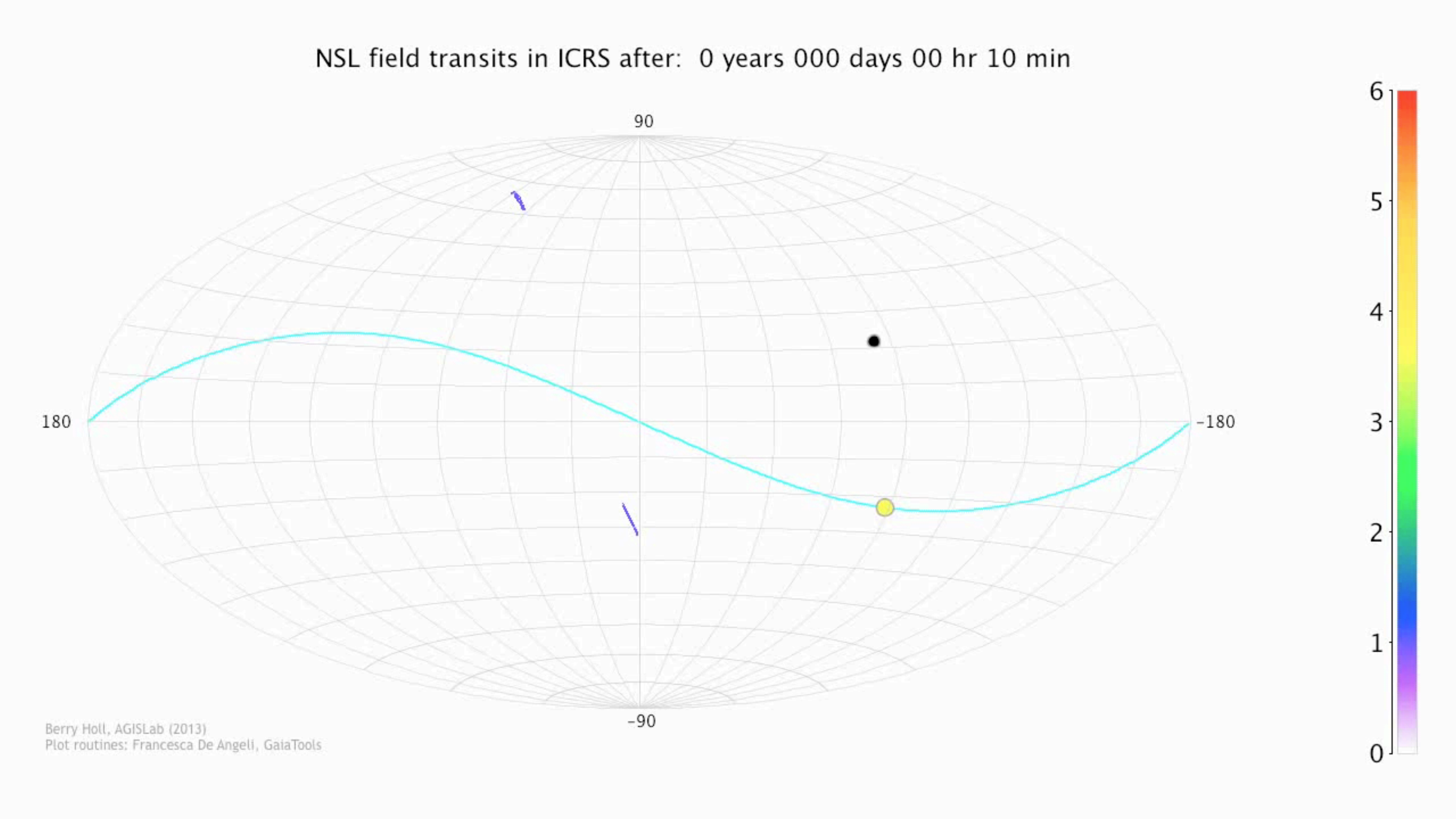

Astrometric precision of future surveys

Space-based, optical telescopes

Current: *Gaia, HST*

Future: *Theia*, WFIRST

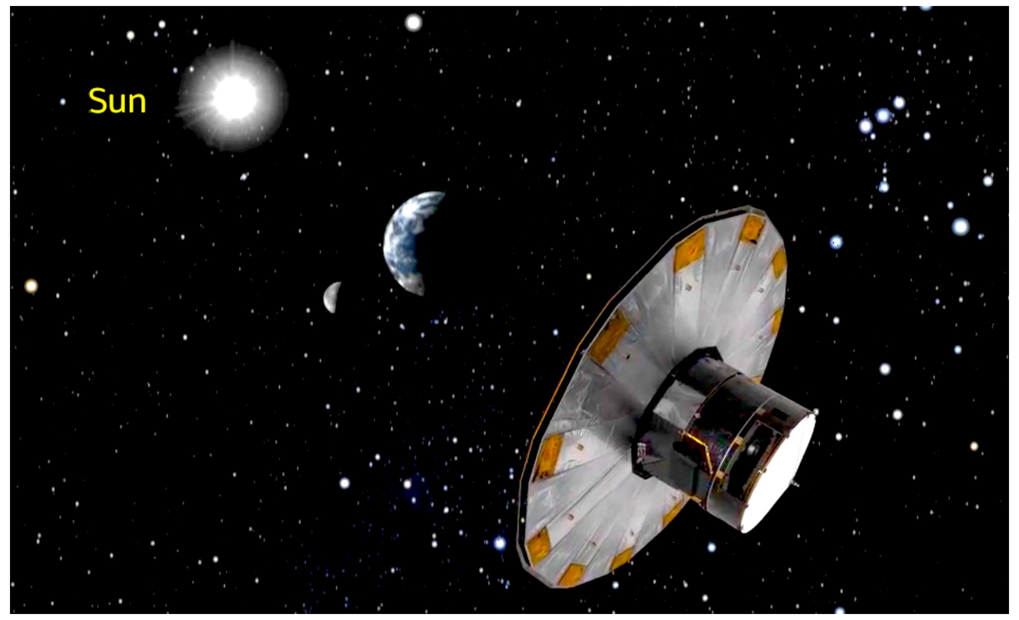

Ground-based, radio interferometry

Current: VLA (Very Large Array)

Future: SKA (Square Kilometer Array)

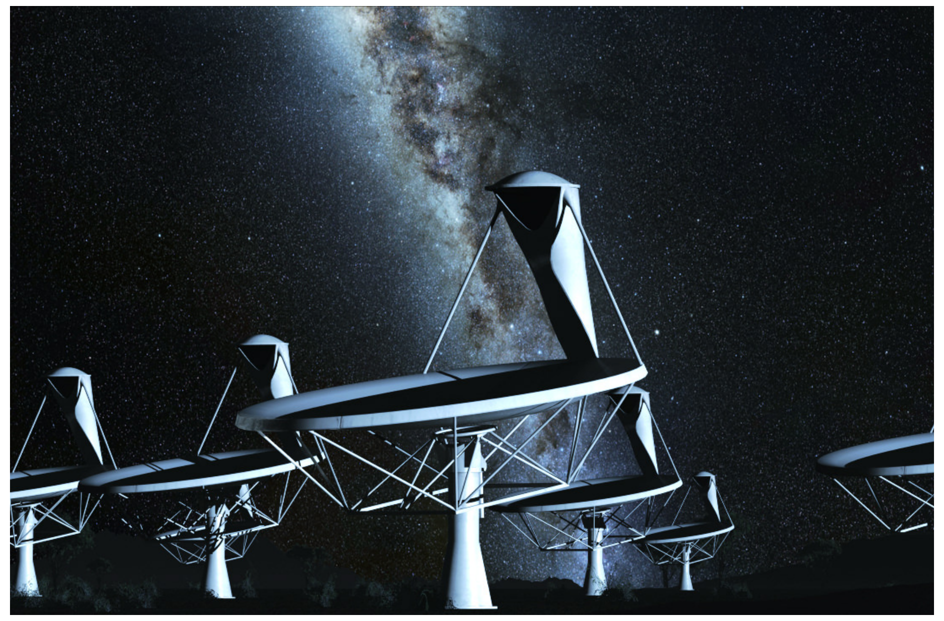

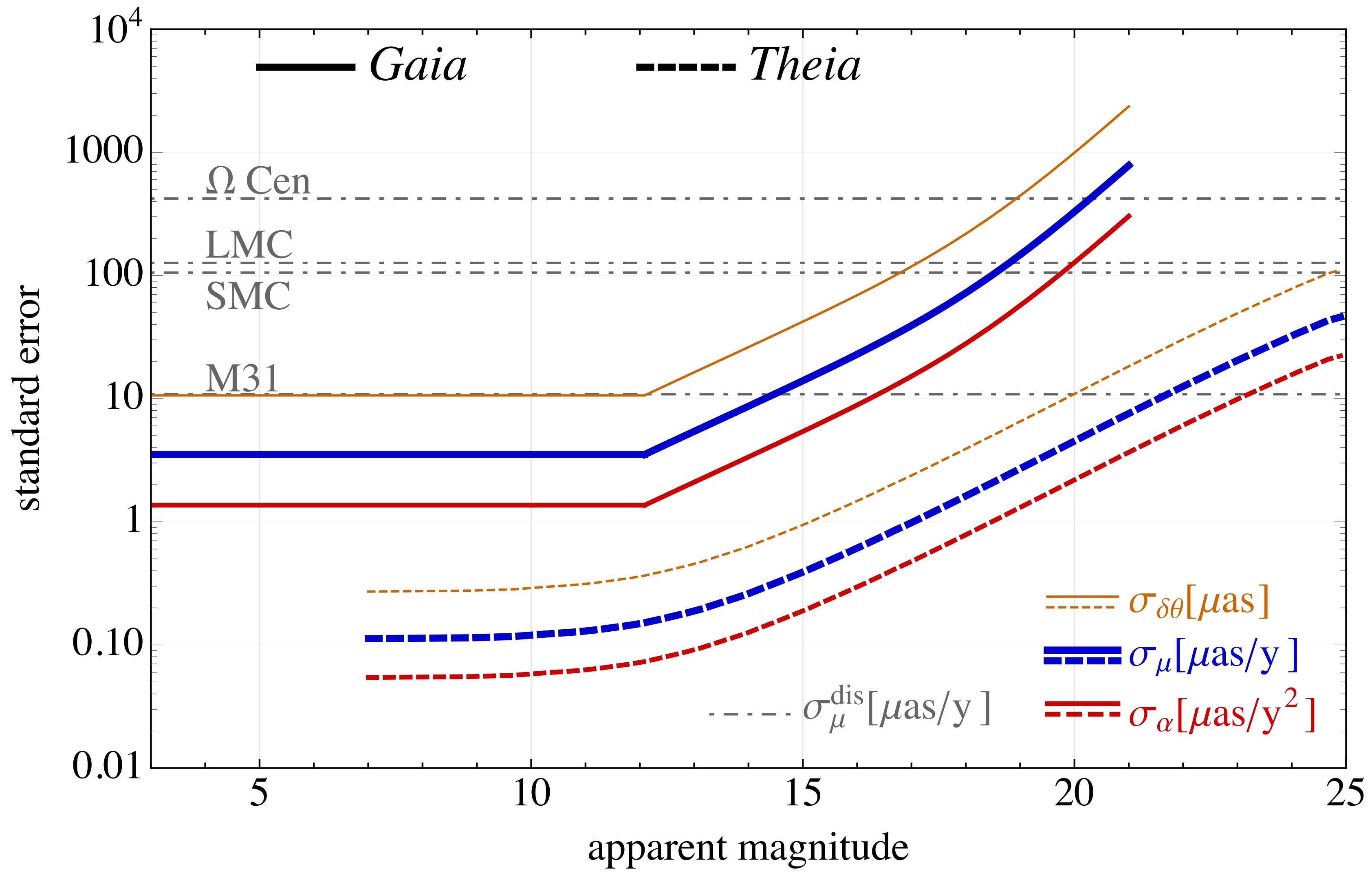

Baseline noise configuration

$$\sigma_\mu = 1\,\mu\mathrm{as\,yr^{-1}}$$
$$N_q = 10^8$$
$$f_{\rm sky} = 1$$

The lensing signal: point lenses

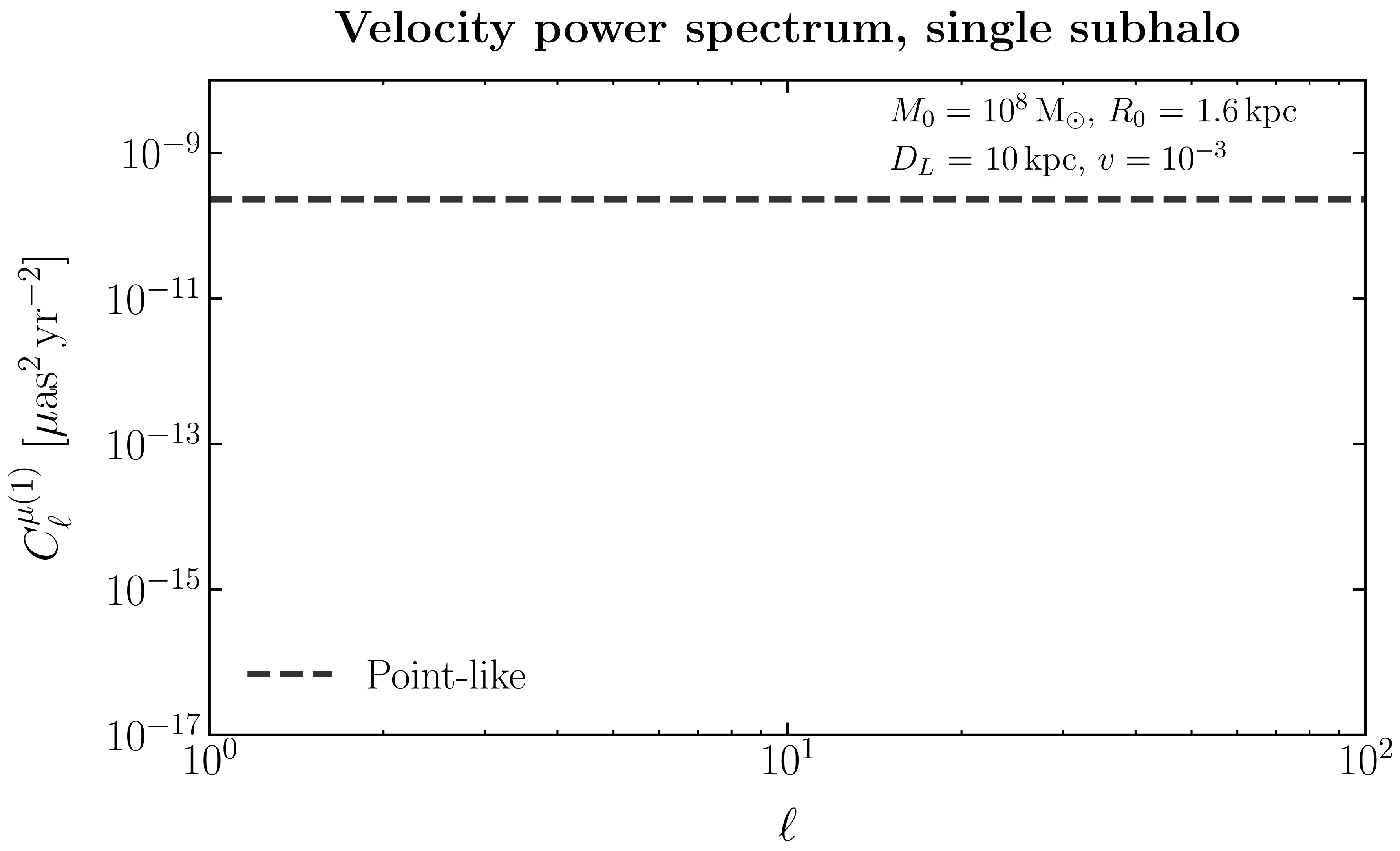

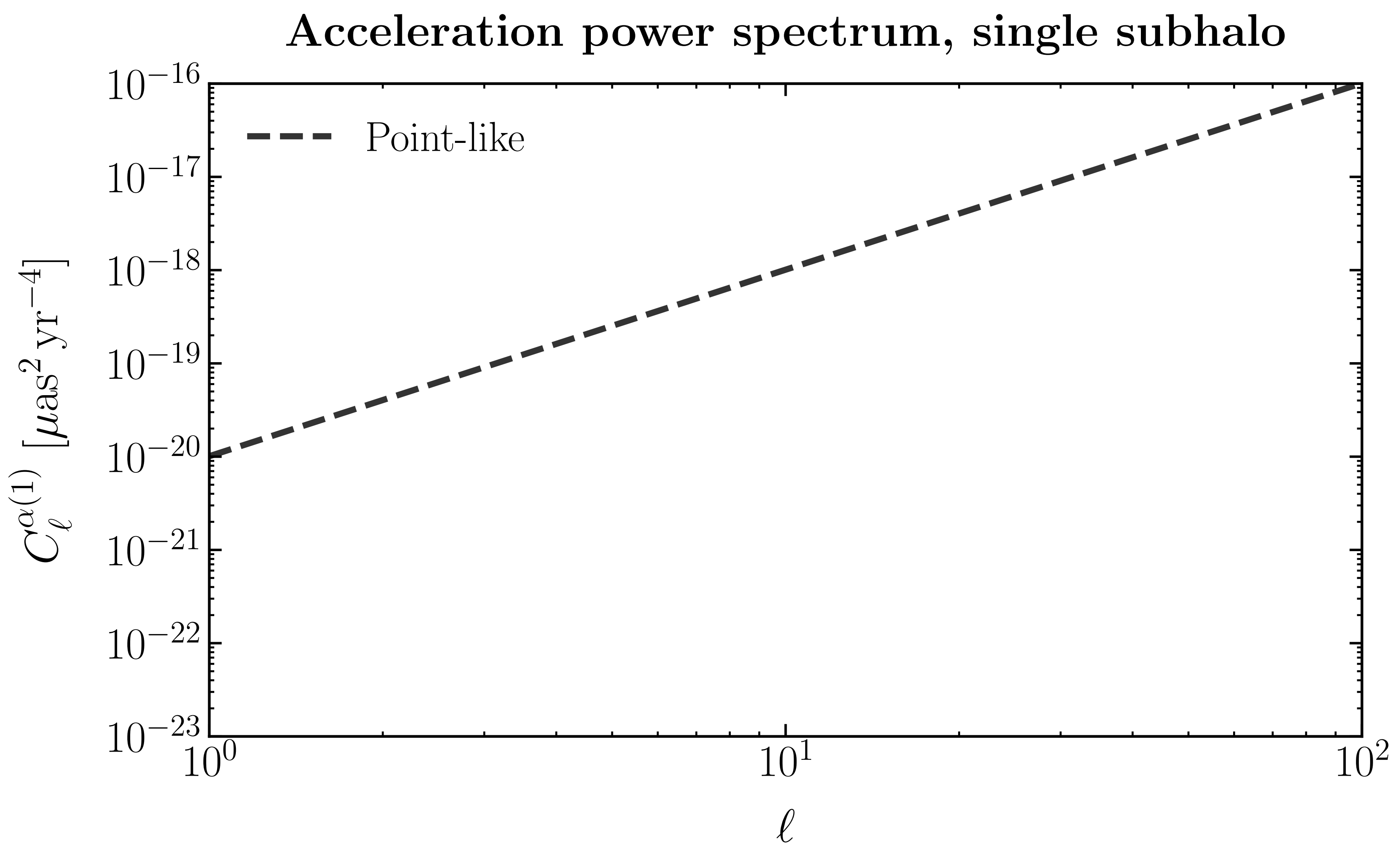

$$C_\ell^{\mu(1)} \simeq \left(\frac{4G_N M_0 v}{D_l^2}\right)^2 \frac{\pi}{2}$$

Acceleration preferentially probes smaller scales

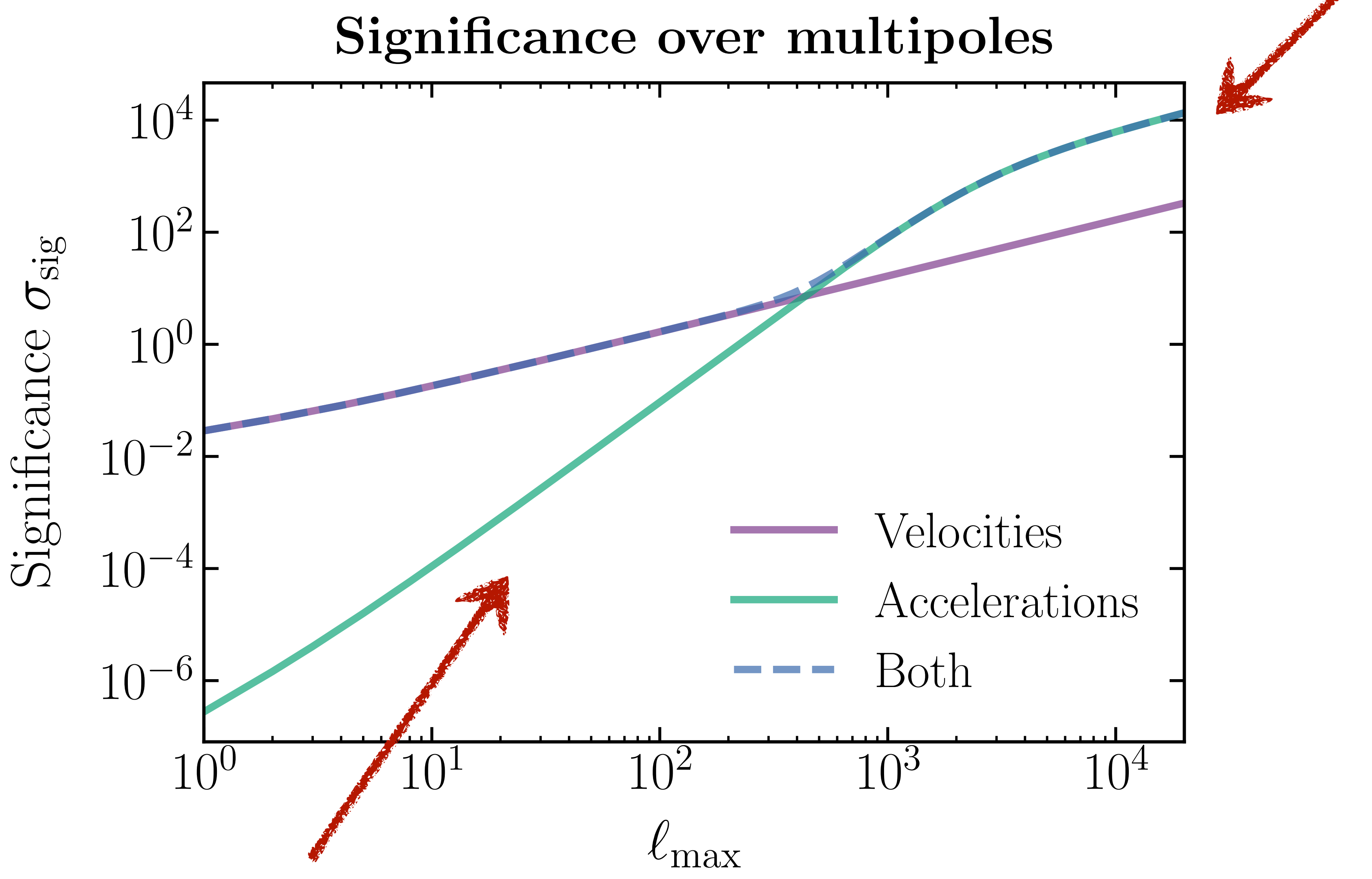

Significance increases linearly with smaller scale

The lensing signal: extended lenses

$$\rho(r) = \frac{M_0}{2\sqrt{2}\pi^{3/2}R_0^3} e^{-r^2/2R_0^2}$$

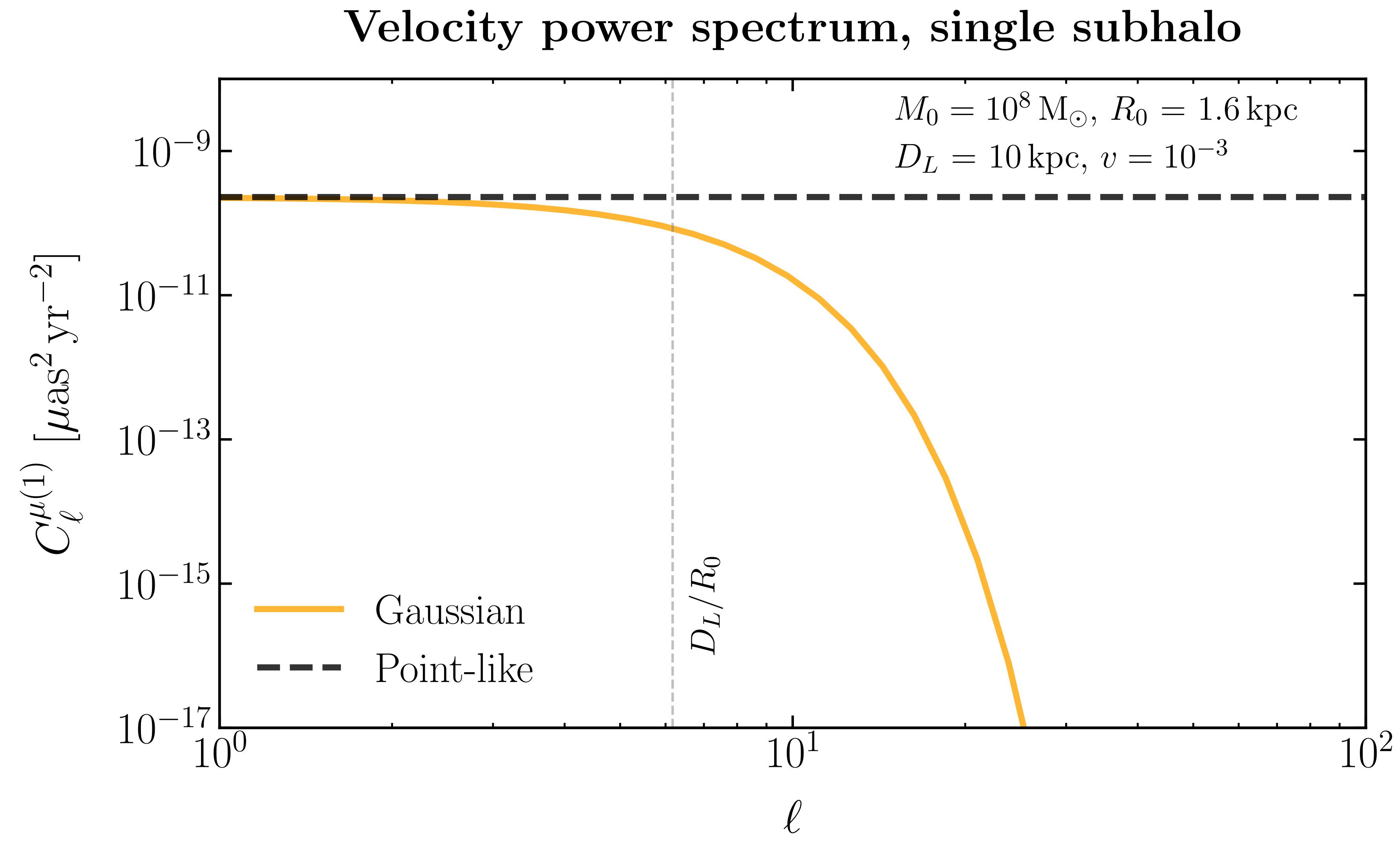

$$C_\ell^{\mu(1)} \simeq \left(\frac{4G_N M_0 v}{D_l^2}\right)^2 \frac{\pi}{2}\, e^{-\ell^2\beta_0^2}$$

Suppression at smaller scales

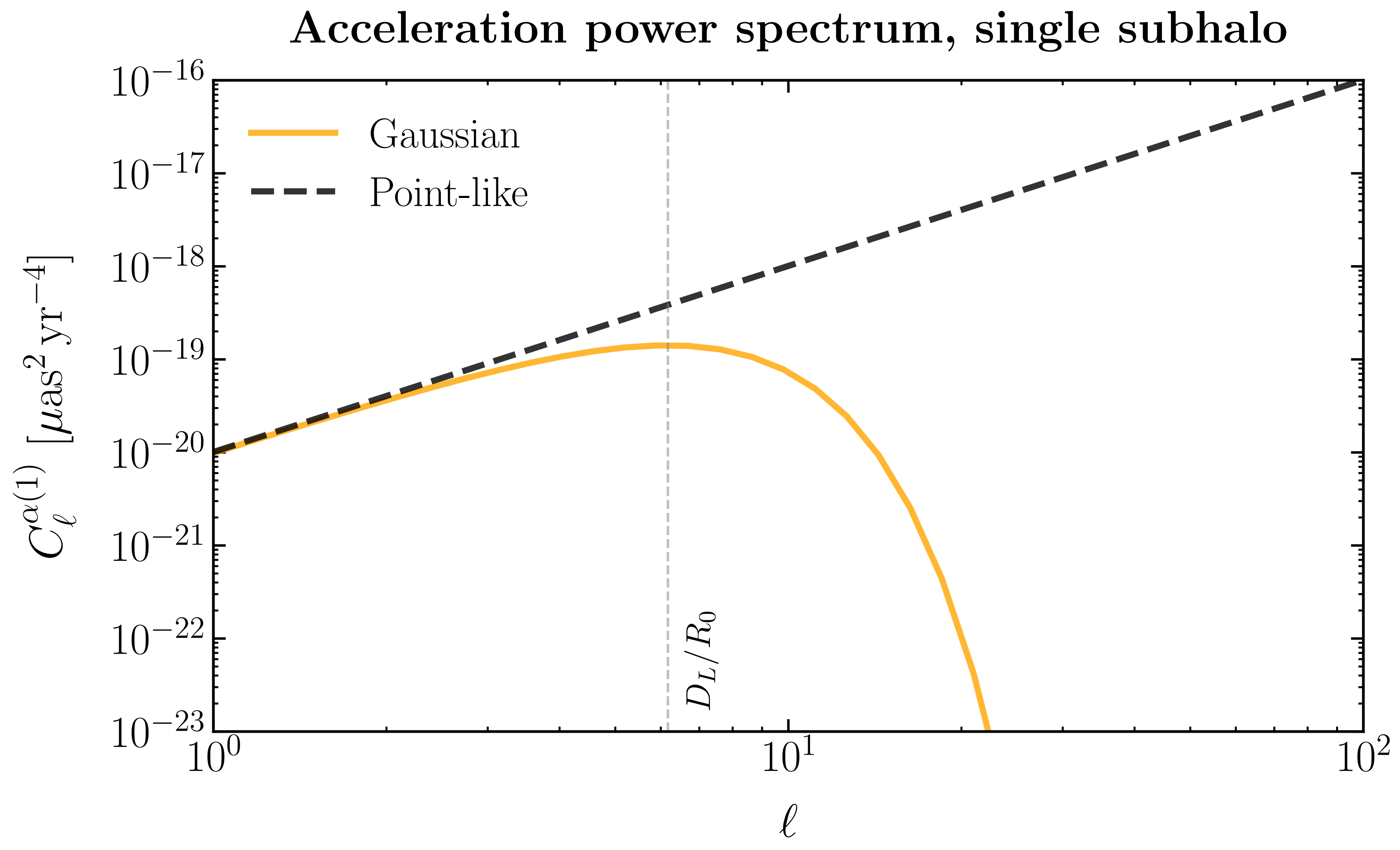

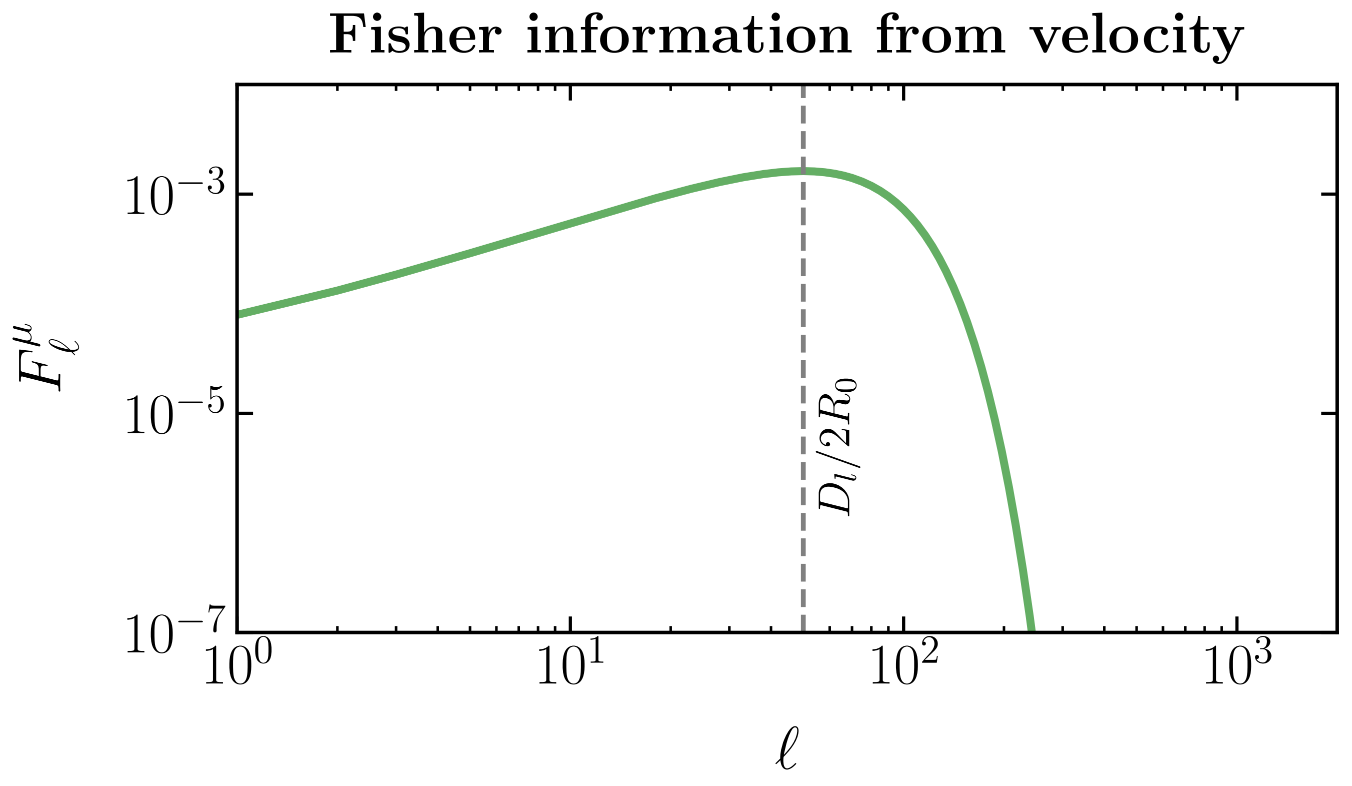

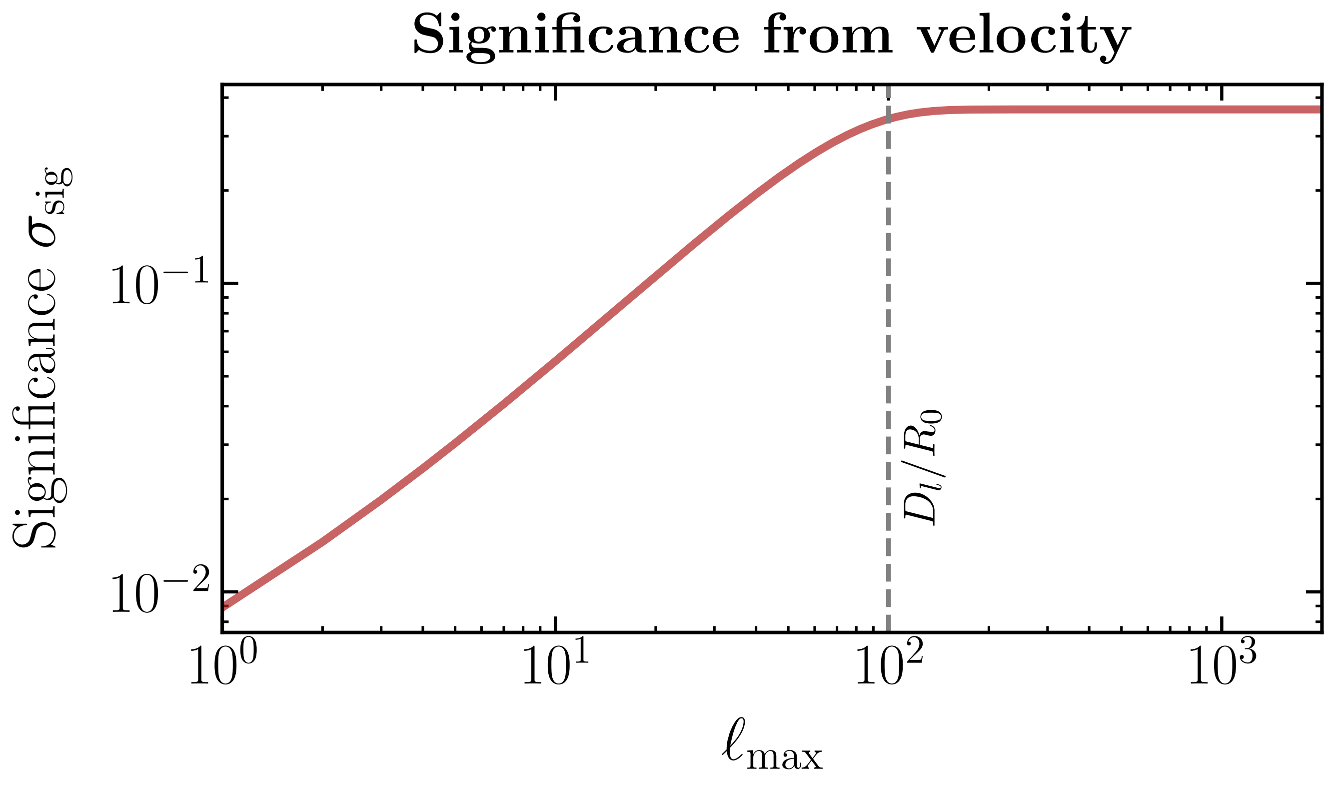

Peak information from scales around angular size of lens

Significance flattens quicker for fluffier lenses

The lensing signal: realistic lenses

$$\rho_{\mathrm{tNFW}}(r) = \frac{M_s}{4\pi r (r+r_s)^2}\left(\frac{r_t^2}{r^2+r_t^2}\right)$$

(truncated) NFW profile: cuspy, describes (tidally stripped) CDM subhalos

$$\rho_{\mathrm{Burkert}}(r) = \frac{M_b}{4\pi (r+r_b)(r^2+r_b^2)}$$

Burkert profile: cored, describes subhalos e.g. in case of DM self-interactions

Truncation effects show up at larger scales

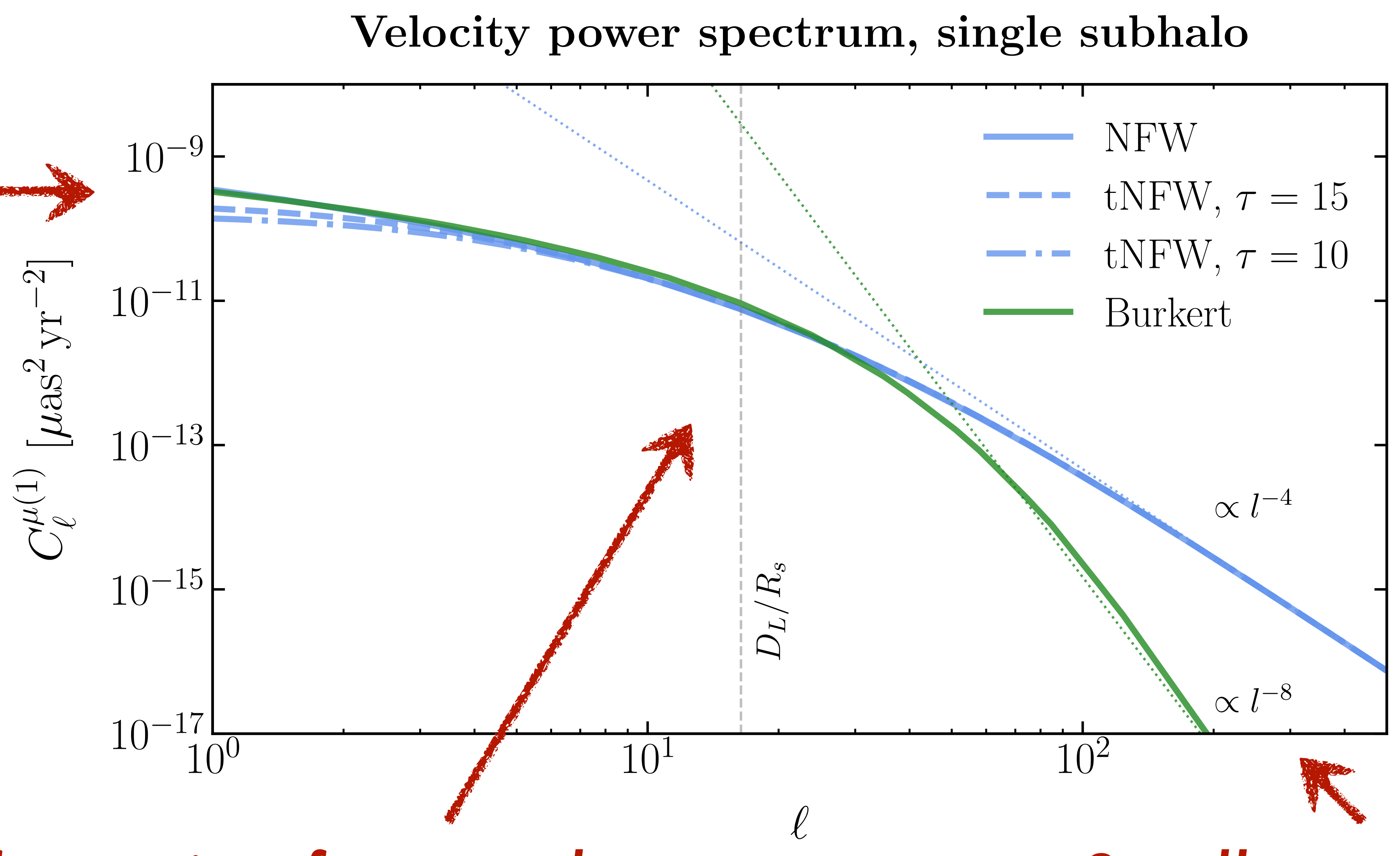

Peak information from scales corresponding to subhalo scale radius

Smaller scales probe subhalo core

Cold dark matter: mass and location in Galaxy

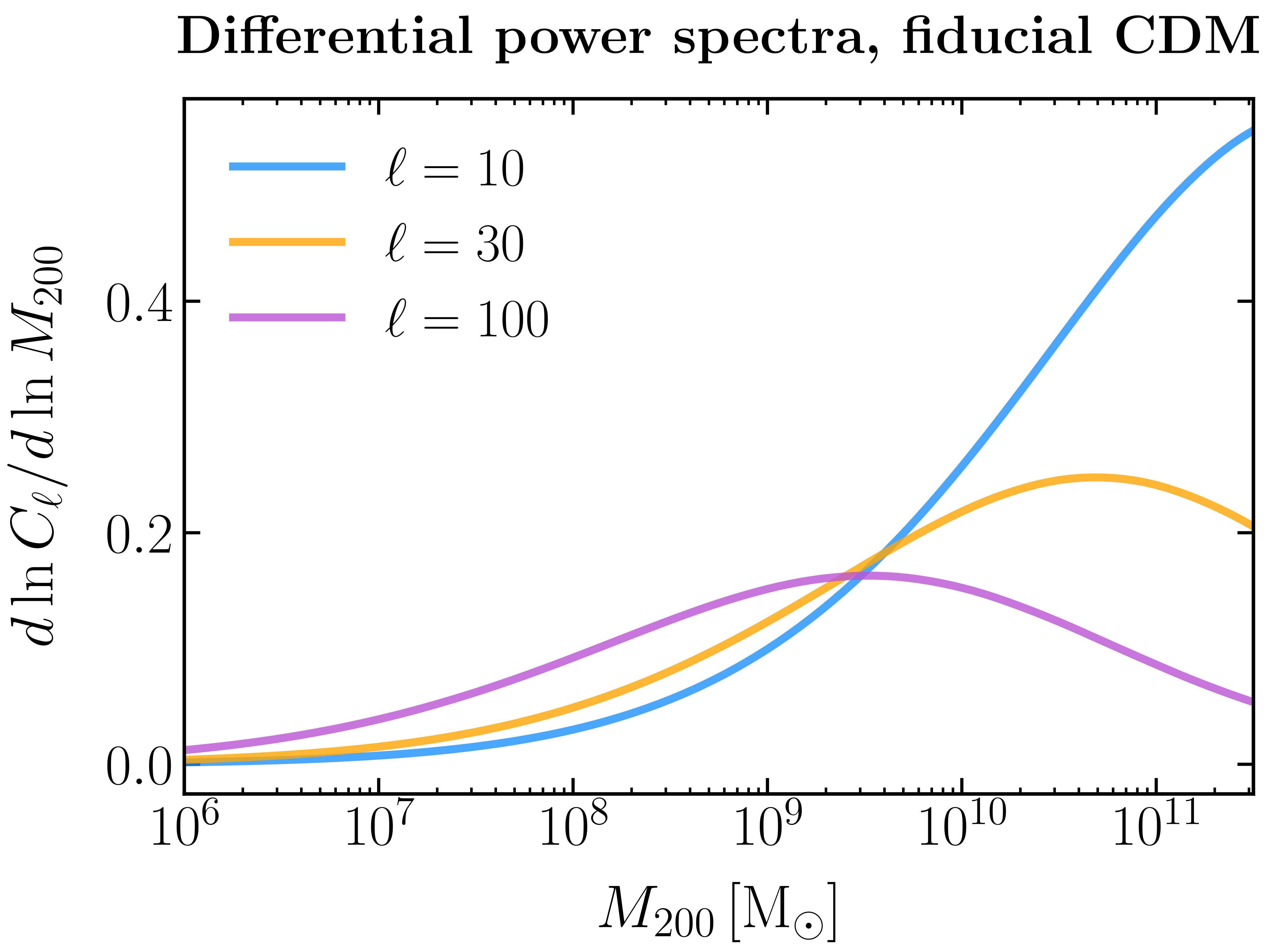

Most of the sensitivity comes from more massive halos

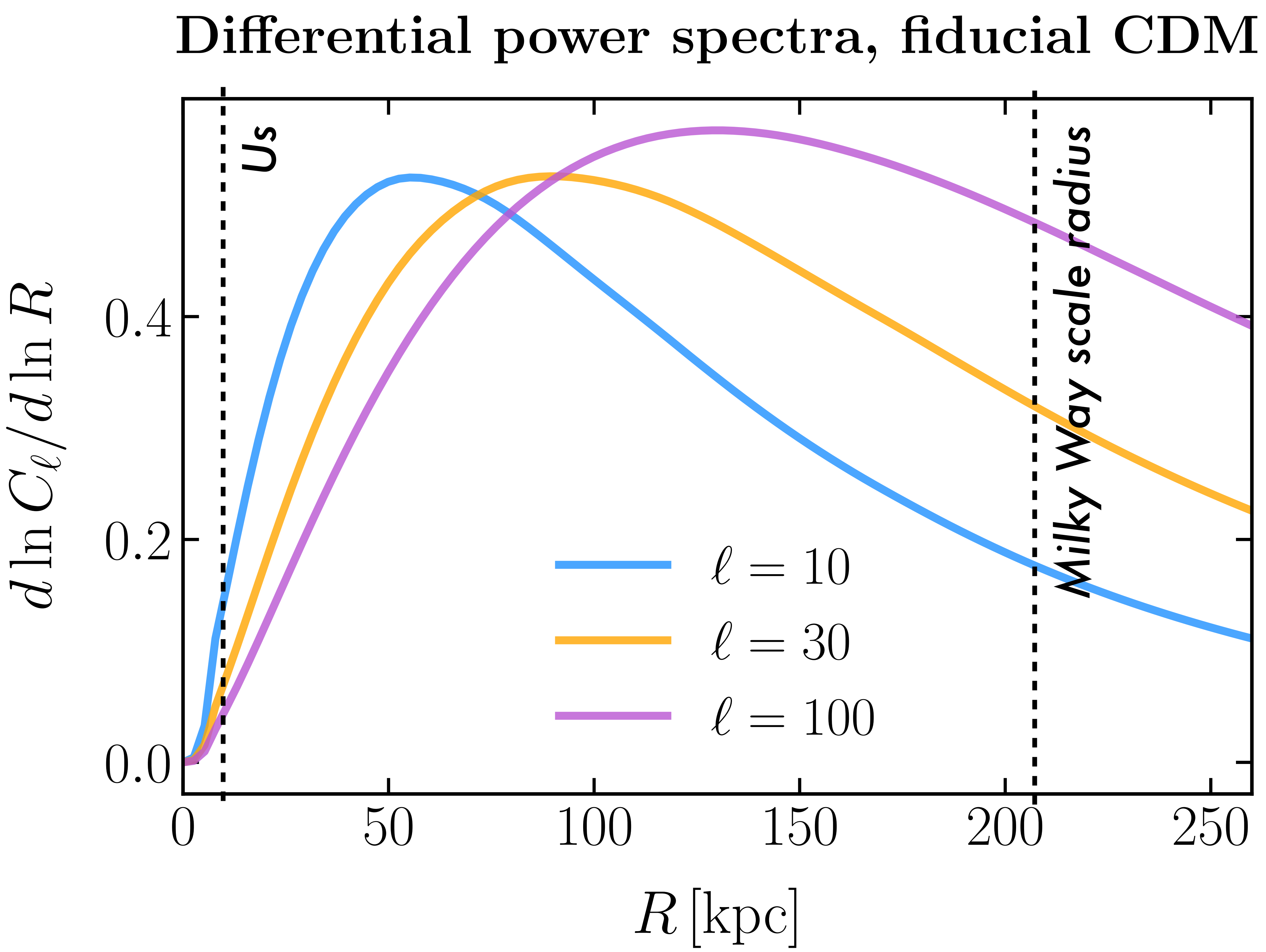

Sensitive to subhalo population in the bulk Milky Way halo

Angular Power Spectra 101

A scalar field $T(\hat{n})$ on a sphere can be expressed as a linear superposition of $Y_{\ell m}(\hat{n})$ spherical harmonics

$$T(\hat{n}) = \sum_{\ell=0}^{\ell_{\max}} \sum_{m=-\ell}^{\ell} a_{\ell m} Y_{\ell m}(\hat{n})$$

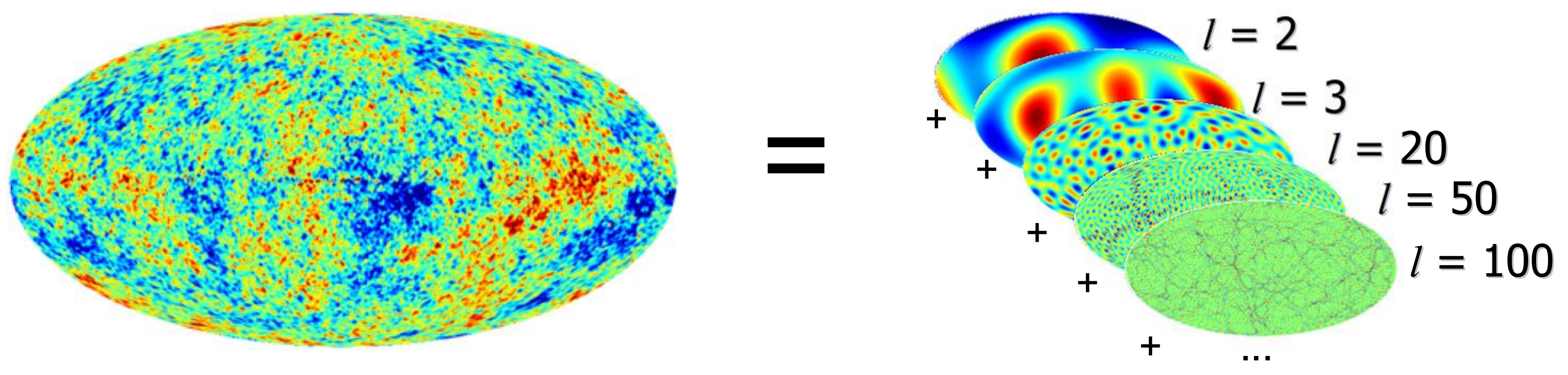

ℓ encodes angular scale

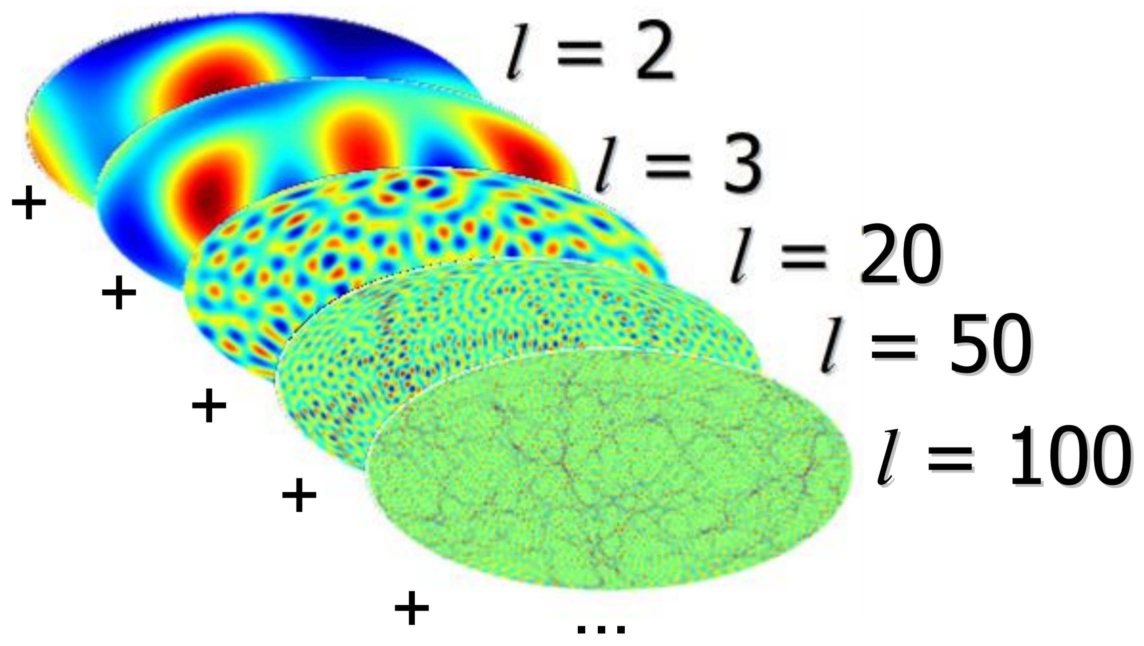

m encodes orientation

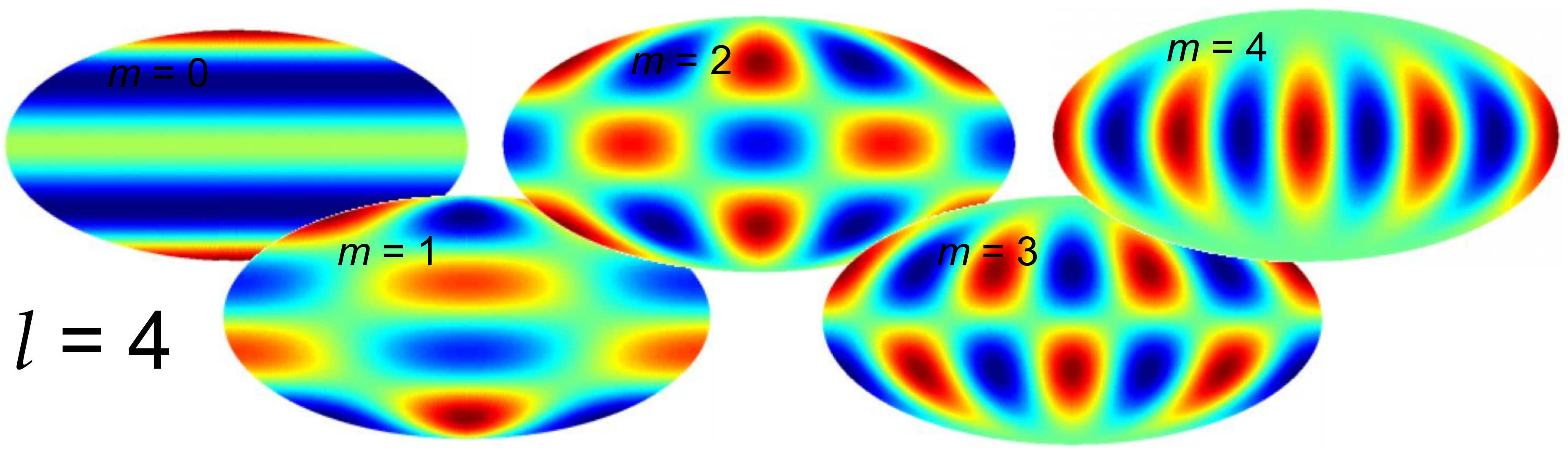

Angular Power Spectra 101

The spherical harmonic coefficient can be determined through a convolution

$$a_{\ell m} = \int_{4\pi} T(\hat{n}) Y^*_{\ell m}(\hat{n}) d\Omega$$

Average power over different azimuthal directions to get power per angular mode ℓ

$$C_\ell = \frac{1}{2\ell + 1} \sum_{m=-\ell}^{\ell} |a_{\ell m}|^2$$

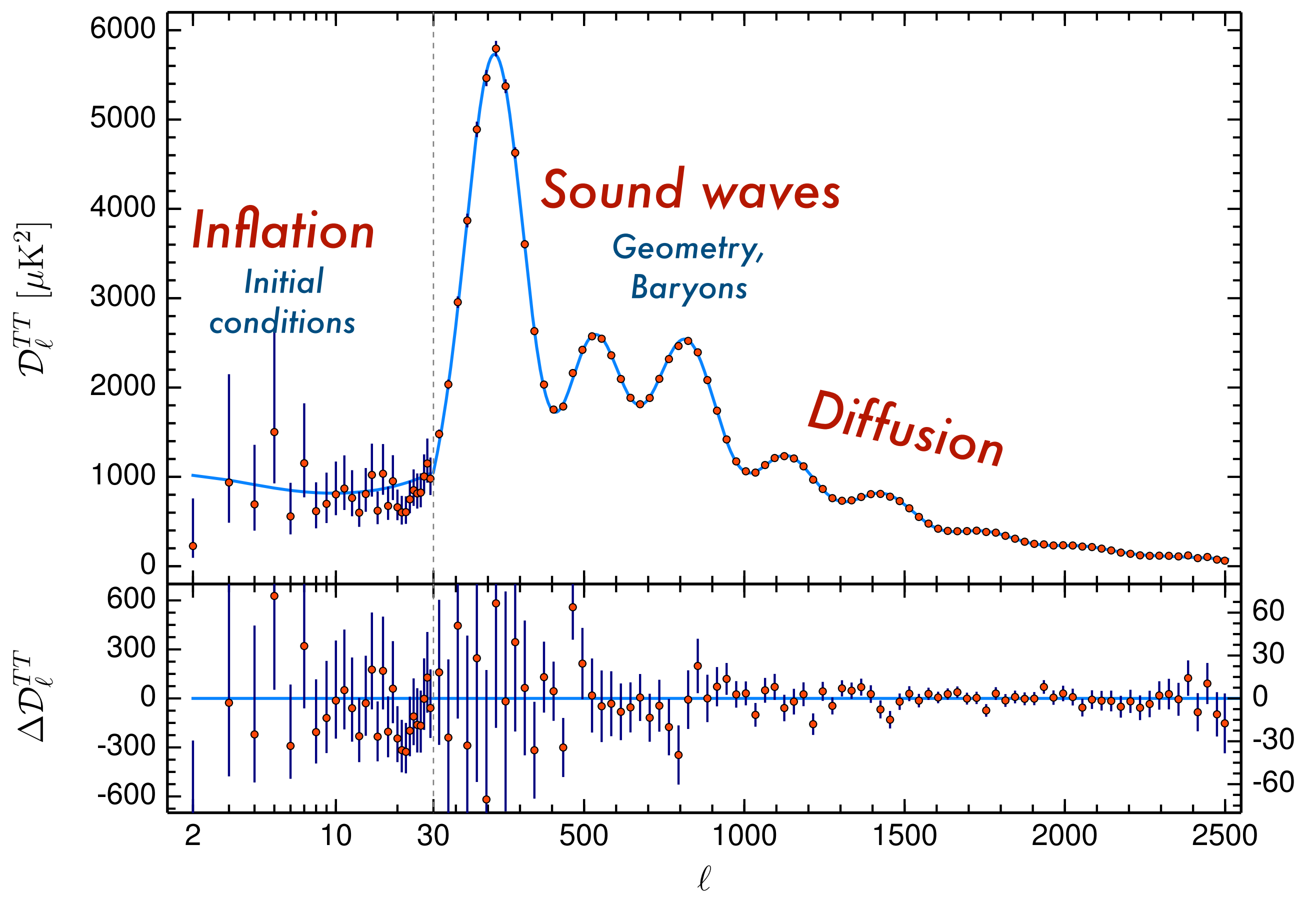

Shape of power spectrum contains a wealth of information about underlying physics

Discovery handles

Can leverage several features of the lensing signal to ensure discovery against systematic/instrumental noise

Curl of lensing signal vanishes

$$C_\ell^{\mu(1)} \equiv \frac{1}{2\ell+1}\sum_{m=-\ell}^{\ell}\left|\mu_{\ell m}^{(1)}\right|^2 \quad = \quad \textit{Signal + Noise}$$

$$C_\ell^{\mu(2)} \equiv \frac{1}{2\ell+1}\sum_{m=-\ell}^{\ell}\left|\mu_{\ell m}^{(2)}\right|^2 \quad = \quad \textit{Noise}$$

$\nabla \times \{$ 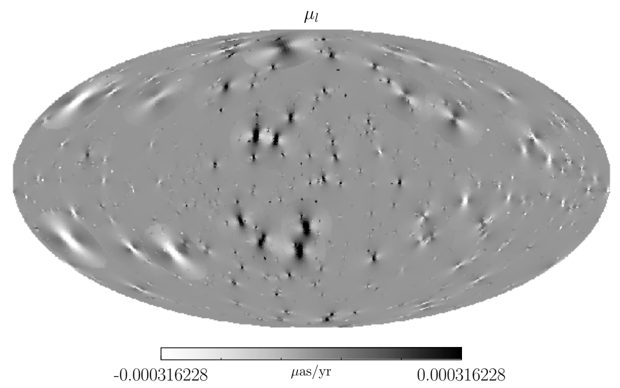

, 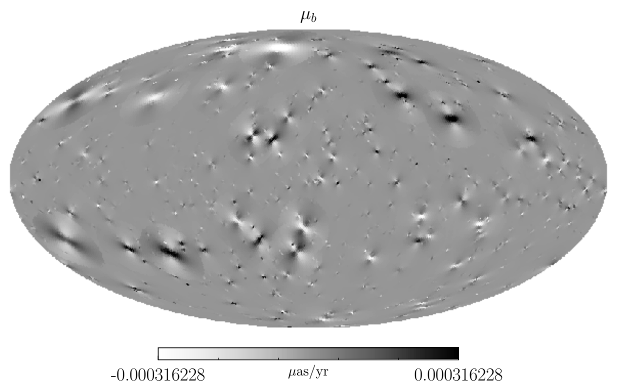

$\} \equiv 0$

Use divergence-free modes as control region

Preferred velocity due to Sun's motion induces azimuthal asymmetry in global lensing signal

$$\mu_{\ell m}^{(1)} = -\frac{\ell(\ell+1)}{D_l}\int \mathrm{d}\Omega\,\psi(\boldsymbol{\beta})\mathbf{v}\cdot\boldsymbol{\Psi}_{\ell m}^*$$

Asymmetric

$$C_{\ell,\mathrm{low}-m}^{(1)} = \left\langle \sum_{m=0}^{\mathrm{floor}(\ell_{\max}/2)} \left|\mu_{\ell m}^{(1)}\right|^2 \right\rangle$$

$$C_{\ell,\mathrm{high}-m}^{(1)} = \left\langle \sum_{m=\mathrm{floor}(\ell_{\max}/2)}^{\ell_{\max}} \left|\mu_{\ell m}^{(1)}\right|^2 \right\rangle$$

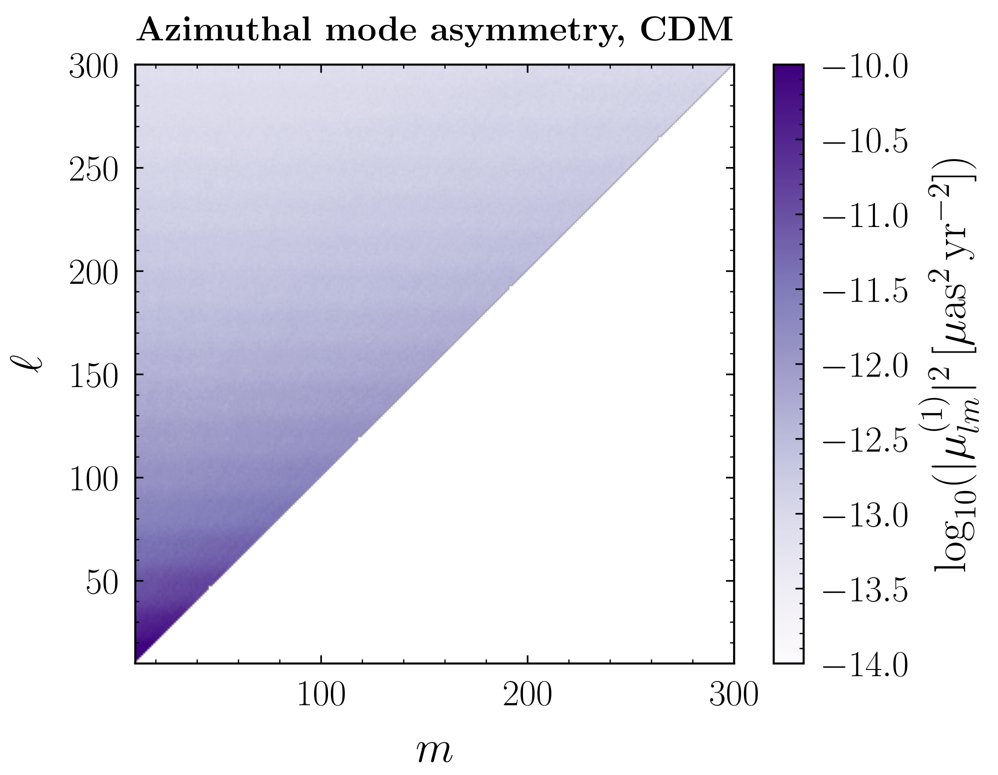

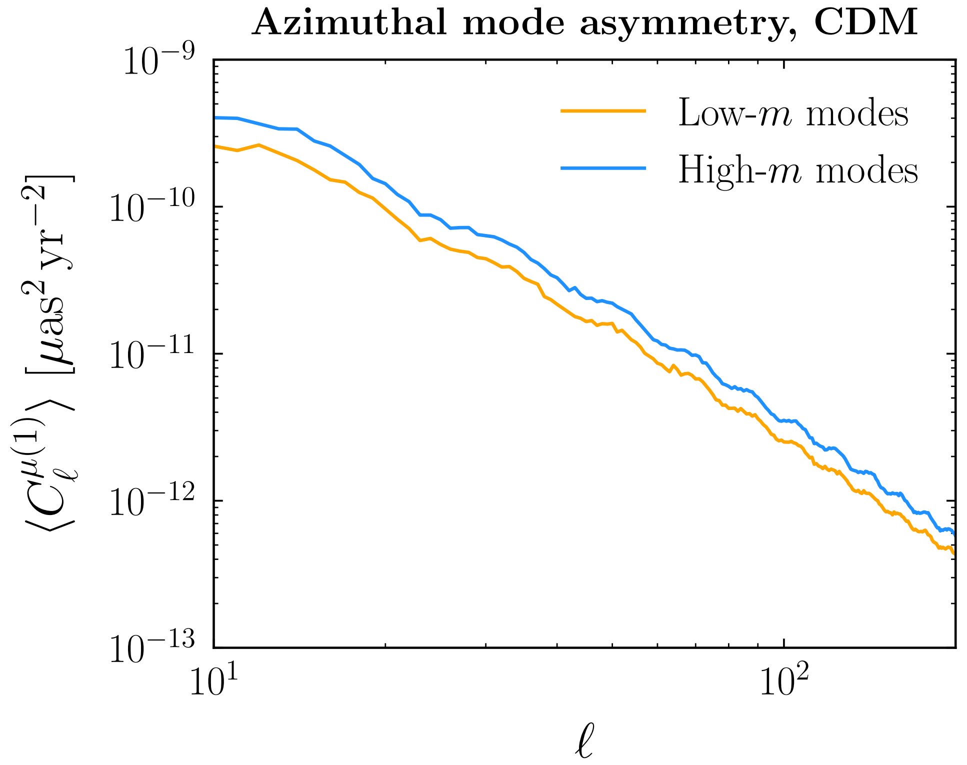

Use systematic asymmetry in m-modes as discriminant

Induced velocity dipole pattern

Gaia DR2 quasars

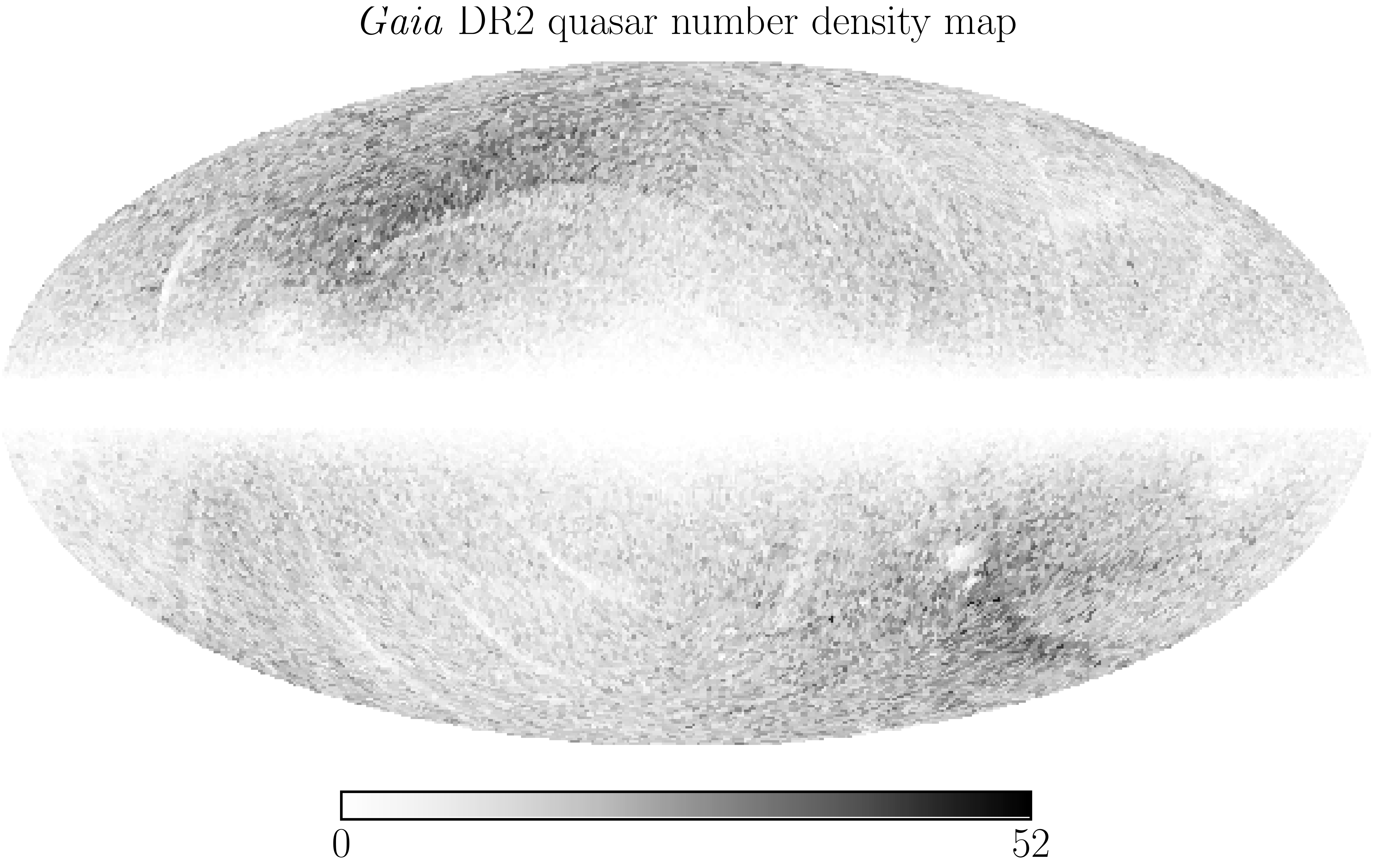

Proper motions

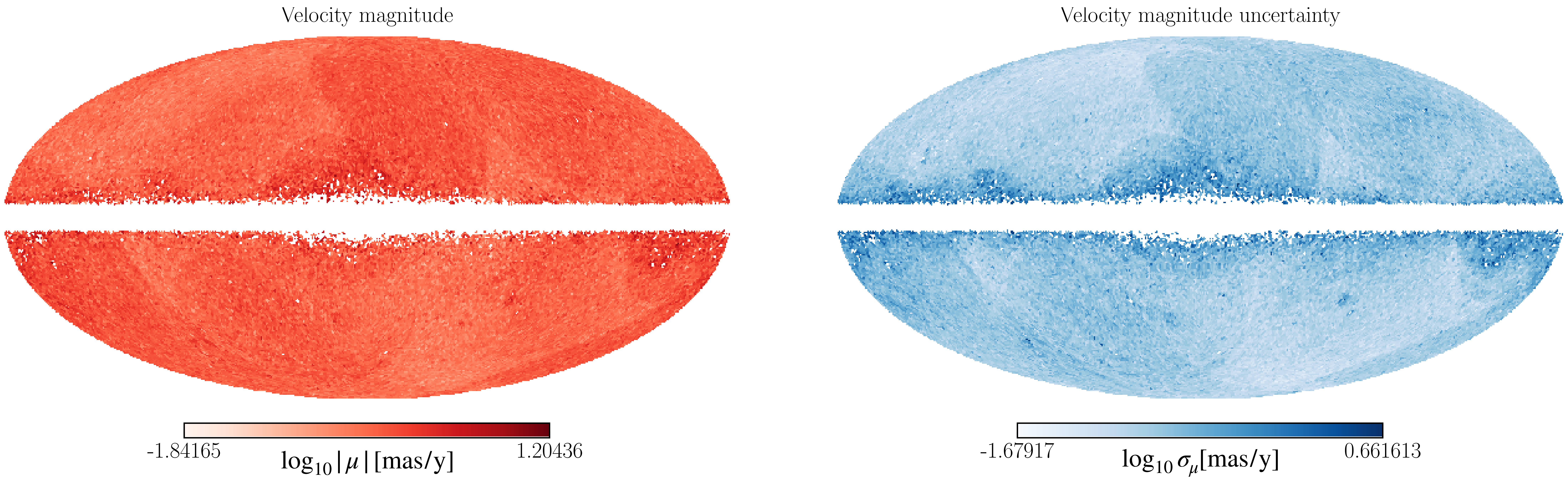

Practically, need *unbiased estimator* to account for non-uniform noise and sky sampling

Proper motions

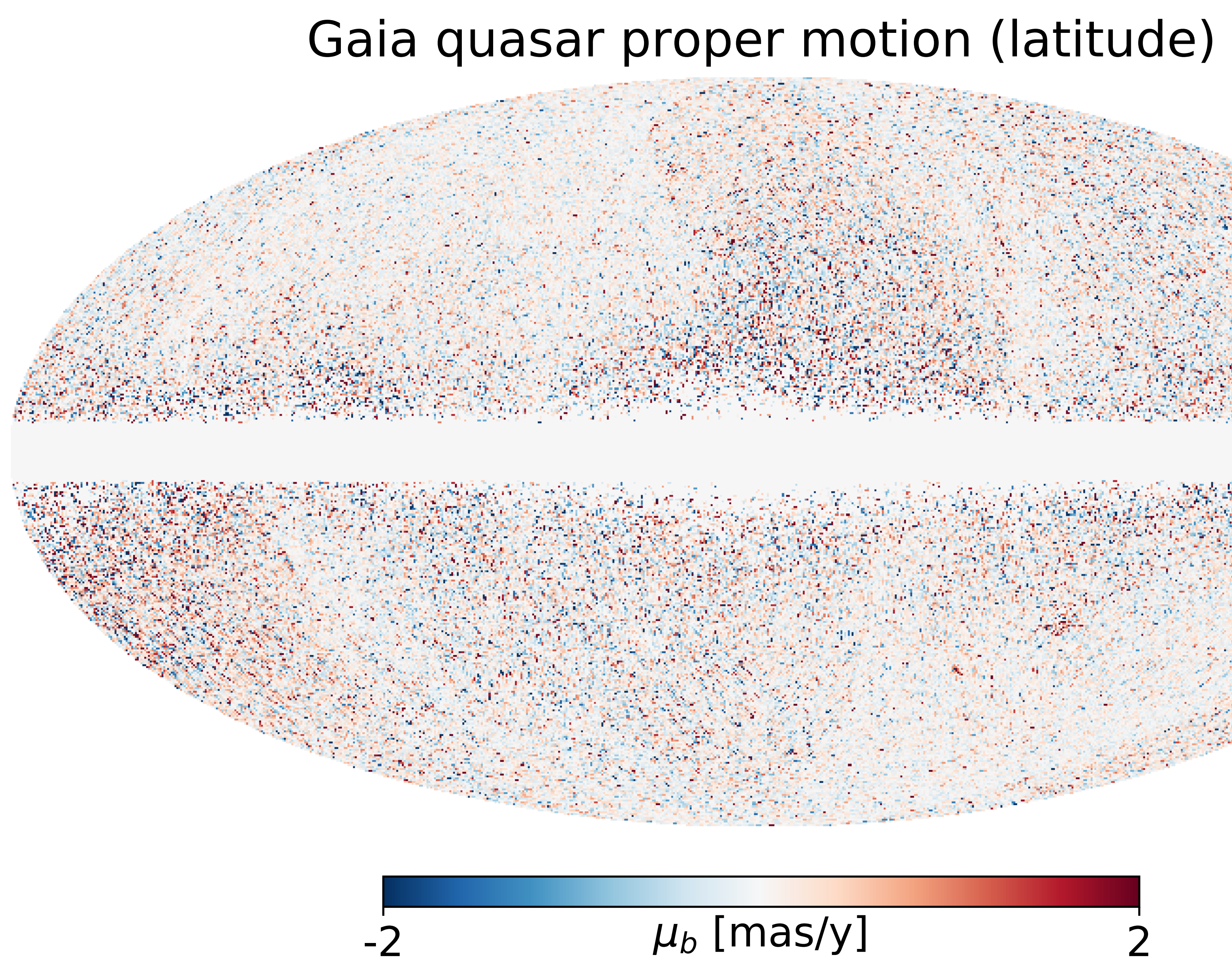

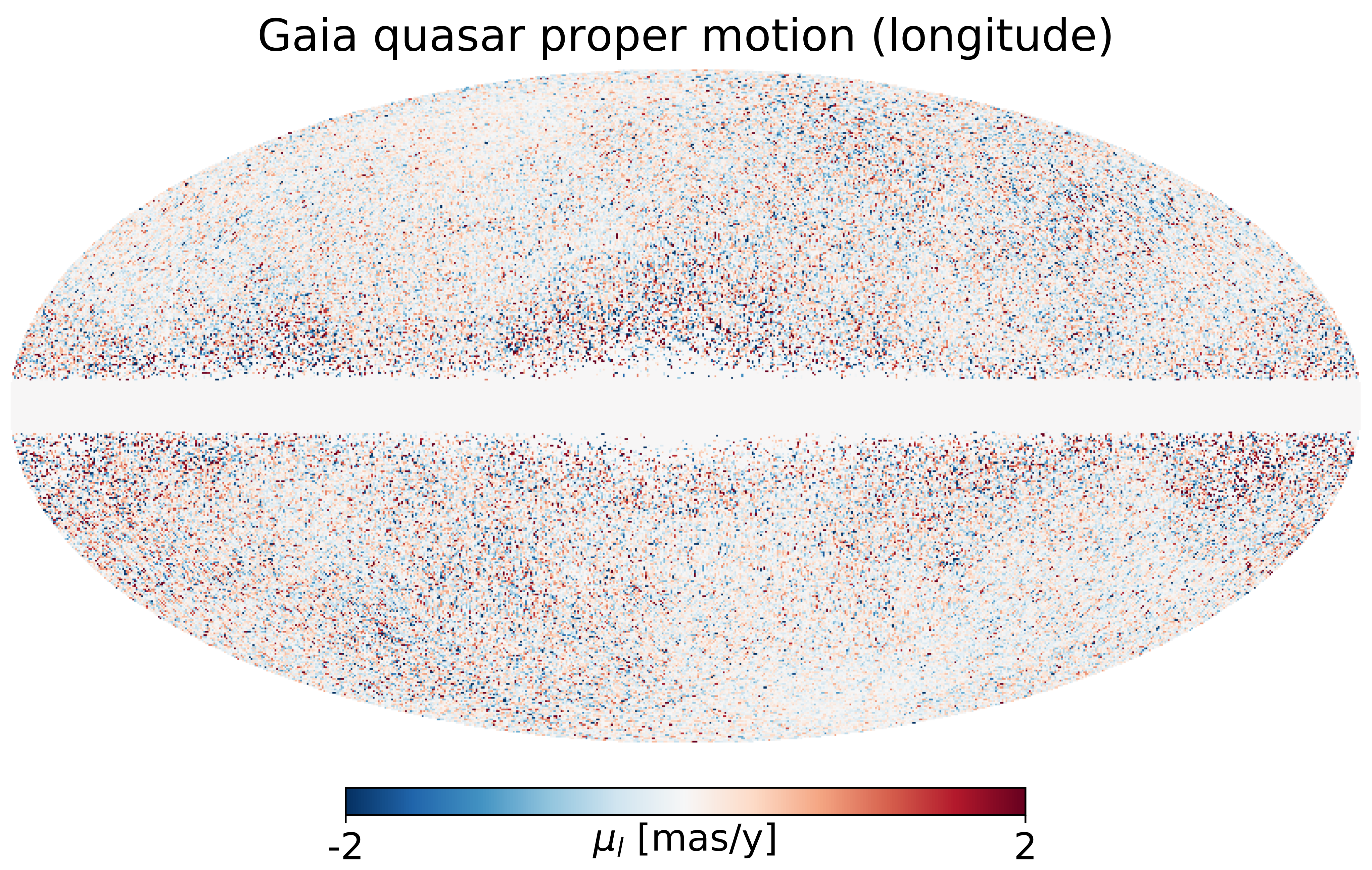

Estimator for power spectrum

$$\overrightarrow{\mu}(\hat{n}) = \sum_{\ell m} \mu^{(1)}_{\ell m} \overrightarrow{\Psi}_{\ell m}(\hat{n}) + \mu^{(2)}_{\ell m} \overrightarrow{\Phi}_{\ell m}(\hat{n})$$

$$\hat{S}^{(1)}_{\ell m} = \frac{1}{2} \sum_{\ell' m'} \left(F^{(1)}\right)^{-1}_{\ell m \ell' m'} \sum_{i \alpha j \beta} \frac{\mu_{i\alpha}}{\sigma^2_{\mu_i}} \frac{\mu_{j\beta}}{\sigma^2_{\mu_j}} \Psi^{\ell' m'}_{i\alpha} \Psi^{\ell' m' *}_{j\beta}$$

Curl-free modes

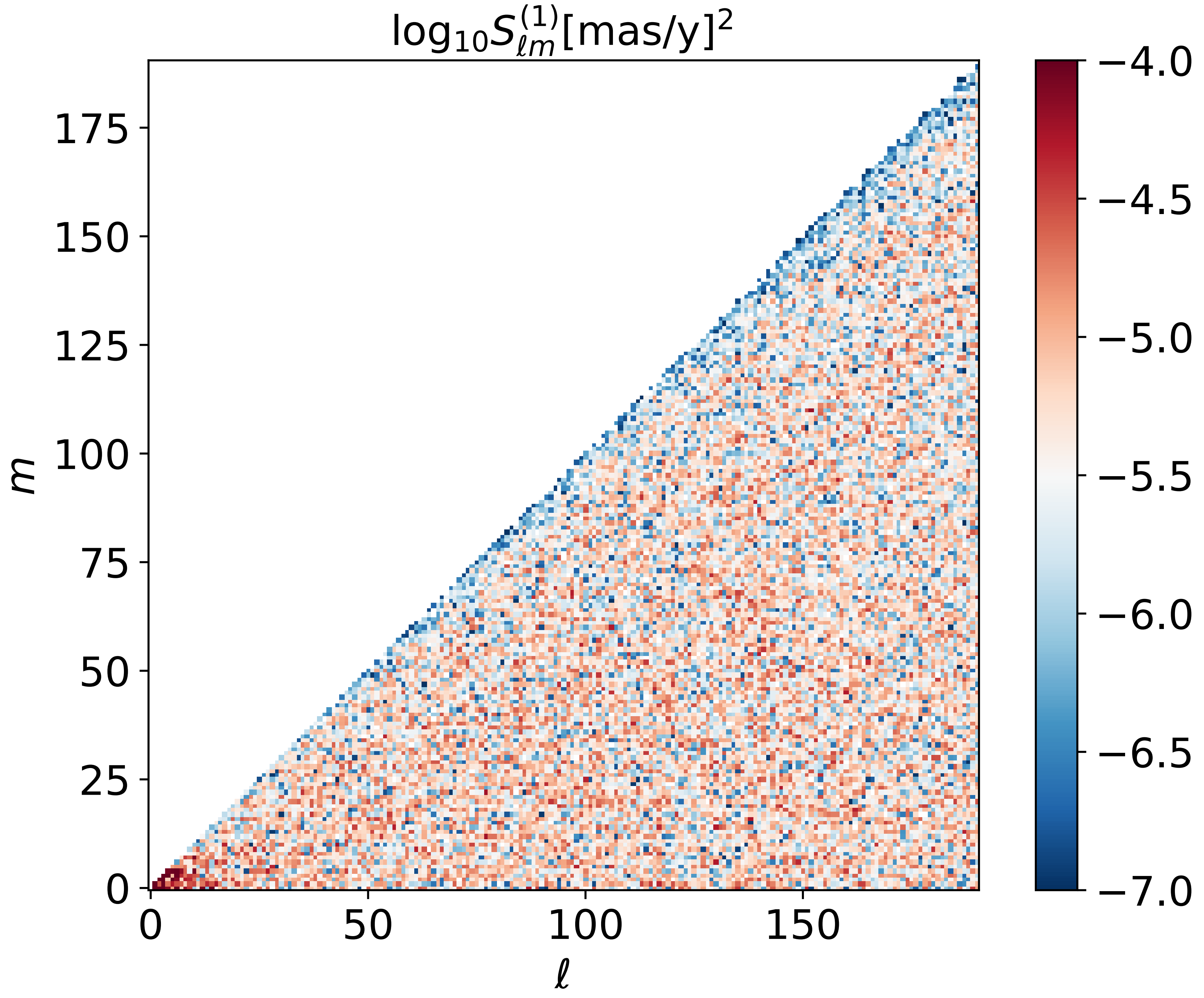

Divergence-free modes

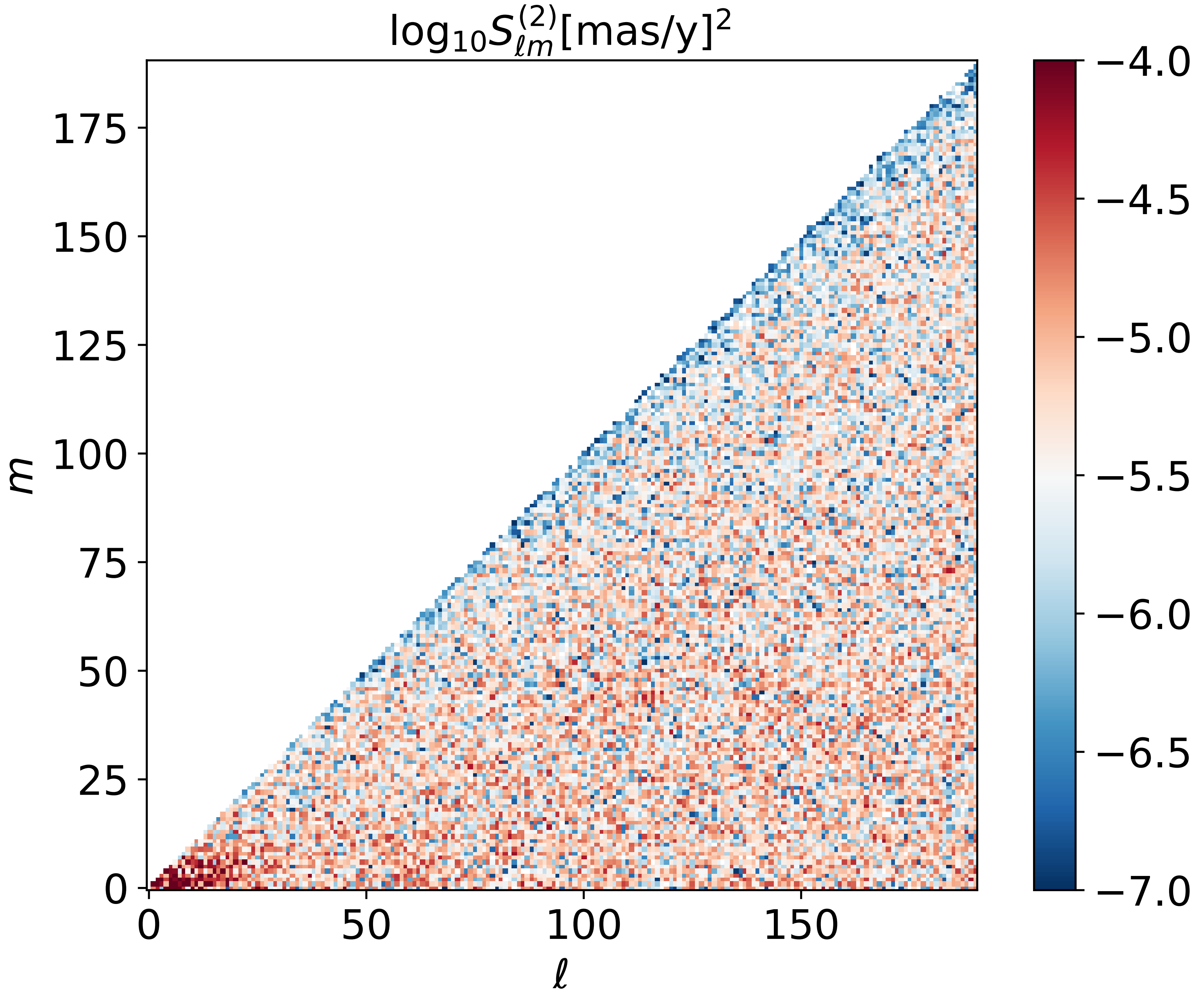

Quasar power spectra

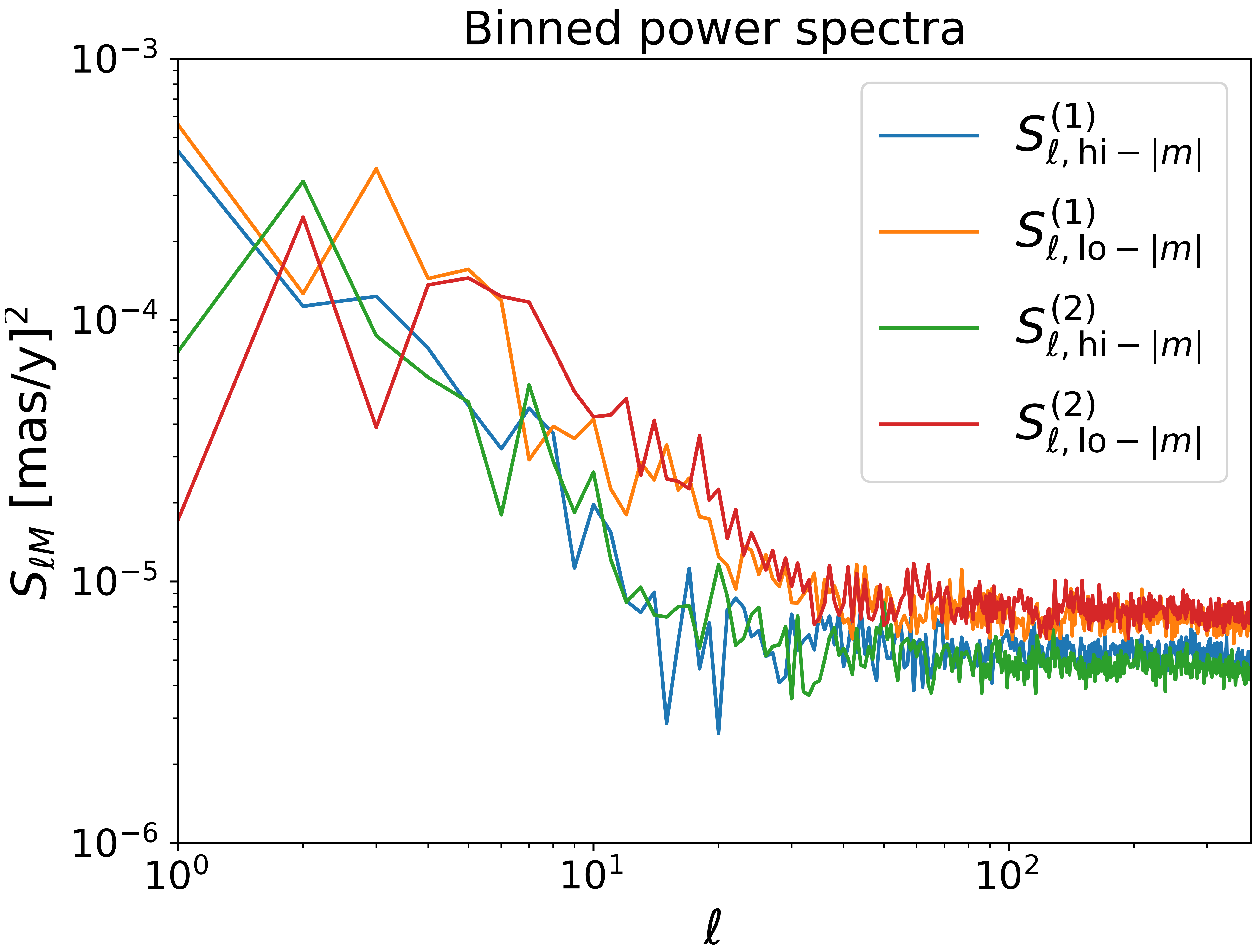

Total power spectra from convolution

Get total expected signal as *convolution over subhalo distribution properties*

$$C_\ell^{\text{tot}} = \int_{M,r,v} d^3v d^3r dM f_\oplus(\mathbf{v}, t) \frac{dN}{d\mathbf{r}} \frac{dN}{dM} C_\ell \left(M, \mathbf{v}, D_l(\mathbf{r}), \mathbf{r}\right)$$